In vivo silencing of A20 *via* TLR9-mediated targeted siRNA delivery potentiates anti-tumor immune response

Inauguraldissertation

zur

Erlangung des akademischen Grades eines

Doktors der Naturwissenschaften
(Dr. rer. Nat.)

der

Mathematisch-Naturwissenschaftlichen Fakultät

der

Ernst-Moritz-Arndt-Universität Greifswald

vorgelegt von
Floriane Claudia Maria Braun
geboren am 14.09.1983
in Berlin, Deutschland

Greifswald, der 31.08.2015

Dekan der Mathematisch-Naturwissenschaftlichen Fakultät
Prof. Dr. Klaus Fesser

1. Gutachter: Prof. Dr. Barbara M. Bröker

2. Gutachter: Prof. Dr. Andreas Thiel

Tag der Promotion:

10.02.2016

“Die Neugier ist die mächtigste Antriebskraft im Universum,
weil sie die beiden größten Bremskräfte im Universum überwinden kann:
die Vernunft und die Angst.”

(Walter Moers)

CONTENTS

1 ZUSAMMENFASSUNG

Krebserkrankungen zählen zu den häufigsten Todesursachen in den westlichen Industrieländern. Heutige Therapieoptionen sind bislang hauptsächlich die operative Entfernung, Bestrahlung und Chemotherapie. Dank intensiver Forschung nehmen alternative Verfahren, wie die Gentherapie und vor allem Immuntherapien stark zu und stellen vielversprechende neue Behandlungsoptionen dar. Der grundlegende Gedanke bei Immuntherapien ist es das körpereigene Immunsystem des Patienten zu unterstützen und zu stimulieren, damit es so in die Lage versetzt wird Tumorzellen eigenständig eliminieren zu können. Ein optimales Ziel dafür sind die Dendritischen Zellen, da sie sehr potente Antigen-präsentierende Zellen sind und im Immunsystem die Weichen stellen in welche Richtung eine Immunantwort verlaufen soll. Eine Stimulation dieser Zellen durch Aktivierung interner Signalwege führt zu ihrer Reifung, zur Hochregulation von Oberflächenrezeptoren sowie zur Sekretion von Zytokinen. Derart manipulierte Dendritische Zellen können zu einer verstärkten Bildung von Effektorzellen und dem Durchbrechen einer Immunsuppression führen. Eine Möglichkeit zur Aktivierung zellulärer Signalwege ist die Blockierung des natürlichen Regulators A20. Zur Herunterregulation der A20 Expression wird in diesem Projekt die Methode der RNA-Interferenz angewendet. Dafür muss eine, gegen A20 gerichtete, siRNA in das Zytoplasma der Zielzellen gelangen. Als Transportsystem wird eine CpG DNA-Sequenz verwendet. Diese CpG-Sequenzmotive sind charakteristische Bausteine von bakterieller DNA und werden daher von Immunzellen als alarmierendes Signal wahrgenommen. Immunzellen, die den Toll-like Rezeptor 9 exprimieren, wie zum Beispiel Dendritische Zellen nehmen diese DNA auf. Infolgedessen kommt es zur Stimulation und Aktivierung dieser Zellen. CpGs werden bereits als immunstimulierende Zusätze bei Impfungen und auch in der Krebstherapie eingesetzt. Die Kopplung einer siRNA zur Blockierung von A20 an CpGs ermöglicht eine selektive Regulation von A20 in Zellen, die den Rezeptor zur CpG-Erkennung besitzen und führt zu ihrer verstärkten Stimulation.

Ziel dieses Projekts war es durch den Einsatz von CpG-siRNA A20 Konstrukten gezielt Tumor-assoziierte Immunzellen zu stimulieren, um eine vom Tumor induzierte Immunsuppression zu durchbrechen und eine potente anti-Tumor Immunantwort zu induzieren.

Als Modell für die Untersuchung von Internalisation und stimulatorischer Kapazität der CpG-siRNA A20 Konstrukte wurde aus Knochenmarkzellen der Maus eine Langzeitkultur Dendritischer Zellen generiert. Die Konstrukte waren bereits nach einer Stunde in den Zellen nachweisbar und führten zu deutlich verstärkter Zellstimulation im Vergleich zu CpG ohne A20 siRNA. Im Folgenden wurden die Konstrukte auf ihre immunstimulatorische Wirkung bei intraperitonealer Applikation in gesunden Mäusen untersucht. Auch hier konnten deutliche Zeichen der Zellaktivierung detektiert werden. Neben lokalen zellulären Veränderungen im Peritoneum war vor allem die erhöhte Expression der Zytokine IL-6 und TNF-α Anzeichen immunmodulatorischer Effekte. In den darauf folgenden Experimenten wurde das Potential dieser Effekte auf *subcutan* wachsende Tumore untersucht. In einem Maus-Tumormodell mit Melanomzellen führte die A20 Blockade zu einer Verstärkung der CpG-induzierten Immunstimulation mit deutlich erhöhter Expression der Zytokine IL-6, TNF-α, IFN-γ und IL-12. Infolgedessen konnten signifikant mehr Tumor-spezifische zytotoxische T-Zellen im Blut und im Tumor nachgewiesen werden. Das Wachstum der aggressiven Tumore konnte messbar verlangsamt und dadurch das Überleben der Tiere verlängert werden.

Eine Prüfung auf Übertragbarkeit der Ergebnisse von Mäusen auf den Menschen, erfolgte in Dendritischen Zellen isoliert aus dem Blut gesunder Spender. In ersten Versuchen konnte im Vergleich zu CpG eine verstärkte Stimulation der Zellen und eine erhöhte Expression der Zytokine IL-6 und TNF-α nachgewiesen werden. Obwohl die Spenderzellen unterschiedlich stark auf die Behandlung ansprachen, zeigten sich vielversprechende Parallelen zu den Versuchen bei Mäusen.

Die gewonnenen Erkenntnisse aus den durchgeführten *in vitro* und *in vivo* Experimenten bestätigen die zentrale Rolle von A20 bei der Regulation des immunstimulatorischen Potentials Dendritischer Zellen. Es konnte gezeigt werden, dass die neuartigen CpG-siRNA A20 Konstrukte eine gute Möglichkeit zur simultanen A20-Regulation und CpG-basierten Stimulation darstellen. Darüber hinaus konnten mit diesen neuartigen Konstrukten deutliche anti-Tumor Effekte induziert werden, die das Überleben von Mäusen mit aggressiven Melanomen verlängern konnte.

Die einfache Applikation eines einzigen synthetischen Moleküls und die starke immunstimulatorische Kapazität machen diese Konstrukte zu einem Immunstimulans mit Zukunftspotential, das die Immuntherapie humaner Tumorerkrankungen ergänzen und verbessern könnte.

2 SUMMARY

Cancer is one of the leading causes of death in industrialized nations. Nowadays, cancer therapy mainly consists of surgery, radiation and chemotherapy. Thanks to intensive research alternative treatment strategies like gene therapy and especially immunotherapies are on the rise. Immunotherapies base on the idea of stimulating and supporting the patients` immune system to generate an effective anti-tumor immune response. Dendritic Cells are perfect targets for this purpose, since these potent antigen-presenting immune cells influence the balance of the immune system by defining the route of action. Stimulation of these cells by activation of cellular signaling pathways results in maturation, upregulation of surface molecules and secretion of cytokines. A20 has been identified as a regulator of dendritic cell maturation and attenuator of their immune stimulating properties. Hence, the blockade of that natural inhibitor reveals an elegant way to activate cellular pathways of DCs. A siRNA against A20 obtains a functional blockade via RNA interference if it can be delivered into the cytoplasm of the target cells. CpG oligodeoxynucleotides can be used for this intracellular transport. CpGs contain DNA motifs similar to those found in bacteria. Innate immune cells can detect this DNA via the toll-like receptor 9 getting activated and stimulated. CpG oligodeoxynucleotides are already in clinical use as adjuvants in vaccines and in cancer therapy approaches. Linking A20-specific siRNA to CpG enables A20 regulation and cell stimulation selectively in toll-like receptor 9 expressing cells, like dendritic cells.

Aim of this study was to investigate if these constructs trigger immune cell activation and if they are able to break immune-suppression in the tumor environment to enhance anti-tumor immunity.

A long-term growth factor dependent bone marrow-derived dendritic cell culture has been established in order to analyze the CpG-siRNA A20 effects on murine dendritic cells. The constructs were internalized shortly after administration (1 hour) and led to cell stimulation/activation. The intraperitoneal treatment with the constructs induced local cellular activation and systemic IL-6, TNF-α cytokine production in healthy mice. Subcutaneous growing B16 melanoma tumors were treated peritumorally to analyse whether the observed immune-stimulation has effects on established tumors. The silencing of A20 enhances CpG-induced activation of NF-κB followed by elevated expression of IL-6, TNF-α and IL-12 in this tumor model.

These changes led to enhanced anti-tumor immune responses manifested by increased numbers of tumor-specific cytotoxic T cells, high levels of tumor cell apoptosis and delayed tumor growth.

New constructs were designed and tested on dendritic cells isolated from healthy donors in order to test whether the obtained results for the murine system are applicable to the human system. CpG-siRNA A20 constructs induced cell activation and cytokine expression (IL-6, TNF-α) significantly more than CpG alone. Even though responds of the donor DCs were variable, there are promising similarities to the results of the mouse experiments.

The significant role of A20 in controlling the immune-stimulatory activity of DCs has been confirmed in this study. The novel CpG-siRNA A20 constructs provide a strategy for simultaneous A20 silencing and CpG-mediated cell stimulation directly *in vivo*. This therapeutic approach induces potent adaptive and innate immune responses against established tumors in mouse melanoma model leading to prolongation of survival.

CpG-targeted A20 blockade is a new immune-stimulatory approach, which could be suitable for supplementation or optimization of clinical tumor treatments.

3 ABBREVIATIONS

A20 = TNFAIP3	Tumor Necrosis Factor Alpha Induced Protein 3
ABIN-1	A20 Binding and Inhibitor of NF-kappaB 1
A. dest.	Aqua destillata
AP1	Activator Protein 1
APC	Allophycocyanin (= a fluorescent protein)
APC	Antigen-Presenting Cell
AUC	Area Under the Curve
B220	Isoform of CD45
ß2MG	Beta-2-Micro-Globulin
BMDC	Bone Marrow-derived Dendritic Cell
BSA	Bovines Serum Albumin
CBA	Cytometric Bead Array
CD	Cluster of Differentiation
cDNA	complementary DNA
CEBP	CCAAT-Enhancer-Binding Protein
CpG	Cytosine triphosphate deoxynucleotide (C), phosphodiester link (p), Guanine triphosphate deoxynucleotide (G)
CpG-siRNA	CpG oligoneoxynucleotide linked to siRNA via carbon chain linker
CTL	Cytotoxic T Lymphocyte
ΔΔCT	delta delta of Threshold Cycle
DC	Dendritic Cell
DEPC	Diethylpyrocarbonate (DEPC) treated, RNase free water
DNA	DesoxyriboNucleinAcid
dNTP	desoxyNukleotidTriPhosphat
DTT	DithioThreiTiol
EDTA	EthyleneDiamineTetraacetic Acid
et al.	et alii
FACS	Fluorescence Activated Cell Sorter
FCS	Fetal Calf Serum
FITC	FluoresceinIsoThioCyanat (= a fluorescent protein)
GFP	Green Fluorescent Protein
GM-CSF	Granulocyte Macrophage Colony-Stimulating Factor
h	hour
HBS	Hepes – Buffered Saline

HBSS	Hank's Balanced Salt Solution
HPLC	High Performance Liquid Chromatography
HRP	Horse Radish Peroxidise
IDO	Indoleamine 2,3-DiOxigenase
IFN-α/ -γ	Interferon alpha/ gamma
IκBα	NF-kappa-B Inhibitor alpha
IKK	Inhibitor of KappaB kinase
IL	Interleukin
i.p.	intraperitoneal
IRAK	Interleukin-1 Receptor-Associated Kinase
kb	kilobase
kDa	kiloDalton
Ly6-G	Lymphocyte antigen 6 complex, locus G (also known as Gr-1)
MALDI-TOF	Matrix Assisted Laser Desorption/Ionization - Time of Flight
MAP	Mitogen-Activated Protein
MEM	Minimum Essential Medium
MHC I/ II	Major Histocompatibility Complex class 1/ 2
mRNA	messenger RNA
mDC	myeloid Dendritic cell
MyD88	Myloid Differentiation primary response gene 88
MΦ	Macrophage
NEAA	Nonessential Amino Acids
NF-κB	Nucleo Factor-kappa B
NK	Natural Killer cell
NKT	Natural Killer T cell
n.s.	not significant
ODN	Oligodeoxynucleotide
PAGE	Polyacrylamide Gel Electrophoresis
PAMP	Pathogen-Associated Molecular Pattern
PBMC	Peripheral Blood Mononuclear Cell
PBS	Phosphat-Buffered Saline
pDC	plasmacytoid Dendritic Cell
PerCP	Peridinin-Chlorophyll (= a fluorescent protein)
PFA	Paraformaldehyde
PI3K	Phosphoinositide 3-kinase

PMSF	Phenylmethylsulfonylfluorid
RIP1	Receptor-Interacting Protein 1
RBC	Red Blood Cell
RNF11	Ring Finger Protein 11
RNA	Ribonuclein Acid
RPMI	Cell culture medium (named after “Roswell Park Memorial Institute”)
RT	Reverse Transkriptase
RT-qPCR	Real Time - quantitative Polymerase Chain Reaction
s.c.	subcutaneous
scr	scrambled
SDS	Natriumdodecylsulfat
siRNA	small interfering RNA
STAT3	Signal Transducer and Activator of Transcription 3
TAX1BP1	T-cell leukemia virus type 1 Binding Protein 1
Tc1	CD8-positive T cells type 1
TCR	T Cell Receptor
TDF	Tumor-Derived Factor
TDLN	Tumor Draining Lymph Node
TH1/ 2	T Helper cell type 1 or 2
TLR	Toll-Like Receptor
TNF	Tumor Necrosis Factor
TNFAIP3	Tumor Necrosis Factor Alpha Induced Protein 3
TNFR1	Tumor Necrosis Factor Receptor 1
Treg	regulatory T cell
TRAF6	Tumor Necrosis Factor (TNF) Receptor-Associated Factor 6
Trp-1	Tyrosinase related protein-1 (= Tyrp1, gp75)
VEGF	Vascular Endothelial Growth Factor

4 INTRODUCTION

4.1 Tumor development and immune escape mechanisms

Cancer is one of the leading causes of death and it is on the way of becoming the most frequent lethal disease in industrialized nations. Nowadays, cancer therapy mainly consists of radiation, chemotherapy, surgery, gene therapy and immunotherapy. Immunotherapy is a promising field on the rise, especially in treatment of hematological cancers and with regards to metastasis or relapse. A central question of cancer immunotherapy is how antigenic tumors can grow in immune-competent hosts. Immune suppression can partly explain why tumors develop and progress even in the presence of tumor-specific immune effector cells [1]. Nearly 100 years ago Paul Ehrlich drew up the “immunosurveillance theory” describing the ability of the immune system to recognize and eliminate primary developing tumors [2]. The “cancer immunoediting” hypothesis by Burnet and Thomas added the different mechanisms of tumor-immune escape to this theory [3]. The process of cancer immunoediting contains three phases in this hypothesis. The first phase is called “elimination” and refers to cancer immunosurveillance in which the cells of the immune system recognize and destroy developing tumors. The second phase “equilibrium” is a long period in which tumor and immune system enter into a dynamic equilibrium. The third phase is the “escape”, in which tumor variants emerge by an immune selection process from the “equilibrium” phase and develop into clinically apparent tumors growing in an immune-competent host [3]. Some tumor cells have the ability to manipulate the immune system by generating a tolerant microenvironment with immunosuppressive factors like Interleukin-10 and Vascular Endothelial Growth Factor (VEGF) [4]. Most cancer patients have an immune system, which is deficient or tolerant and unable to overcome tumor-induced immune-regulatory barriers [1]. Despite the discovery of numerous new therapeutic agents (like antibodies and vaccinations), there is still no entirely successful therapy, as cancer immunotherapy generally requires patients to be immune-competent. Therefore, breaking tumor-induced immunosuppression is one of the major obstacles in improving cancer immunotherapy. Promising target cells for this purpose are the professional antigen-presenting dendritic cells (DCs).

4.2 Dendritic cells and their role in tumor environment

Dendritic cells (DCs) are nature`s best antigen-presenting cells (APCs) expressing higher levels of antigen-presenting molecules than any other cell [5]. During steady state the majority of DCs are resting/ immature [6]. In response to environmental signals DCs can switch from immature antigen-processing cells to mature T cell stimulating cells [5]. Mature DCs have higher expression of antigen-presenting molecules (CD1a, MHC-I, MHC-II), co-stimulatory molecules (CD40, CD80, CD83, CD86) and are the source of many cytokines (IFN-α, IL-1, IL-6, IL-12) necessary for the development of primary immune responses [5][7][8][9]. Aberrant maturation of DCs is an indicator for tumor-mediated immunosuppression by tumor-derived factors (TDFs) like IL-6, IL-10 and GM-CSF [10][11][12]. Presentation of tumor antigens and priming of T cells is done by macropahges, B cells and most notably dendritic cells [4]. However, the immunosuppressive environment in which DCs most likely encounter tumor antigens induces and maintains T cell tolerance to tumor antigens [4]. DCs are the main innate immune cells directing the adaptive immune response. Mature DCs are providing not just the first and second signal for T cell activation, based on the direct interaction between MHC and TCR/CD3 complex (signal 1) and between CD80/CD86 and CD28 (signal 2), respectively, but also the third signal by providing the cytokine stimulus [13][14]. Therefore, activated DCs have the ability to initiate primary T cell-mediated immune responses. They also dictate the development of T cell-mediated immune responses into either type Th1 or Th2 [15][4]. The balance between activating and inhibitory pathways in DCs was proposed to play a crucial role in determining these divergent T cell outcomes [4]. A negative regulator of the Toll-like receptor (TLR) and tumor necrosis factor (TNF) receptor signalling pathways, the zinc-finger protein A20, was found to be a factor in controlling maturation, cytokine production and immune-stimulatory potency of dendritic cells [16].

4.3 A20 functions and effects on dendritic cells

A20, also called tumor necrosis factor alpha induced protein 3 (TNFAIP3), is a negative regulator of the NF-κB pathway. The transcription factor NF-κB is a key regulator of cellular growth and survival and its aberrant activation is characteristic in various diseases including cancer. With its dual ubiquitin-editing function, A20 leads to proteasomal degradation of the receptor-interacting protein 1 (RIP1), an essential mediator of TNF receptor 1 (TNFR1) signalling complex [17] [18] [19], the TNF receptor associated factor 6 (TRAF6) [18] [20], and the I-κB kinase (IKK) [18] [21]. Moreover, A20 was shown to adjust NF-κB and MAP Kinase signalling pathways as well as TNF-α-induced cell death by cooperation with the E3 ubiquitin ligases Itch and RNF11 and the adaptor proteins TAX1BP1 and ABIN-1 [17] [18] [22]. A20 is a transcriptional target of NF-κB itself and therefore a potent executor of a negative feedback loop mechanism leading to termination of NF-κB signalling [23] [24]. The important role of A20 has been clearly shown in A20 knock-out mice experiments. These mice fail to regulate TNF-α induced NF-κB as well as cell death responses and die prematurely because of severe inflammation and cachexia [18] [25] [26]. $A20^{fl/fl}$ CD11c-cre mice, with DC-specific loss of A20, develop normally, but they have an accumulation of DCs in the spleen combined with a derangement of splenic architecture. The A20 deficient DCs from these mice are hypersensitive to endotoxins, CpG motifs and TNF-α and are more potent in stimulating B cells [27]. Transient A20 knockdown in DCs enhances expression of co-stimulatory molecules, pro-inflammatory cytokines and therefore, allows murine DCs to hyperactivate CTLs and Th and inhibit Tregs. Infiltration of the tumor by lymphocytes is enhanced consequently. [28]. The inhibitory effects of A20-silenced DCs on Tregs may tip the balance from immune suppression to anti-tumor immunity [28]. However, DCs need to be fully mature to activate naive T cells and by this, generating an effective anti-tumor immune response. This can be achieved by several stimuli, for example inflammatory signals, CD40 cross-linking, and TLR ligands. The importance of TLR-mediated DC activation has been highlighted recently. [29]. It was demonstrated that tolerogenic mechanisms, impeding productive anti-tumor immune response, can be overcome by TLR activated DCs [30].

4.4 CpG ODNs in immunotherapy

The innate immune system can be activated by exposure to pathogen associated molecular patterns (PAMPs), which are expressed by a diverse group of microorganisms. The recognition of PAMPs is mediated by members of the Toll-like receptor (TLR) family. TLRs are ancient receptors that are highly conserved from *Drosophila* to humans and recognize molecular patterns specific to microbial antigens. Signalling through TLRs strongly activates DCs to upregulate co-stimulatory molecules (CD80, CD86) and to produce pro-inflammatory cytokines (TNF-α, IL-6, IL-12) [31]. The resulting antigen-specific immunity is characterized by the production of high-affinity antibodies and the generation of cytotoxic T cells. Bacterial DNA is a potent PAMP. Coley`s toxin is an early form of immunotherapy based on killed bacterial cultures (*Streptococcus pyogenes* and *Serratia marcescens*) designed in the 1890s to boost the immune system [32][33]. In contrast to eukaryotes, prokaryotes have unmethylated CpG motifs at a much higher frequency in the genome [34]. The innate immune system detects these unmethylated CpG motifs using TLR9 [35][36]. Synthetic oligonucleotides (ODNs), which contain CpG motifs that are similar to those found in bacterial DNA, are able to stimulate a strong TLR9-mediated immune response. CpG ODNs are rapidly internalized by immune cells, presumably involving phosphatidylinositol 3-kinases (PI3Ks), and they interact with TLR9 that is present in endocytic vesicles. This is a highly specific interaction. Cells that lack TLR9 do not respond to CpG DNA [35].

In humans, TLR9 is mainly expressed by B cells and plasmacytoid DCs (pDCs). Activation of these cells by CpG DNA initiates an immune-stimulatory cascade that culminates in the indirect maturation, differentiation and proliferation of natural killer (NK) cells, T cells and monocytes/ macrophages [35]. Together these cells secrete cytokines and chemokines creating a pro-inflammatory (IL-1, IL-6, IL-18, TNF) and Th1-biased (IFN-γ, IL-12) immune milieu [35]. In mice, immune cells of the myeloid lineage (including monocytes, macrophages and myeloid DCs) express TLR9 and respond to CpG stimulation.

The interactions between CpG-DNA and TLR9 connect innate and adaptive immunity by direct stimulation/activation of innate immune cells (DCs, MΦ, NK cells) which than in turn initiate adaptive immune responses (T and B cells). Due to their immune-stimulatory capacities, CpG ODNs are already used in several phase I/II studies to optimize immunotherapy approaches.

4.5 CpG ODNs as tool for targeted siRNA delivery

During the last years CpG research became a rapidly growing field in immunotherapy. There are already several CpG subtypes (CpG-A, -B, -C) showing specific stimulatory capacities and modifications for more stability and prolonged function. All CpG ODNs cross cell membranes via sequence-non-specific receptor-mediated endocytosis [37]. Cellular activation by TLR9 involves a signaling cascade through myeloid differentiation primary response gene 88 (MYD88), Interleukin-1 receptor-activated kinase (IRAK) and tumor-necrosis factor receptor-associated factor 6 (TRAF6) [38]. This cascade culminates in the activation of several transcription factors, including nuclear factor-κB (NF-κB), activating protein 1 (AP1), CCAAT/enhancer binding protein (CEBP) and cAMP-responsive element binding protein. These transcription factors directly upregulate cytokine and chemokine gene expression [37].

CpG has beside its stimulatory potential also the capability to transport coupled Oligonucleotides into TLR9 expressing cells. This has been described first by Kortylewski et al. [39]. CpG-siRNA molecules are actively internalized by TLR9+ cells without the need of transfection reagents. Recently it has been shown that TLR9 expression is not necessary for CpG-siRNA uptake, but obligatory for induction of siRNA-mediated gene silencing [40]. Shortly after cellular uptake, a dicer endonuclease in the early endosomes leads to uncoupled CpG and siRNA parts. The siRNA part of the conjugate translocates from the endosome to the endoplasmatic reticulum, where it interacts with the RNA interference machinery [40]. In an *in vitro* study with pooled mice splenocytes, it has been shown that FITC-labeled CpG-Stat3 siRNA were taken up by splenic DCs, MΦ, and B cells [39]. *In vivo* an internalisation has been observed by resident MΦ, DCs, and B cell in lymph nodes in tumor-free mice and by MΦ, DCs, and myeloid cells at injection site and in TDLN (tumor draining lymph nodes) in tumor-bearing mice [39].

Linking siRNA to CpG ODN offers a promising tool for targeted delivery in cytoplasm of TLR9 expressing cells and gene silencing *in vitro* and *in vivo*.

5 OBJECTIVE

The immune system of cancer patients is frequently not able to overcome tumor-induced suppression and to eliminate established tumors. Silencing the natural NF-κB inhibitor A20 in dendritic cells leads to an enhanced stimulatory capacity of these important antigen presenting cells. This switch from immune suppressive factors to immune effector functions could probably disrupt a tumor-induced immune tolerance. The dual role of CpG ODN in targeting and stimulating toll-like receptor 9-expressing DCs is a perfect tool for targeted siRNA delivery simultaneous to cell stimulation. Combination of these activities results in one synthetic molecule consisting of a CpG linked to a siRNA against A20. This molecule is as easy to apply, as it is effective. The construct enables a local, targeted and transient A20 knockdown in tumor associated cell types, especially in DCs, directly *in vivo.* The combined stimulation of two central factors of the immune system by these constructs builds up a great therapeutic potential. The dendritic cells as coordinating force of the immune system get targeted through the CpG. Next to the cell specific delivery the CpG stimulates one of the main activation drivers of immune cells, the NF-κB pathway, whose long lasting empowerment in turn is guaranteed by the siRNA. Construct-mediated NF-κB activation in DCs is leading to a multitude of activating and stimulating factors (illustrated in Fig. 1). The construct effects are assumed to culminate in activation of antigen presenting cells (DCs, Macrophages), antigen-specific cytotoxic T cells, and a strong Th1 response.

The major objectives of this study are to examine whether TLR9 mediated A20 silencing via the novel CpG-siRNA constructs is possible, and, if this knockdown acts synergistically to the CpG ODN induced cell stimulation. In healthy mice it will be studied whether these constructs can be utilized to stimulate immune cells directly *in vivo*. The final goal is to improve anti-tumor immune responses and to break tumor-induced immune suppression for prolongation of survival in a mouse tumor model.

An additional interesting question is the transferability of this approach from the murine to the human system. This interesting issue could give rise to future application possibilities in the clinics and will be tested by *in vitro* treatment of healthy donor DCs.

In summary, objective of this project is the validation of the innovative CpG-siRNA A20 constructs as immunotherapeutic reagent to improve cancer immunotherapy.

Figure 1: Illustration of assumed CpG-siA20 construct function

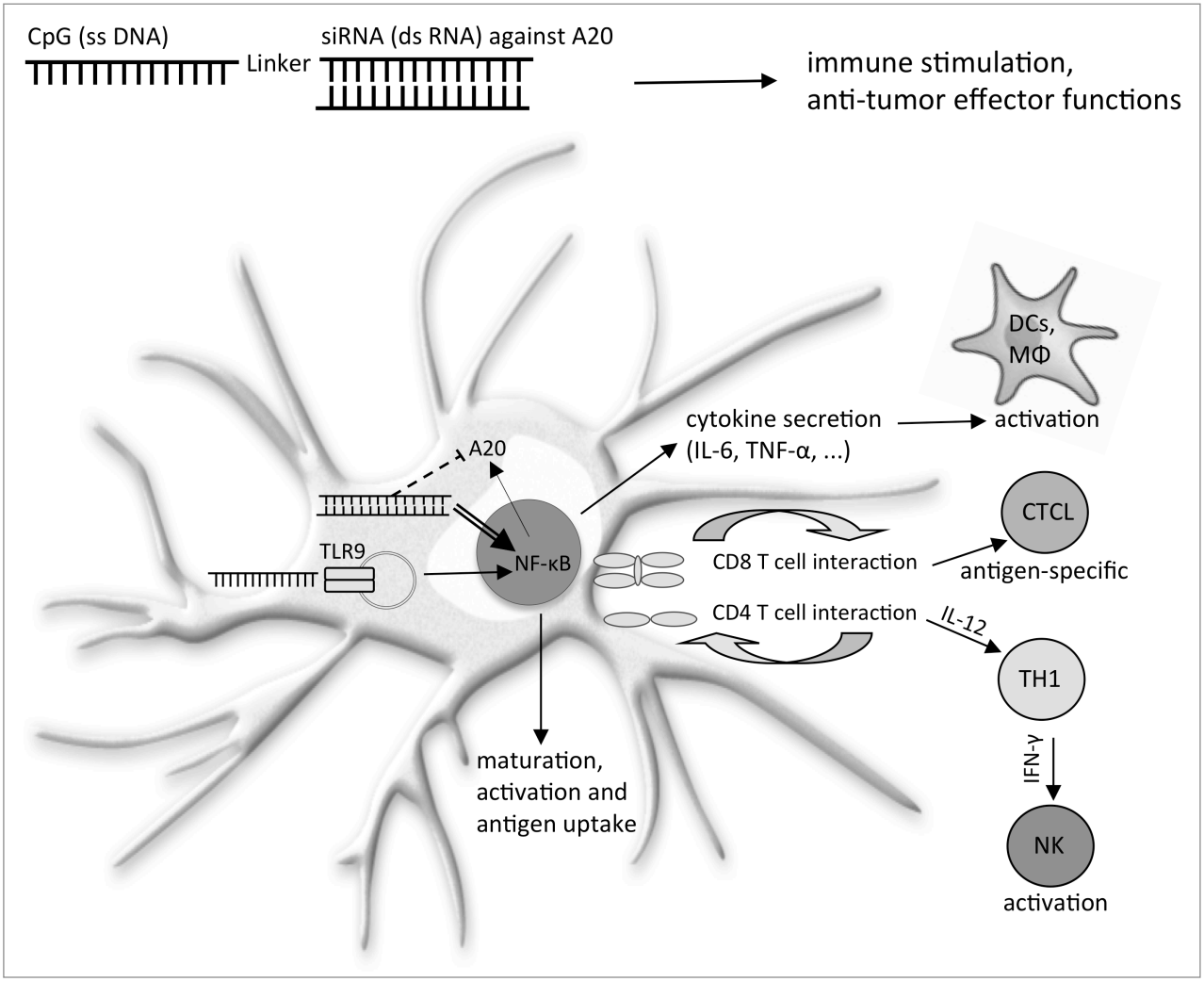

Figure 1: Illustration of assumed CpG-siA20 construct function. The CpG-siA20 construct consists of a single strand DNA oligodeoxynucleotide binding endosomal toll-like receptor 9 (TLR9) e.g. in dendritic cells (DCs) and a double strand siRNA against the natural NF-κB inhibitor A20. CpG interacting with TLR9 is leading to NF-κB activation and production of target genes like A20, which is than silenced by the siRNA part of the constructs. Construct uptake is leading to a powerful NF-κB activation and by this to a multitude of activating and stimulating factors. The construct effects culminate presumably in activation of antigen presenting cells (DCs, Macrophages), NK cells, antigen-specific CTLs, and a strong TH1 response.

6 MATERIALS AND METHODS

6.1 Materials

6.1.1 Cells, cell lines and mice

All cells and cell lines were cultured at 37 °C, 5% CO_2 and 90% humidity.

- Murine immature Dendritic cell line JAWSII (ATCC® CRL-11904™)
  Organism: Mus musculus, mouse
  Strain: C57BL/6
  Tissue: bone marrow
  Cell type: immature dendritic cell; monocyte
  Cells were maintained in MEMalpha medium with addition of 20% FCS,
  4 mM L-Glutamin, 1 mM Sodium Pyruvate, supplemented with 5 ng/ml recombinant murine GM-CSF before use.

- Murine melanoma cell line B16-F1 (92101203 Sigma)
  Organism: Mus musculus, mouse
  Strain: C57BL/6
  Tissue: skin
  Cell type: melanoma cells
  Cells were maintained in DMEM+GlutaMAX™-I with addition of 10% FCS and 0.2% Plasmocin.

- Bone marrow-derived murine Dendritic cells
  Organism: Mus musculus, mouse
  Strain: C57BL/6
  Tissue: bone marrow
  For generation protocol see methods section.

Cells were maintained in RPMI-1640 medium with addition of 10% FCS (inactivated, filtered), 1% MEM NEAA, 1% Sodium Pyruvate, and 0.2% Plasmocin, supplemented with 800 U/ml recombinant murine GM-CSF before use.

- For all in *vitro* and *in vivo* experiments C57BL/6N mice were used.
  Strain information: Developed by C.C. Little in 1921, from a mating of Miss Abby Lathrop's stock that also gave rise to strains C57BR and C57L.
  Strain code: 027
  Coat color: black
  MHC haplotype: H2b
  The mice were obtained from Charles River Laboratories. All *in vivo* experiments were performed in the Central Core & Research Facility of Laboratory Animals, University of Greifswald, Greifswald, Germany.

- Human DC analyses were performed with DCs isolated from whole blood of healthy donors provided by the blood donation unit of the University Medicine Greifswald (Greifswald, Germany).

Donor DCs	Blood group	Gender	Age
DC 1	A+	Male	35
DC 2	0+	Female	33
DC 3	AB+	Female	63
DC 4	AB+	Male	47
DC 5	0-	Male	53
DC 6	AB+	Female	32
DC 7	AB+	Female	23
DC 8	AB+	Male	47

  For isolation protocol see methods section.
  Cells were maintained in RPMI-1640 medium with addition of 10% FCS (inactivated, filtered), 1% MEM NEAA, 1% Sodium Pyruvate, and 0.2% Plasmocin, supplemented with 800 U/ml recombinant human GM-CSF and 50 U/ml recombinant human IL-4 before use.

6.1.2 Reagents for cell culture

Reagent	Source
RPMI 1640 (1x) + GlutaMAX™-I	Gibco® by Life Technologies™ (61870-010)
DMEM (1x) + GlutaMAX™-I	Gibco® by Life Technologies™ (31966-021)
Minimum Essential Medium Eagle Alpha Modification	Sigma-Aldrich (M8042)
GlutaMAX™-I (100x)	Gibco® by Life Technologies™ (35050-038)
Sodium Pyruvate 100mM (100x)	Gibco® by Life Technologies™ (11360-039)
MycoZap™ Prophylactic	Lonza (VZA-2031)
Recombinant Murine GM-CSF	PeproTech® (315-03)
Recombinant Human GM-CSF	PeproTech® (300-03)
Recombinant Human IL-4	PeproTech® (200-04)
0.5% Trypsin-EDTA (10x)	Gibco® by Life Technologies™ (15400-054)
PBS (without Ca^{2+}, Mg^{2+})	Biochrom/ Merck Millipore (L1825)
Aqua ad iniectabilia	Braun (2351744)

6.1.3 Reagents for human DC isolation

Reagent	Source
Leucosep™ (with separation medium)	Greiner bio-one (227 288)
RBC Lysis Solution	Qiagen (158904)
Blood Dendritic Cell Isolation Kit II, human	MACS Miltenyi Biotec (130-091-379)

6.1.4 CpG-ODN-siRNA constructs

The used constructs were synthesized and hybridized from Bio-Synthesis (Texas, USA) including quality check by MALDI-TOF mass spectrometry, HPLC and PAGE, quantity was proven by UV spectrophotometry.

Mouse:

Name	Description	Sequence
CpG1668	DNA	5`TsCsCsAsTsgsAsCsgsTsTsCsCsTsgsAsTsgsCsT 3`
CpG-siA20_5	RNA, sense	5` CCUCgAACUACACAggUAgCCUCAA 3`
	RNA, antisense	5`TsCsCsAsTsgsAsCsgsTsTsCsCsTsgsAsTsgsCsT-[3(CH2)]-UUgAggCUACCUgUgUAgUUCgAgg 3`
CpG-siA20_6	RNA, sense	5`gCACACUCggAAgCACCAUgUUUgA 3`
	RNA, antisense	5` TsCsCsAsTsgsAsCsgsTsTsCsCsTsgsAsTsgsCsT-[3(CH2)]-UCAAACAUggUgCUUCCgAgUgUgC 3`
CpG-scr	RNA, sense	5` UgUAUAUUggAACggCUggUgCgUC 3`
	RNA, antisense	5`TsCsCsAsTsgsAsCsgsTsTsCsCsTsgsAsTsgsCsT-[3(CH2)]-gACgCACCAgCCgUUCCAAUAUACA 3`

Human:

Name	Description	Sequence
CpG D19	DNA	5`gsgsTgCATCgATgCAggsgsgsgsg 3`
CpG-siA20_59	RNA, sense	5`CAAAgUUggAUgAAgCUAAtt 3`
	RNA, antisense	5`gsgsTgCATCgATgCAggsgsgsgsg-[3(CH2)]-UUAgCUUCAUCCAACUUUgcg 3`
CpG-siA20_60	RNA, sense	5`ggAUgUUACCAggACAUUUtt 3`
	RNA, antisense	5`gsgsTgCATCgATgCAggsgsgsgsg-[3(CH2)]-AAAUgUCCUggUAACAUCCtg 3`
CpG-scr	RNA, sense	5`CUAACgAgAgCAggUUCAUAA 3`
	RNA, antisense	5`gsgsTgCATCgATgCAggsgsgsgsg-[3(CH2)]-UUAUgAACCUgCUCUCgUUAg 3`

s= phosphorothionation, DNA = underlined
FITC-labeled constructs: FITC located at 3`end of RNA antisense strand

6.1.5 Reagents for flow cytometry analysis

Reagent	Source
FACSFlow Sheath Fluid	BD FACSFlow™ (342003)
FACS Clean Solution	BD FACS™ (340345)
FcR Blocking Reagent Mouse	MACS Miltenyi Biotec (130-092-575)
FcR Blocking Reagent Human	MACS Miltenyi Biotec (130-059-901)
Annexin V : PE Apoptosis Detection Kit I (Annexin V-PE, 7-AAD, and Annexin V Binding Buffer)	BD Pharmingen™ (559763)
Annexin V-APC	BD Pharmingen™ (550474)
Propidium iodide	Sigma-Aldrich (25535-16-4)
RNase	Sigma-Aldrich
FIX&PERM	Nordic MUbio (GAS-002A-1, -002B-1)
Perm/Wash Buffer	BD Biosciences (554723)

6.1.6 Antibodies for flow cytometry analysis

Name	Clone	Reactivity	Fluorescence	Company
CD80 (B7-1)	BB1	Human	FITC	BD Pharmingen™ (555683)
CD83 (HB15)	HB15e	Human	FITC	BD Pharmingen™ (556910)
CD86 (B7-2)	2331 (FUN-1)	Human	APC	BD Pharmingen™ (560956)
CD11c (ITGAX)	B-ly6	Human	FITC	BD Pharmingen™ (561355)
HLA-DR	G46-6	Human	APC	BD Pharmingen™ (560744)
TLR9	eB72-1665	Human	APC	BD Pharmingen™ (560428)
CD80	16-10A1	Mouse	FITC	Abcam (ab95550)
CD83	Michel-19	Mouse	APC	BD Pharmingen™ (558206)
CD86 (B7-2)	GL1	Mouse	APC	BD Pharmingen™ (558703)
CD11c	HL3	Mouse	APC	BD Pharmingen™ (550261)

CD11c	N418	Mouse	FITC	MACS Miltenyi Biotec (130-091-842)
CD11b	M1/70	Mouse, Human	PerCP	BioLegend (101229)
MHC Class II I-Ad	AMS-32.1	Mouse	APC	eBioscience (17-5323)
CD45R/ B220	RA3-6B2	Mouse	PerCP	BD Pharmingen™ (553093)
CD69	H1.2F3	Mouse	PerCP-Cy5.5	BD Pharmingen™ (551113)
NK-1.1	PK136	Mouse	PerCP-Cy5.5	BD Pharmingen™ (551114)
CD49b (Integrin alpha-2)	DX5	Mouse	APC	BD Pharmingen™ (560628)
CD3e	145-2C11	Mouse	PerCP	BD Pharmingen™ (553067)
CD4 (L3T4)	RM4-5	Mouse	APC	BD Pharmingen™ (553051)
CD4	GK1.5	Mouse	FITC	MACS Miltenyi Biotec (130-091-608)
CD8a (Ly-2)	53-6.7	Mouse	APC	BD Pharmingen™ (553035)
CD8	53-6.7	Mouse	FITC	MACS Miltenyi Biotec (130-102-806)
Foxp3	FJK-16s	Mouse, Rat	APC	eBioscience (17-5773)
CD25	PC61	Mouse	PerCP	BioLegend (102027)
CD19	6D5	Mouse	APC	LS Bio (LS-C43606/ 44237)
CD22	OX-96	Mouse	FITC	LS Bio (LS-C44385/ 44238)
IDO	-	Human, Mouse, …	Alexa Fluor 647	Bioss (bs-15493R-A647)
IFN- γ	XMG1.2	Mouse	PerCP/Cy5.5	Biolegend (505822)
H-2Kb/TRP-1 Multimer (TWHRYHLL)	222-229	Mouse	APC	TCMetrix

6.1.7 Reagents for confocal microscopy analyses

Reagent	Source
FIX&PERM® Kit	ADG Bio Research (GAS-002)
Paraformaldehyde (PFA) powder -> 2% Solution in sterile PBS	Sigma-Aldrich (P6148)
Hank's balanced salt solution (HBSS)	Gibco® Life Technologies (14025092)
NucBlue™ Live Cell Stain (Hoechst 33342 Special Formulation)	Life Technologies (R37605)
Hoechst 33342 nucleic acid stain	Life Technologies (H21492)
Oregon Green® 488 DHPE	Life Technologies (O-12650)

6.1.8 Reagents for cytokine analysis

Reagent	Source
EDTA (0.5 M, pH 8.0)	Ambion/ Applied Biosystems (AM9261)
Human Enhanced Sensitivity Flex Set for: TNF IFN-γ IL-2 IL-6 IL-12p70	BD™ Cytometric Bead Array (561521) (561516) (561515) (561517) (558276) (561518)
Mouse Inflammation Kit	BD™ Cytometric Bead Array (552364)
Mouse Enhanced Sensitivity Flex Set for: TNF IFN- γ IL-2 IL-4 IL-6 IL-10 IL-12p70	BD™ Cytometric Bead Array (562246) (562336) (562233) (562262) (562272) (562236) (562263) (562264)

6.1.9 Reagents for RNA isolation

Reagent	Source
TRIzol® Reagent	Life Technologies (15596-018)
QIAzol Lysis Reagent	Qiagen (79306)
Chlorophorm, stabilized (~0.75% ethanol)	J.T.Baker® (257-02)
2-Propanol (Isopropanol)	J.T.Baker® (9334-03)
Ethanol absolute -> for 75% solution dilution with A.dest	CHEMSOLUTE® (2273.1000)
DEPC water	Carl Roth® (T143.1)

6.1.10 Reagents for RT-qPCR

Reagent	Source
SuperScript™ II ReverseTranscriptase (supplied with 5x First Strand Buffer, 100 mM DTT)	Invitrogen (18080-044)
Random Primers	Promega (C1181)
dNTP Mix 100 mM	Applied Biosystems® (4303443)
Platinum SYBR Green qPCR SuperMix	Invitrogen/ Life Technologies (11733-038)

Primers for RT-qPCR were obtained from TIB MOLBIOL Laboratories.

Human:

Name	Length in bp	Sequence	orientation	T_M in °C
B2MG-f41-62	22	5`- CTCgCgCTACTCTCTCTTTCTg	forward	57.4
B2MG-r188	25	5`- AgTCAACTTCAATgTCggATggATg	reverse	60.5
TNFAIP3-fo	20	5`- CTgggACCATggCACAACTC	forward	60.0
TNFAIP3-re	20	5`- CggAAggTTCCATgggATTC	reverse	59.0

Mouse:

Name	Length in bp	Sequence	orientation	T_M in °C
mB2MGf	20	5`- AAgTATACTCACgCCACCCA	forward	54.9
mB2MGr	20	5`- AAgACCAgTCCTTgCTgAAg	reverse	54.2
mTNFAIP3-f-3	20	5`- CACTCggAAgCACCATgTTTg	forward	60.0
mTNFAIP3-r-3	20	5`- gCTTAggTgCTggCACTCCAT	reverse	60.7
mIL6-f-44	20	5`- TgggACTgATgCTggTgACA	forward	59.0
mIL6-r-254	22	5`- TCTgCAAgTgCATCATCgTTgT	reverse	59.4
mTNF-a-f-77	20	5`- ACTCCAggCggTgCCTATgT	forward	61.3
mTNF-a-r-326	20	5`- CTCAgCCACTCCAgCTgCTC	reverse	60.3
IkBa 2-for	20	5`- TggAgCACTTggTgACTTTg	forward	56.4
IkBa 2-rev	20	5`- TggAgATTTTCCAgggTCAg	reverse	55.6
mTLR9-3-F	20	5`- TCCATCTCCCAACATggTTC	forward	55.6
mTLR9-3-R	20	5`- gAAACggggTACAgACTTCA	reverse	54.2
mTRP1-1185-f	20	5`- AgCACTgAgggTggACCAAT	forward	58.8
mTRP1-1434-r	20	5`- CCgTTCCATTCAggAAgAgg	reverse	57.8

6.1.11 Reagents for protein isolation, detection

Reagent	Source
RIPA Lysis Buffer System: • 1X lysis buffer (pH 7.4 ±0.1) • PMSF in DMSO (200mM) • protease inhibitor cocktail in DMSO • sodium orthovanadate in water (100mM)	Santa Cruz Biotechnologie (sc-24948)
Phosphatase inhibitor cocktail B	Santa Cruz (sc-45045)
Micro BCA Protein Assay Reagent Kit (supplied with Albumin Standard Ampules, 2mg/mL)	Pierce Biotechnology (23235)

6.1.12 Reagents for Westen Blot

Reagent	Source
Western-Star™ Immunodetection System with Goat Anti-Mouse IgG AP conjugate (containing Blocker, Wash Buffer, Assay Buffer, Substrate)	Life Technologies (T1046)
Western-Star™ Immunodetection System with Goat Anti-Rabbit IgG AP conjugate (containing Blocker, Wash Buffer, Assay Buffer, Substrate)	Life Technologies (T1048)
Mini-PROTEAN TGX Stain Free Gradient Gel (4-15%) 10, 12, 15 well	BioRad (456-1081, **-1085,** -1086**)**
10x Tris/Glycine/SDS electrophoresis buffer	BioRad (161-0732)
Lane Marker Sample Buffer	Thermo Scientific (39000)
PageRuler Plus Prestained Protein Ladder	Thermo Scientific (26620)
PageRuler™ Plus Prestained Protein Ladder	Fermentas (SM1811)
10x Tris/Glycine electrophoresis buffer	BioRad (161-0734)
Methanol	J.T.Baker® (9093-02)

Antibodies	Company, origin, used dilutions, molecular weight
Actin (N-terminal)	Sigma-Aldrich (A2066), rabbit, polyclonal, 1:1500, 42 kDa
A20/TNFAIP3 (D13H3)	Cell Signaling (#5630), rabbit, monoclonal, 1:1000, 82 kDa
IkBa (L35A5)	Cell Signaling (#4814), mouse, monoclonal, 1:1000, 39 kDa
Phospho-IkBa (5A5)	Cell Signaling (#9246), mouse, monoclonal, 1:2000, 40 kDa
Goat Anti-Rabbit	2nd Antibody-AP goat anti-rabbit IgG, 1:3000
Goat Anti-Mouse	2nd Antibody-AP goat anti-mouse IgG, 1:3000

6.1.13 Consumable material

Consumables	Company
AHD 2000® desinfection	Lysoform (0128-6)
Hamilton Microliter®-Syringes, Model 7002 KH	Carl Roth (X058.1)
Micro-Fine™ Insulin syringe (29G)	BD (324827)
Plastipak™ syringe 1ml	BD (300013)
Discardit™ II syringe 20ml	BD (300296)
Microlance™ 3 Needles 18G, 26G, 27G	BD (301900, 303800, 302200)
Disposable scalpel	Pfm medical (02.001.30.011)
Polystyrene round-bottom tube	FALCON® Corning Brand (352052)
Cell Strainer 70µm Nylon	FALCON® Corning Brand (352350)
Filtropur S 0.45	Sarstedt (83.1826)
µ-Dish 35mm, low, ibiTreat	Ibidi GmbH
WillCo-Dish® glass bottom dish	WillCo (GWSt-5040)
Tissue culture dish 35x10mm	Sarstedt (83.1800)
6 Well Suspension Culture Multiwell Plate	Cellstar® Greiner bio-one (657185)
12 Well Suspension Culture Multiwell Plate	Cellstar® Greiner bio-one (665102)
24 Well Suspension Culture Multiwell Plate	Cellstar® Greiner bio-one (662102)
Cell Culture Flasks with Filter Cap 25cm^2	Cellstar® Greiner bio-one (690175)
Cell Culture Flasks with Filter Cap 75cm^2	Cellstar® Greiner bio-one (658175)
Peha-soft® nitrile fino	Hartmann (942197)
Polypropylene conical tube 50 ml	FALCON® Corning Brand (352070)
Polypropylene conical tube 15 ml	Sarstedt (62.554.502)
PS-Microplate, sterile, 96 W	Greiner bio-one (655161)
Roti®-PVDF 0.45	Carl Roth (T830.1)
Gel-Blotting-Papers, Whatman 3MM	Carl Roth (A126.1)
Safe-Lock Tubes 2.0 ml	Eppendorf (0030 120.094)
Serological pipette 10 ml	Sarstedt (86.1254.001)
Terralin® liquid desinfection	Schülke (23184-A)
Tube 1.5 ml, conical, screw-cap, DNase-, RNase-free	Biozym Scientific (710052)
Tube 0.5 ml, conical, screw-cap, DNase-, RNase-free	Biozym Scientific (710051)

SafeSeal Microcentrifuge Tubes 0.65 ml	Sorensen BioScience (11160)
SafeSeal-Tips® professional: 1000 µl 200 µl 100 µl 20 µl 10 µl	Biozym (770400) (770200) (770100) (770050) (770030)
MACS® Cell Separation Columns MS	MACS Miltenyi (130-042-201)
MACS® Cell Separation Columns LD	MACS Miltenyi (130-042-901)

6.1.14 Equipment and software

Device	Company
7500 Realtime PCR system, software v2.0.3	Applied Biosystems
Analytical balance, 210 g, 0.01 mg resolution	Sartorius
Analytical balance, Scout Pro 400g	OHAUS
Digital-Micrometer "PDM-501" (0-25mm, 0,001mm resolution, 5,5st.LCD-Anzeige)	MC Check
Ice system, AF 10	Scotsman
MiniMACS™, MidiMACS™ Separator	MACS Miltenyi Biotec
Molecular Imager®, ChemiDoc™ XRS+	BIO-RAD
Heating block, Thermomixer comfort	Eppendorf Research
Incubator, Hera Cell 150	Heraeus
Fluorescent cytometer FACSCalibur and software WinMDI 2.8	Becton Dickinson
Flowing Software (free flow cytometry data analysis software)	Project of Cell Imaging Core, Turku Centre for Biotechnology
Light microscope (473012-9901)	Zeiss
Fluorescence microscope IX70, Power Supply and Burner U-RFL-T	Olympus
Fluoview FV1000 LSM microscope, FV1200 ASW system software	Olympus
Confocal laser scanning microscope TCS SP5 II	Leica

Hybrisisation oven OV3	Biometra
Mono/Bi dest. processing plant, 2108	GFL
SenTix 97/T pH electrode	WTW
Bench pH/mV routine meter pH 538	WTW
Pipettes	Eppendorf Research
Pipettes	Gilson/Pipetman
Pipette filler, Pipetus®	Hirschmann
Plate photometer GENios, Magellan V3.11 software	TECAN
Shaker, PMS 1000	Grant Instruments
Safety cabinets, Hera safe	Heraeus
PowerPac™ HC (250 V, 3.0 A)	Bio-Rad
ThermalCycler C1000™	Bio-Rad
Thermocycler, GeneAmp 2400	Applied Biosystems
Vortex Mixer, neolab 7-2020	Neolab
Vortex Mixer, VF2	Janke & Kunkel
Western Blot Tank System, Mini Protean 3	Bio-Rad
Trans-Blot SD Cell (50W)	Bio-Rad
Neubauer cell counting chamber	Paul Marienfeld
Centrifuge 5415R	Eppendorf Research
Centrifuge, Megafuge 1.OR	Heraeus
Centrifuge, Varifuge 3.ORS	Heraeus
Waterbath W 22	Medingen
Cooling device (4°C, -20°C)	Kirsch/ Bosch
Hera freeze (-80°C)	Heraeus
SAS 9.3 XP_ProWindows NT Server Version	SAS Institute Inc.
GraphPad Prism (scientific graphing, statistics)	GraphPad Software

6.2 Methods

6.2.1 Cell culture

The murine immature DC cell line JAWSII (ATCC® CRL-11904™) was cultured in Complete Growth Medium (Alpha minimum essential medium with ribonucleosides, deoxyribonucleosides, 4mM L-glutamine, 1 mM sodium pyruvate, 20% FCS, and 0.5% MycoZap) supplemented with 5 ng/ml recombinant murine GM-CSF (PeproTech) at density of 1 x 10^6 cells/ ml in 25 cm^2 culture flasks (Greiner Bio-One). The cultures were fed every second day by removing adherent cells by Trypsine-EDTA 0,5% (Gibco®) treatment, pooling adherent and suspension cells, centrifugation (5 min, 300xg), resuspension of pelleted cells in fresh medium supplemented with GM-CSF, and placed in new culture flasks.

Mouse bone marrow-derived DCs (preparation protocol see below) were cultured in RPMI 1640 +Glutamax (Gibco®) supplemented with 10% FCS, 1% MEM NEAA (Gibco®), 1% Sodium pyruvate (Gibco®) and 0.5% MycoZap™ Proylactic (Lonza) and 800 U/ml recombinant murine GM-CSF (PeproTech).

Human DCs (isolation protocol see below) were cultured in RPMI 1640 +Glutamax (Gibco®) supplemented with 10% FCS, 1% MEM NEAA (Gibco®), 1% Sodium pyruvate (Gibco®) and 0.5% MycoZap™ Proylactic (Lonza) and 800 U/ml recombinant murine GM-CSF (PeproTech) and 50 U/ml recombinant human IL-4 (PeproTech) before use.

Murine melanoma cell line B16-F1 (Sigma-Aldrich) was cultured in DMEM (Gibco®) supplemented with 1% Glutamine (Gibco®), 1% MEM NEAA, 0.5% MycoZap™ Proylactic, 10% FCS. The cultures were fed every second day by removing the adherent cells using Trypsine-EDTA 0,5% treatment, seeding 1:2 to 1:5 in new culture flasks.

6.2.2 Generation of mouse bone marrow derived DCs (BMDCs)

After removing all muscle tissues from the femurs and tibias, mice bones were washed twice with sterile PBS, and transferred into a fresh dish with RPMI 1640 medium. Both ends of the bones were cut with scissors, and the marrow was flushed out using sterile RPMI 1640 with a syringe and 25-gauge needle. The marrow cells were suspended, passed through nylon mesh (70 µm Cell Strainer, BD 50 ml Falcon tube) to remove small pieces of bones, and red blood cells were lysed with RBC Lysis Solution (Qiagen). After washing, 1-2 x 10^6 cells were placed in 6-well plates (Greiner CELLSTAR® multiwell suspension culture plates with lid) in 2 ml of RPMI 1640 medium. After 1-2 hours the medium with all suspension cells were discarded and adherent cells remained on the plates with addition of 2 ml fresh RPMI 1640 medium supplemented with 800 U/ml GM-CSF and cultured at 37°C. The cultures were fed every 2-3 days by removing complete medium, centrifugation (5 min, 500xg), resuspension of pelleted cells in fresh medium supplemented with 800 U/ml GM-CSF, and placed back to the plates with the adherent cells. After 7 days DC grade reached more than 80%, after 14 days of this procedure the number of non-adherent granulocytes decreased remarkably. Adherent macrophages also expanded in these cultures, but most of them remained firmly attached to the culture dish. In this microenvironment cells can survive more than 300 days (no longer tested so far). By harvesting non-adherent and loosely adherent cells DC grades from about 80-90% can be reached. Further selection, for example positive selection with CD11c MicroBeads or negative selection with Anti-Ly-6G Microbeads, is possible at any point of culturing for getting pure DC suspensions.
For *in vitro* experiments mainly DCs from day 7 to day 14 were taken.

6.2.3 Isolation of human DCs from blood

Human DCs were isolated out of buffy-coats from healthy donors provided by the clinical blood donation centre Greifswald.
The buffy-coats were containing 60-75 ml blood, which was diluted 1:2 with PBS and portioned in four Leucosep^{TM} tubes for Ficoll separation.

After centrifugation (1000xg, 10 min) the interphase containing peripheral blood mononuclear cells (PBMCs) were collected and washed with 35 ml PBS (300xg, 5 min). To get rid of remaining red blood cells PBMC pellets were dissolved in 35 ml RBC lyses solution, incubated for 15 min at room temperature, centrifuged (300xg, 5 min) and washed with PBS (300xg, 5 min). With the obtained cells procedure of DC selection using “Blood Dendritic Cell Isolation Kit II” for human (MACS Miltenyi Biotec) was performed. Therefor cells were put through pre-separation filters (30 µm nylon mesh) to get a single cell suspension. Determination of cell numbers by Neubauer counting chambers was the bases for reagent and buffer volume calculations. Per 10^8 total cells 300 µl pre-cooled buffer (PBS 0.5 % BSA) was used for cell resuspension. FcR Blocking Reagent (100 µl per 10^8 cells) and Non-DC Depletion Cocktail (100 µl per 10^8 cells) were added, mixed and incubated for 15 min at 2-8°C. During incubation LD columns were placed in the magnetic field and prepared for separation with 2 ml buffer. Cells were washed with 5-10 ml buffer (300xg, 10 min), resuspended in buffer (500 µl for up to 1.25x10^8 cells) and applied onto the columns. The magnetic labeled Monocytes and B cells (CD14, CD19) were binding to the column in this selection step and the unlabeled cells containing DCs were collected. Washing twice with 1 ml buffer flushed all unlabeled cells into the collection tube. Cells were centrifuged (300xg, 10 min) and resuspended in 400 µl buffer before the second selection. Then DC Enrichment Cocktail was incubated for 15 min at 2-8°C and subsequently centrifuged (300xg, 10 min), resuspended in 400 µl buffer. During this procedure MS Columns were placed in the magnetic field and prepared with 500 µl buffer. By applying cell suspension onto column labeled DCs (CD304, CD1c, CD141) were bound and positively selected. Unlabeled cells were flushed through by washing three times with 500 µl buffer. The labeled cells were collected by removing column from the magnetic field on a suitable tube, addition of 500 µl buffer and immediately pushing plunger into the column.

The first enriched and then positively selected DCs were suspended in 24 ml RPMI1640 (+10% FCS, 1% NEAA, 1% Sodium pyruvate, 1ml MycoZap) with addition of human recombinant GM-CSF (100 U/ml), human recombinant IL-4 (50 U/ml) and placed in 24-well plates (1 ml/ well). Additional cytokine administration was performed 48 hours later.

72 hours after selection procedure the cells were taken for in vitro experiments testing effects of CpG-siRNA A20 constructs on cDNA and cytokine levels.

6.2.4 CpG-siRNA A20 treatment of mouse DCs *in vitro*

Model systems for the CpG/ CpG-siRNA construct experiments in mouse DCs *in vitro* were the immature murine dendritic cell line JAWSII (ATCC® CRL-11904™) and murine bone marrow derived dendritic cells (see methods section 6.2.2). BMDCs were taken from day 7 to day 14 of culturing.
Both cell types were cultured in 12-/24-well culture dishes. They were transferred in fresh medium 24 hours before the experiments started. CpG oligonucleotide and the CpG-siRNA constructs were added to the cells at concentrations of 0.5 nmol/ml or 1 nmol/ml diluted in DEPC water. After treatment cells were collected at several time points for RNA isolation/ cDNA analysis, protein isolation, and fluorometric analysis, supernatants were collected for cytokine analysis. DCs treated with FITC-labeled constructs additionally were taken for confocal microscopy.

6.2.5 CpG-siRNA A20 treatment of human DCs *in vitro*

For *in vitro* testing of human CpG-siRNA A20 constructs peripheral blood DCs were used. Blood from healthy donors were provided by the clinical blood donation centre Greifswald. Following PBMC isolation by Ficoll separation and RBC lysis, DCs were isolated by negative and positive bead selection (MACS Blood Dendritic Cell Isolation Kit II). For DC isolation protocol see method section 6.2.3.
DCs were treated with 1 nmol/ml of CpG/ CpG-siRNA constructs (A20 siRNA or scrambled siRNA). Cells were collected for RNA and FACS analyses at several time points starting at 1 hour after treatment until 18 hours; supernatants were taken for cytokine analysis. The DCs were checked for maturation stage and percentage of construct internalization (FITC-labeled constructs).

6.2.6 CpG-siRNA A20 treatment in healthy mice *in vivo*

Mouse care and experimental procedures were performed under specific pathogen free conditions in accordance with established institutional guidance and approved protocols from the animal facility of the Central Core & Research Facility of Laboratory Animals, University of Greifswald. All treatments were performed under Sevofluran anesthesia, and all efforts were made to minimize suffering. The *in vivo* experiments in healthy mice were performed in C57BL/6N wild type mice (8-12 weeks old, female) obtained from the Central Core & Research Facility of Laboratory Animals, University of Greifswald.
The mice were divided into groups of 4 to 6 animals. They were treated intra peritoneal (i.p.) with 1 nmol CpG/ CpG-siRNA constructs (against A20 or scrambled) in 200 µl volume using 1 ml Micro-FineTM Insulin syringes or PlastipakTM syringe (29G). As a non-treated control mice of one group were injected with sterile PBS of the same volume.
The application plan differed in number and interval of treatment. During the experiments blood were collected every second day from mice tail to analyze cytokine levels. At the end of the experiment mice were sacrificed with CO_2 inhalation. To analyze direct effects on cells in the peritoneal cavity a peritoneal lavage was performed and the cells analyzed by fluorometric analyses. Whole blood was collected by heart puncture and the immune cell populations were determined. Spleen and lymph nodes were also analyzed for amount and status of immune cell populations.

6.2.7 CpG-siRNA A20 treatment in mouse tumor model *in vivo*

Mouse care and experimental procedures were performed under specific pathogen free conditions in accordance with established institutional guidance and approved protocols from the animal facility of the Central Core & Research Facility of Laboratory Animals, University of Greifswald. All treatments were performed under Sevofluran anesthesia, and all efforts were made to minimize suffering. The *in vivo* experiments in mouse tumor model were performed in C57BL/6N wild type mice (8 weeks old, female) obtained from Charles River Laboratories. The mice were divided into groups of 6 animals.

For tumor treatment experiments B16-F1 melanoma cells (Sigma-Aldrich) were cultured. Directly before experiment start the cells were harvested using Trypsin/EDTA, washed and dissolved in cold PBS.

Before experiment start blood was collected (retro-orbital) for determining the neutral point of cytokine and cellular status. At the right side of the waist a small area was prepared by removal of hair. In this region 1x10^6 B16 melanoma cells in 100 µl volume were injected subcutaneously (s.c.) using 1 ml Micro-FineTM Insulin syringes or PlastipakTM syringe (29G).

The mice were checked daily for physical conditions, body weight, and tumor development. From day 4 tumors reached a measurable size, which was checked with a digital outside micrometer in diameter. The starting point for tumor treatment differs in the performed experiments between day 4 and day 7. The mice were treated peritumorally with 1 nmol or 2 nmol CpG/ CpG-siRNA constructs (against A20 or scrambled) in 5 µl volume using Hamilton Microliter®-Syringes. As a non-treated control, mice of one group were injected with sterile PBS of the same volume. Treatment was repeated daily for 7 days. Mice were sacrificed with CO_2 inhalation when the tumor reached 1 cm in diameter or the mice developed critical physical conditions.

During the whole time of the experiment small amounts of blood were collected from the tail for cytokine analyses every second day. At the individual endpoint of experiment (day 10 to day 18) mice were sacrificed with CO_2 inhalation. Whole blood was collected by heart puncture to determine differences in immune cell populations. Spleen and tumor draining lymph node were dissected and the cells analyzed for amount and status of immune cell populations. Tumors were analyzed for weight, apoptotic cells, cell cycle and infiltrating immune cell populations.

The *in vivo* tumor model experiments using the amount of 2 nmol CpG/ CpG-constructs were performed in collaboration with Sören Thomas (Master student).

All mouse *in vivo* experiments were done in cooperation with Dr. Jens van den Brandt (ZSFV, University Greifswald).

6.2.8 Processing of mouse material for analyses

During the *in vivo* experiments blood were collected every second day from mice tail to analyze cytokine levels. The blood (10 drops) was collected in tubes containing EDTA (0.5 M). Cells were removed from plasma by centrifugation (2,000xg, 10 min). The plasma was collected and stored at -80°C for cytokine analysis (see method section 6.2.20).
In healthy mice *in vivo* experiments constructs were applied intra peritoneal (i.p.). To analyze direct effects on cells in the peritoneal cavity a peritoneal lavage was performed. Using a 2 ml syringe and 27G needles sterile filtered PBS (0.5 % BSA) was injected for collecting all cells in the peritoneum. Peritoneal cells were washed with PBS twice (5 min, 300xg) and prepared for cytofluorometric analyses.
In tumor model mice experiments the animals were sacrificed (CO_2 inhalation) at the individual end of *in vivo* experiment determined by tumor size and/or physical condition. Whole blood was collected by heart puncture using Micro-Fine^{TM} Insulin syringe (29G). The blood was collected in tubes containing EDTA (0.5 M). Blood cells were prepared for cytofluorometric analyses by RBC lysis and washing with PBS twice (5 min, 300xg).
In tumor model experiments spleen, lymph node, and tumors were removed from mice as well. The organs were prepared for cytofluorometric analyses by separation through a nylon mesh (70 µm Cell Strainer). In case of spleen an RBC lysis was done. All samples were washed with PBS twice (5 min, 300xg).
For all *in vivo* samples the cell number was determined using Neubauer cell counting chamber.

6.2.9 Measurement of tumor size

In the mouse tumor model experiments, tumor size was checked every day. Starting from day 3 to 4 after injection of 1x10^6 B16 melanoma cells the tumor reached measurable size. Tumor size was measured with a digital outside micrometer in diameter.

6.2.10 RNA isolation

TRIzol RNA isolation method was used for total RNA extraction.

Homogenization for cells grown in monolayer:

After removing culture medium cell monolayer was washed with PBS once. By adding 1 ml of TRIzol Reagent per 3.5 cm diameter dish cells were directly lysed in the culture dish. The cell lysate was passed several times through a pipette, collected in a 1.5 ml tube and vortexed thoroughly.

Homogenization for cells grown in suspension:

The cells were collected and centrifuged (5 min, 300xg) for removing media. Pelleted cells were washed with PBS once (5 min, 300xg). The cells were lysed with 1 ml of TRIzol Reagent per 5-10x10^6 cells by repetitive pipetting and vortexed thoroughly.

The homogenized samples were incubated for 5 minutes at room temperature to permit the complete dissociation of nucleoprotein complexes. Till the RNA extraction samples were stored at -20°C.

Phase separation:

The samples were defreezed at room temperature for proceeding with RNA isolation. Per 1 ml of TRIZOL Reagent 0.2 ml of chloroform were added. After vigorously shaking for 15 seconds the samples were incubated at room temperature for 2 to 3 minutes. Following centrifugation (12,000xg, 10 min, 4°C), the mixture separated into lower red (phenol-chloroform phase) an interphase, and a colorless upper aqueous phase. The RNA containing aqueous phase was transferred carefully without disturbing the interphase into fresh tube.

RNA precipitation:

To precipitate the RNA from the aqueous phase 0.5 ml of isopropyl alcohol was added and mixed. The samples were incubated at room temperature for 10 minutes and centrifuge (12,000xg, 10 min, 4°C). The RNA precipitate formed a gel-like pellet on the side and bottom of the tube.

RNA washing:

Following complete removing of the supernatant the RNA pellet was washed once with 75% ethanol. The samples were mixed until the pellet detached. After centrifugation (7,500xg, 5 min, 4°C) all leftover ethanol was removed.

Dissolving RNA:

The RNA pellet was air-dried for 5-10 minutes and dissolved in 15 µl DEPC-treated water by passing solution a few times through a pipette tip.

6.2.11 cDNA synthesis

cDNA synthesis was performed using SuperScriptTM II RT (Invitrogen).

For each reaction the following components were combined:

Component	Amount
dNTP Mix 100 mM	0.5 µl
Random Primer	0.5 µl

This Master-Mix was added to 5.5 µl RNA sample and incubated for 5 min at 65°C in a Thermo-Cycler, then put on ice.

In a separate tube the second Master-Mix was prepared with the following components for each reaction:

Component	Amount
5x Buffer	2.0 µl
DTT 100 mM	1.0 µl
SuperScriptTM II RT	0.5 µl

After addition of these 3.5 µl per the samples were placed back in the Cycler running the following program:

25°C 2 min -> 25°C 15 min -> 42°C 50 min -> 70°C 15 min -> 4°C ∞

The reaction product was diluted 1:10 with distilled water and stored at -20°C.

6.2.12 Real-time RT-qPCR analysis

Quantification of mRNA expression was analyzed by real-time quantitative PCR with Platinum SYBR Green qPCR SuperMix (Invitrogen).
For each reaction the following components were used:

Component	Amount
A.dest.	9.5 µl
Platinum SYBR Green Mix	12.5 µl
Primer forward 10 µM	0.5 µl
Primer reverse 10 µM	0.5 µl
Sample cDNA	2.0 µl

Using 7500 Realtime PCR System (Applied Biosystems) the cDNA was amplified with the following program: 50°C 2 min -> 95°C 10 min -> 40 Cycles (95°C 15 sec -> 64°C* 1 min)
*temperature depending on melting temperature of used primers
The obtained data were calculated by ΔΔCT method. The housekeeping gene ß2MG was used as a reference gene for normalization. Genes of interest were for example A20, IκBa, IL-6, TNF-α (complete list see material section 6.1.10).

6.2.13 Protein isolation

The cells for protein isolation were collected and washed twice with PBS (500xg, 10 min). The supernatant was removed completely. Cells were lysed in RIPA lysis buffer (Santa Cruz). To prepare complete RIPA 10 µl PMSF solution, 10 µl sodium orthovanadate solution, 10 µl protease inhibitor cocktail solution, and 10 µl phosphatase inhibitor cocktail solution per 1 ml of 1xRIPA Lysis buffer were added directly before applying to cells. The used volume RIPA was dependent on cell pellet size. During incubation on ice samples were mixed by thoroughly repetitive vortexing. After 30 to 45 minutes the resulting mixture was centrifuged at 15,000xg for 15 min at 4°C. This separated the total protein in the supernatant from the cellular debris in the pellet. The supernatant was transferred to a new tube for further analysis and was stored at -80°C.

6.2.14 Protein detection

The quantitation of total protein was performed using the Micro BCA Protein Assay Reagent Kit (Pierce Biotechnology).

Preparation of diluted albumin (BSA) standards:

The albumin stock solution (2 mg/ml) was diluted with A.dest to get the top standard concentration of 80 µg/ml. A serial dilution with A.dest was added in three replicates on the 96 well PS-Microplate (Greiner bio-one).

Preparation of diluted samples:

For each protein sample three dilutions were prepared (1:250, 1:500, 1:1,000). The samples were added in three replicates to the 96-well-plate.

Sample/ standard distribution on the 96-well-plate:

	1	2	3	4	5	6	7	8	9	10	11	12
A	standard 80 µg/ml			sample 1 1:250			sample 1 1:500			sample 1 1:1000		
B	standard 40 µg/ml			sample 2 1:250			sample 2 1:500			sample 2 1:1000		
C	standard 20 µg/ml			sample 3 1:250			sample 3 1:500			sample 3 1:1000		
D	standard 10 µg/ml			sample 4 1:250			sample 4 1:500			sample 4 1:1000		
E	standard 5 µg/ml			sample 5 1:250			sample 5 1:500			sample 5 1:1000		
F	standard 2,5 µg/ml			sample 6 1:250			sample 6 1:500			sample 6 1:1000		
G	standard 1,25 µg/ml			sample 7 1:250			sample 7 1:500			sample 7 1:1000		
H	A. dest.			sample 8 1:250			sample 8 1:500			sample 8 1:1000		

Preparation of Micro BCA Working Reagent:

For a complete 96-well-plate 5 ml MA, 4.8 ml MB, and 0.2 ml MC were mixed. 100 µl of this mixture were added per well.

The plates were covered using sealing tape and incubated at 37°C for 2 hours protected from light, gently shaking, in the hybridization oven.

After cool down at room temperature the absorbance at 562nm was measured in the GENios plate photometer (Tecan). For determination of protein concentration in the samples a standard curve was prepared by plotting the average Blank-corrected 562nm reading for each BSA standard vs. its concentration in µg/mL (Magellan Software V3.11).

6.2.15 Western Blot analysis

Protein separation:

For Western Blot analyses 25 µg protein/ sample/ lane were prepared with 4 µl sample buffer (Thermo Scientific) and Aqua dest. ad 16 µl. Equal protein amounts were separated by SDS-PAGE. BioRad Mini-PROTEAN TGX Stain Free Gradient Gels (4-15%) with 10, 12 or 15 wells, depending on sample number, were used. To determine protein size a prestained protein ladder (Thermo Scientific/ Fermentas) was added to one lane on the gel. The separation was performed in 1x Tris/Glycine/SDS buffer (BioRad) using Western Blot Tank System Mini Protean 3 and PowerPacTM HC with 250 V.

Protein transfer:

For protein transfer from gel to PVDF membrane gels were washed for 15 min in 1x Tris/Glycine buffer with methanol. Membranes were prepared for transfer by 2 min incubation in methanol followed by 15 min in 1x Tris/Glycine buffer with methanol. The transfer was performed by semi-dry blotting method using Trans-Blot SD Cell (BioRad) and PowerPacTM HC. The transfer was complete after 30 min at 0.25 A per gel. Equal protein transfer was proven by Ponceau staining.

The protein-specific detection was performed with the Western-SuperStar™ Immunodetection System (Applied Biosystems). To reduce unspecific binding the blot was incubated with Western-SuperStar Blocker for 1 hour at room temperature and mild shaking. The primary antibody was diluted in Western-SuperStar Blocker (antibody dilutions see material section 6.1.12). Depending on antibody company recommendation incubations were performed on a shaker for 1 hour at room temperature or over night at 4°C. After washing for 5 minutes in 1X Wash Buffer twice the blot was incubated with the secondary antibody diluted in Western-SuperStar Blocker. Following 1 hour incubation the blot was washed for 5 minutes in 1X Wash Buffer twice and for 2 minutes in 1X Assay Buffer twice.

Chemiluminescent detection:

The blot was placed on a development folder and incubated with SuperStar Substrate for 5 minutes at room temperature protected from light. After draining the blot from excessing substrate the blot was ready for imaging using the Molecular Imager®, ChemiDocTM XRS+ (BioRad).

6.2.16 Fluorescence microscopy

For confocal microscopy, cells were cultured on glass bottom dishes (WillCo-Dish GWSt-5040), fixed using 2% paraformaldehyde, washed, and mounted in Hank's balanced salt solution (HBSS). Cellular staining was performed using Nuc Blue Live Cell Stain (ex 405) for the nucleus and Oregon Green 488 DHPE (ex 448) for the membrane. Internalisation of CpG-siRNA constructs was analyzed by FITC-labeled constructs (ex 494). For confocal microscopy Leica TCS SP5 II Confocal Laser Scanning Microscope with HCX PL APO 63X 1.2 N/A water immersion objective and Olympus Fluoview FV1000 LSM with UPLSAPO 60X 1.2 N/A water immersion objective were used. For postacquisition analysis and preparation of pictures FV1200 ASW system software and ImageJ 1.47v software were used. All confocal microscopy was done in corporation with Dr. Raghavendra Palankar (ZIK-HIKE, University Medicine Greifswald).

6.2.17 Cytofluorometric analysis

All cytofluorometric analyses were performed using the fluorescent cytometer FACSCalibur and the software WinMDI 2.8, Flowing.
The fluorescent cytometer was used for cell characterization of mouse *in vivo* samples. For antibody-staining cells were incubated for 15 minutes at room temperature protected from light, washed with PBS twice and dissolved in FACSFlow for measurement.
Additionally, fluorescent cytometer was used for mouse and human DC surface marker identification. Bone marrow-derived mouse DCs (BMDCs) as well as human DCs isolated from blood were characterized using a panel of surface marker antibodies (listed in material section 6.1.6).
Another cytometer application was the quantification of CpG-siRNA A20 construct uptake. Therefor FITC-labeled constructs were used. The percentage of FITC-positive cells was determined in comparison to non-treated control cells.
Further methods with FACS utilization were Multimer-staining (see 6.2.18), Annexin V/ 7-AAD staining, cell cycle analysis (see 6.2.19), and cytokine detection via CBA (see 6.2.20).

6.2.18 Analysis of tumor-specific immune response

For mouse *in vivo* tumor experiments B16 melanoma cell were used. These tumor cells express the known tumor antigen Trp-1. To determine a tumor-specific immune response Trp-1 specific CTLs in mouse blood and inside the tumor were detected. Mouse PBMCs were isolated using Ficoll cell separation. After RBC lysis and PBS washing twice cells were stained first with H-2Kb/TRP-1 Multimer (TWHRYHLL Multimer 210015.50.APC, TCMetrix, Switzerland) and then with anti-CD8 (FITC Rat-Anti-Mouse CD80, BD Pharmingen^{TM}). Afterwards cells were fixed and permeabilized (FIX&PERM; Nordic MUbio, Susteren, Netherlands) and stained with IFN-γ antibody (PerCP/Cy5.5 anti-mouse IFN-γ, Biolegend) for intracellular IFN-γ staining as indicator of cellular activation. The fluorescence was measured using BD FACSCalibur flow cytometer. The proportion of double positive cells was analyzed with WinMDI 2.8 and Flowing software.

6.2.19 Apoptosis and cell cycle analysis

Annexin V/ 7-AAD staining was used to analyze apoptosis rate of tumor cells.
For detection of early and late apoptosis the tumor cells were suspended in a 50 µl Annexin V binding buffer containing 2.5 µL of Annexin V-APC and 2.5 µl of 7-AAD, and incubated for 15 minutes at room temperature in the dark. The fluorescence was measured using a BD FACSCalibur flow cytometer. The percentage of early apoptotic (7-AAD positive) and late apoptotic (7-AAD and Annexin V positive) cells was analyzed with WinMDI 2.8 software.
Cell cycle analysis was performed using the DNA intercalating fluorescent molecule Propidium iodide. Isolated and fixed cells (1% paraformaldehyde) were permeabilized (Perm solution, Nordic MUbio) and incubated in a mixture of 300 µl PBS, 6 µl RNAse and 6 µl Propidium iodide per sample. After 30 min incubation at room temperature in the dark the samples were ready for measurement at a BD FACSCalibur flow cytometer. The %age of cell in G0-/G1-, S- and G2-/M-phase was analyzed with WinMDI 2.8 and Flowing software.

6.2.20 Cytokine analysis

For detection of released cytokines *in vitro* (in cell culture medium) and *in vivo* (in mouse serum) Cytometric Bead Arrays (CBA Mouse Enhanced Sensitivity Flex Set, Human Enhanced Sensitivity Flex Set) were used. In mouse material the cytokines IL-6, IL-10, IL-12p70, IL-17, MCP-1, IFN-μ, TNF-α and in human material IL-2, IL-6, IL-12p70, IFN-μ, TNF were analyzed.

The procedure was performed like described in the kit manual.

1. Preparing standards (fresh for each experiment!)
2. Mixing capture beads for all cytokines
3. Preparing detection reagents A and B (storing at 4°C, protected from light)
4. Performing the assay:

The mixed capture beads (20 µl) were added to the standard dilutions and each unknown sample (50 µl) and incubated for at least 2 hours at room temperature. After addition of the detection reagent A (20 µl) to all assay tubes, the tubes were mixed gently and incubate for 2 hours at room temperature, protected from light. Following this incubation step the samples were washed with 1 ml buffer (200xg, 5 min), the supernatant was discarded and the detection reagent B (100 µl) was added to each assay tube. After incubate for 1 hour at room temperature, protected from light, the samples were washed with 1 ml buffer (200xg, 5 min). The supernatant was discarded and the tubes were prepared for measurement with 300 µl buffer.

5. Performing instrument setup with Cytometer Setup Beads
6. Acquiring samples using a BD FACSCalibur flow cytometer
7. Data analysis with WinMDI 2.8 and Flowing software

Quantitative cytokine amounts in fg/ml or pg/ml were calculated by cytokine standards using Microsoft Office Excel software.

6.2.21 Statistical analyses

For RT-qPCR and CBA data analyses mean values of technical replicates (measured three times in duplicate) and mean values of biological replicates (number of mice per group) were used, respectively. In addition to the experiment kinetics, the mean values of all time points were integrated by calculating the area under curves (AUC) defined by individual time points. Statistical analyses were performed by applying the Kruskal–Wallis one-way analysis of variance by ranks (non-parametric method) and the Wilcoxon rank-sum test (also called Mann-Whitney U test) using SAS 9.3 (Institute for Biometry and Informatics, University Greifswald) or GraphPad Prism software; n.s. indicates not significant, * indicates $p<0.05$, ** indicates $p<0.01$, and *** indicates $p<0.001$.
The statistical analyses were done in the Institute for Biometry and Informatics, (University Greifswald) with the support of Dr. Bernd Jäger.

7 RESULTS

7.1 Generation of a long-term growth factor dependent mouse DC line

Dendritic cells are very potent antigen presenting cells, which are relevant players in anti-tumor immune response. Murine DC *in vitro* systems were needed for testing CpG-siRNA construct internalization, A20 knockdown efficiency and stimulatory effects on DCs. Beside the immature DC line JAWSII a culture system that ideally mimic physiology of naturally occurring DCs was wanted. The most commonly used DC sources are spleen [40] and blood [41], which, however, only provide limited amounts of cells (e.g. myeloid DCs, represent less than 1% of all peripheral blood mononuclear cells [42]). Moreover, the life span of such cultures is limited as DCs are terminally differentiated and cannot divide. An alternative source of DCs widely used in mouse model studies is bone marrow (BM). BM progenitor cells treated *in vitro* with GM-CSF differentiate into so called Bone Marrow-derived Dendritic Cells (BMDCs) which phenotype resembles the naturally occurring DCs [43][44]. This method provides large quantities of DCs, but requires repetitive sacrifice of mice. To avoid this, a long-term growth factor-dependent DC culture from BM progenitor cells was established (Fig. 2).

Figure 2: Bone marrow-derived DC

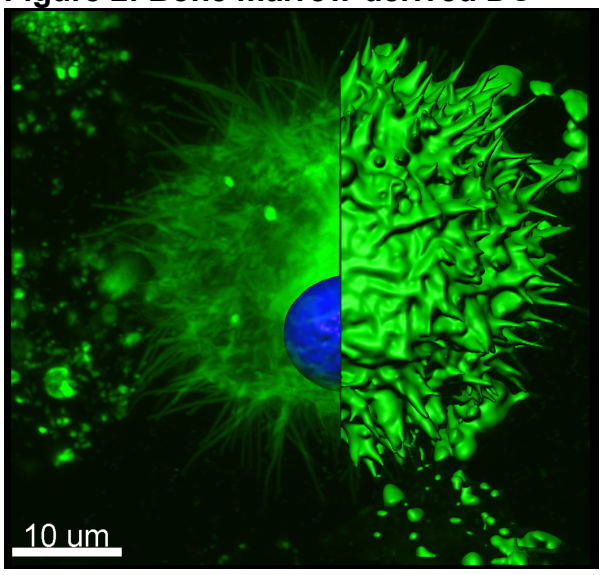

Figure 2: Bone marrow-derived DC. Murine DCs for *in vitro* analyses were generated out of bone marrow cells cultured in presence of GM-CSF. Confocal image showing a BMDC from day 14 of culturing, Nucleus stained with Nuc Blue Live Cell Stain (ex 405), Membrane stained with Oregon Green 488 DHPE (ex 448), using Olympus Fluoview FV1000 LSM microscope, FV1200 ASW system software.

Throughout the entire culturing period, DC-specific surface marker expression was frequently checked by cytofluorometric analysis. CD11c and B220 positive cells increased persistently as well as MHC class II positive cells. After 10 days, more than 80% of the cells expressing these marker maintained high levels between 80 and 95% for the rest of culturing time (more than 1 year). The amount of CD80 and CD86 positive cells did not increase over 20% until day 22. From day 22 onwards, expression stabilized between 70 and 90% (Fig. 3).

Figure 3: Long-term BMDC culture surface marker

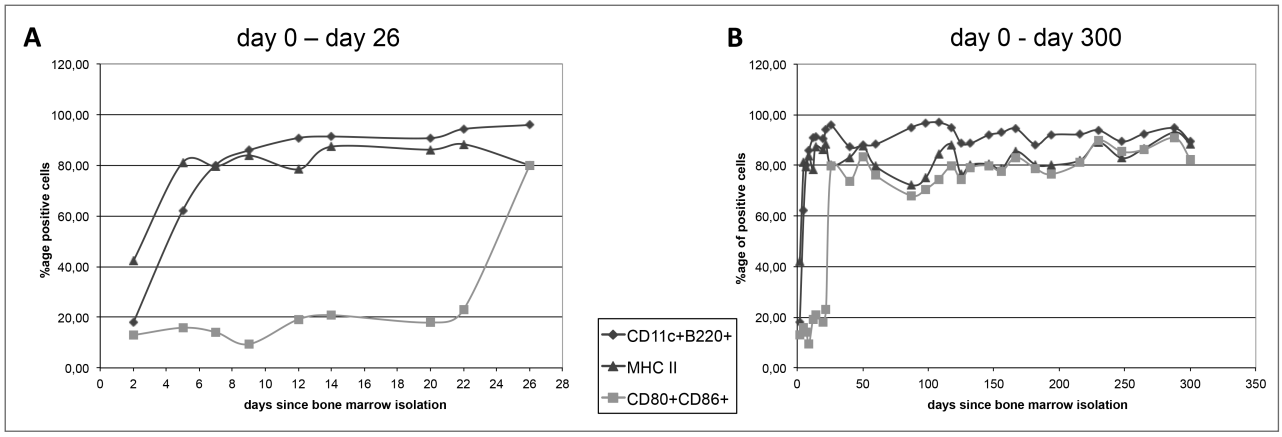

Figure 3: Long-term BMDC culture surface marker. Murine DCs for *in vitro* analyses were generated out of bone marrow cells cultured in presence of GM-CSF. Diagrams showing a selection of characteristical DC surface marker (CD11c, B220, CD80, CD86, and MHC class II). **(A)** Shown are surface marker expression in % from bone-marrow preparation (day 0) until day 26; **(B)** Shown are surface marker expression in % from day 0 until day 300. Cells has been analyzed by FACS Calibur and Win MDI software.

The long-term culturing for more than one year was possible due to the specific environment formed by heterogeneous DCs and "contaminating" cells like monocytes/macrophages and progenitor cells. These cells could be easily selected due to their strong adherence or by sorting. The long term BMDC culture demonstrates a great *in vitro* system by saving time and especially the life of many mice.

Enriched BMDCs were the basis for the *in vitro* testing of CpG-siRNA construct mediated A20 knockdown.

7.2 A20 knockdown in mouse DCs *in vitro*

BMDCs were the basis for all DC *in vitro* experiments. The first question concerning CpG-siRNA function was whether the siRNA is taken up by the BMDCs. For testing the construct internalization confocal microscopy and fluorescence labelled CpG-siRNA constructs were used. The cells were treated with 1 nmol CpG-siA20-FITC or CpG-scr-FITC constructs and incubated for up to 24 hours. After several time points (0, 1, 2, 3, 4, 5, 6, 8, 10, 12, 18, 24 hours) cells were collected, washed, and fixed with PFA. Just before imaging, cells were stained with Nuc Blue to visualize the nucleus. Confocal imaging was performed using a Leica confocal laser scanning microscope TCS SP5 II.

Cellular uptake by BMDCs *in vitro* could be confirmed already 1 hour after FITC–labelled constructs were added to the cells (Fig. 4). There were no considerable differences in CpG-siA20 and CpG-scr construct uptake (data not shown).

Figure 4: Cellular uptake of CpG-siRNA constructs - Confocal images

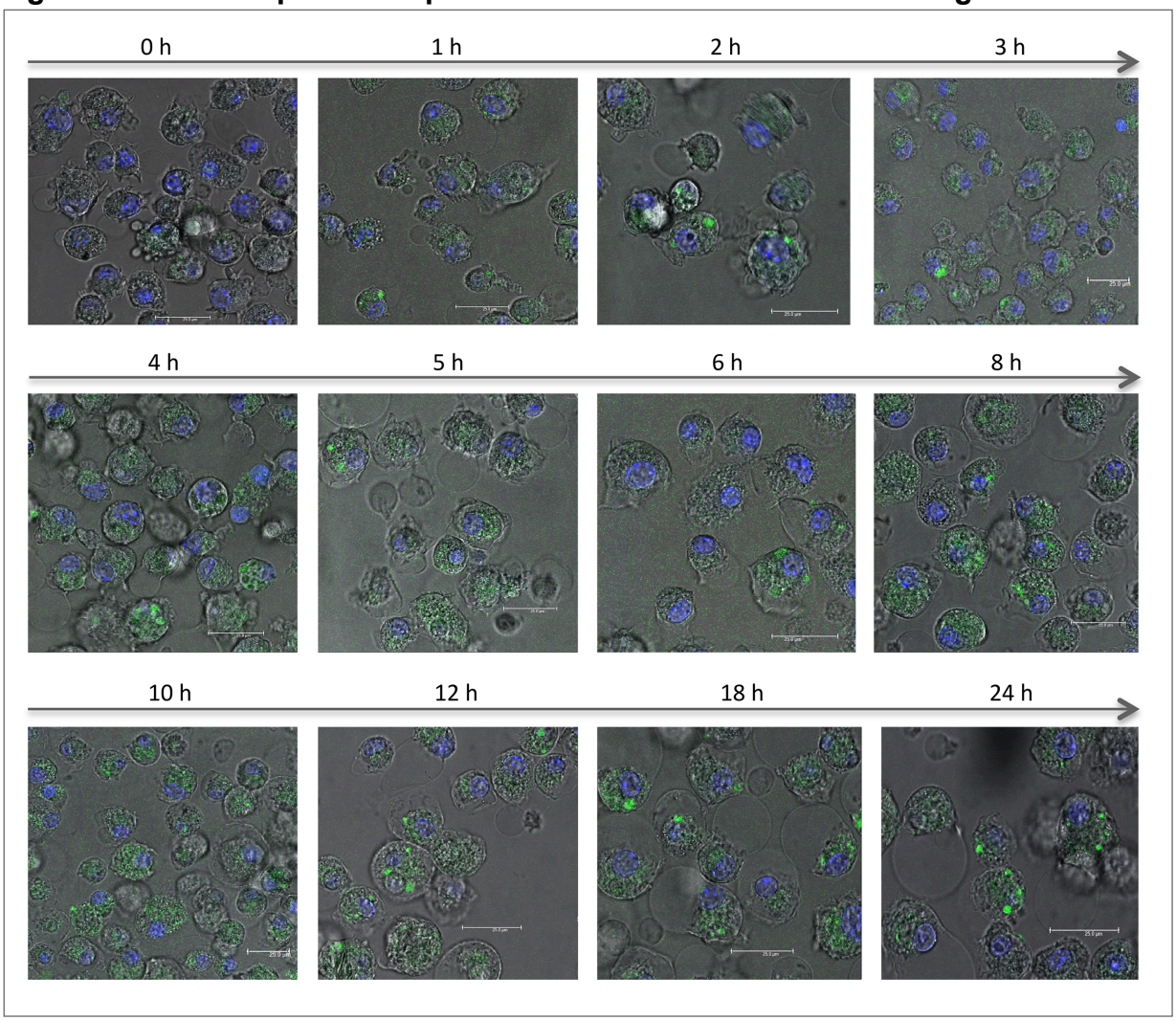

Figure 4: Cellular uptake of CpG-siRNA-FITC constructs by BMDCs. BMDCs at day 7 of culturing has been incubated with 1 nmol CpG-siRNA A20 linked to FITC. Shown are confocal images of CpG-siRNA A20-FITC treated BMDCs from 0-24 hours stained with Nuc Blue (ex 405); Leica confocal laser scanning microscope TCS SP5 II, ImageJ 1.47v software has been used.

The efficiency of the uptake reached its peak (90% mean fluorescent intensity inside the cells) after 2 hours of incubation and approximately 80% of the FITC signal remained for 24 hours (Fig. 5).

Figure 5: Cellular uptake of CpG-siRNA constructs - Kinetic

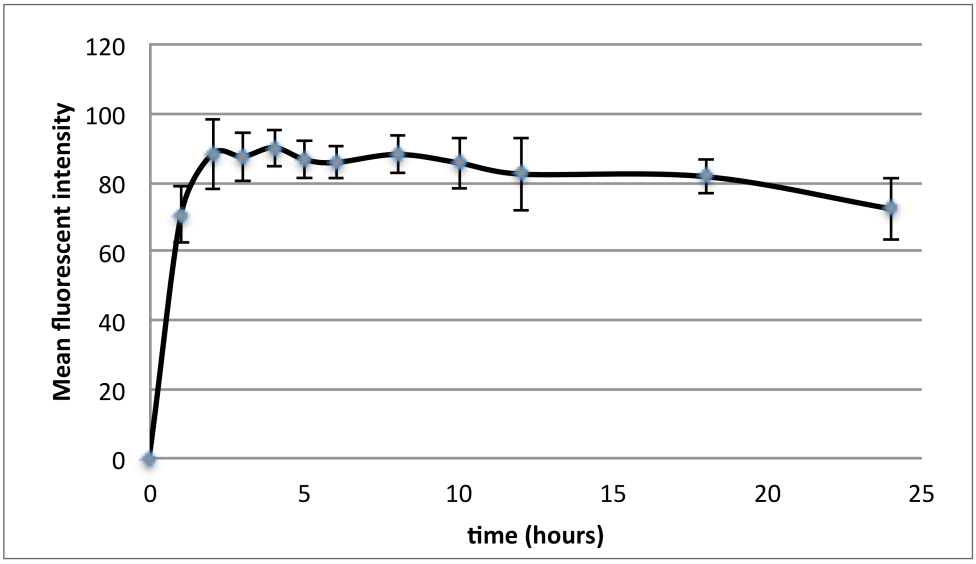

Figure 5: Cellular uptake of CpG-siRNA-FITC constructs by BMDCs. BMDCs at day 7 of culturing has been incubated with CpG-siRNA A20 linked to FITC. Diagrammed are mean fluorescent intensities of FITC in 10 cells/ time point compared to untreated cells over 24 hours; Leica confocal laser scanning microscope TCS SP5 II, ImageJ 1.47v software were used.

After demonstrating the cellular uptake of CpG-siRNA A20 constructs, the next question was whether the siRNA is capable of silencing A20.

A20 was analyzed on protein level in DCs by performing Western Blot. Therefor BMDCs were incubated with 1 nmol CpG, CpG-scr or CpG-siA20 (CpG-siA20_5, CpG-siA20_6) constructs. Since CpGs activate the NF-κB pathway and therefore induce A20 expression, the detection of construct mediated A20 knockdown and its effects was challenging. However, it was possible to eventually localize the time points of interest. Initially, at around 12 to 16 hours after CpG/CpG-construct administration, A20 was upregulated in all samples irrespective of their specifity compared to non-treated control DCs (Fig. 6).

This effect was not surprising since A20 is a target gene of the NF-κB pathway stimulated by CpG ODNs. At later time points (18 to 20 hours) the amount of A20 protein decreased in cells with A20-specific siRNA fused to CpG, indicating a siRNA-mediated A20 knockdown (Fig. 6, 7). Four hours later (at 24 hours) the A20 protein signal was again elevated above the levels observed in control cells and CpG-treated cells (Fig. 6, 7). This most likely shows the consequence of the prolonged and augmented NF-κB activity due to the previous A20 knockdown.

Figure 6: A20 protein in CpG/ CpG-construct treated DCs

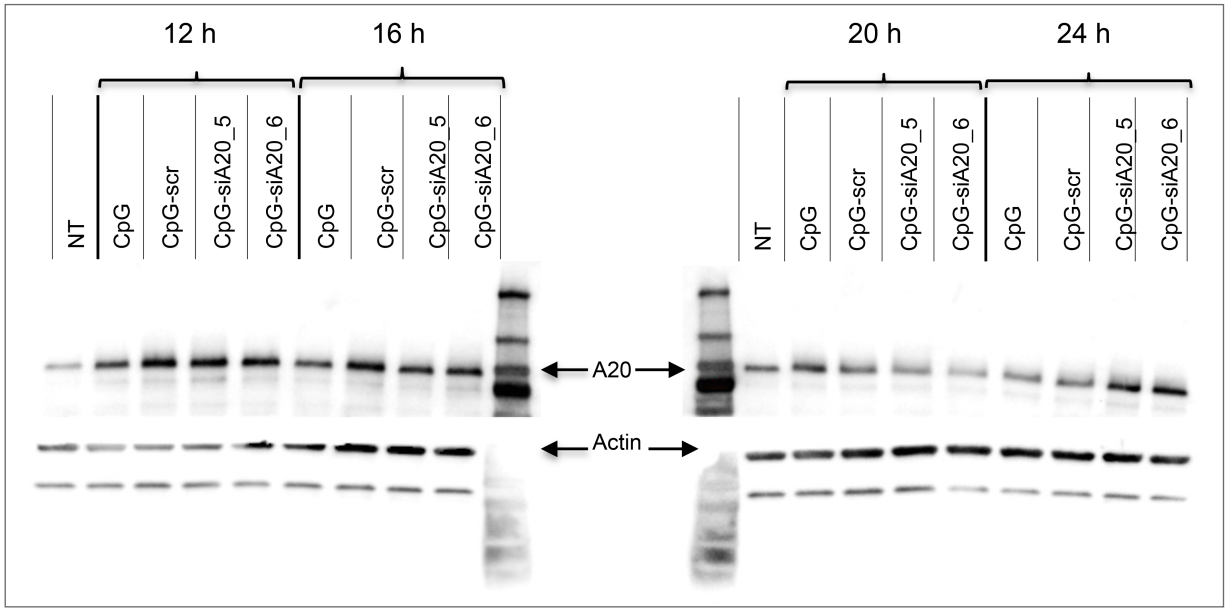

Figure 6: A20 protein expression in CpG/ CpG-construct treated BMDCs. BMDCs at day 15 of culturing have been treated with 1 nmol CpG/ CpG-scrambled siRNA/ CpG-siRNA A20 constructs (CpG-siA20_5, CpG-siA20_6). Western Blot analyses of A20 (82 kDa) and Actin (42 kDa) as loading control for one representative experiment showing A20 upregulation at 12, 16 hours in all treated samples, A20 knockdown at 20 hours due to CpG-siA20, and an additional upregulation at 24 hours exclusively in CpG-siA20 treated BMDCs.

Figure 7: A20 protein in CpG/ CpG-construct treated DCs

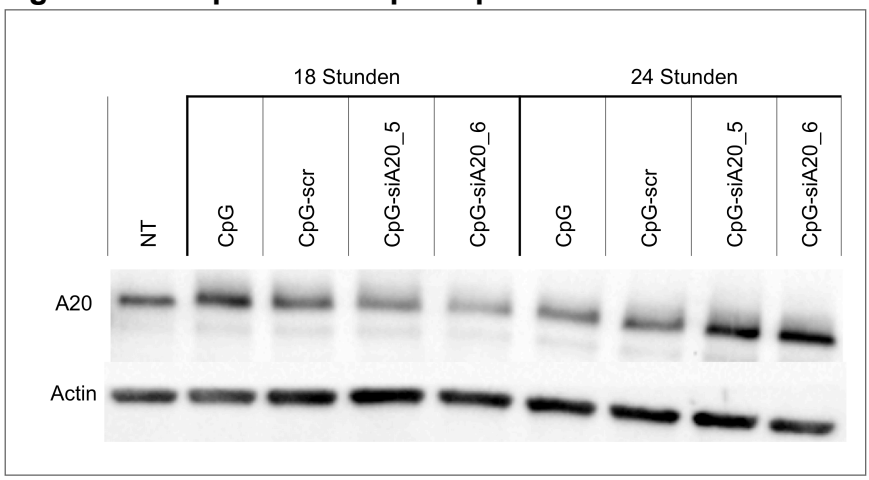

Figure 7: A20 protein expression in CpG/ CpG-construct treated BMDCs. BMDCs at day 12 of culturing has been treated with 1 nmol CpG/ CpG-scrambled siRNA/ CpG-siRNA A20 constructs. Western Blot analyses of A20 (82 kDa) and Actin (42 kDa) as loading control for one representative experiment showing A20 knockdown at 18 hours in CpG-siA20 treated samples and stronger upregulation than in CpG/ CpG-scr treated BMDCs at 24 hours.

In order to confirm CpG-siRNA-mediated A20 knockdown and to analyse NF-κB activation quantitative real-time PCR for A20 and IκBa were performed. At multiple time points (0, 2, 4, 6, 8, 10, 12, 18, 24 hours) mRNA levels were determined. In addition to the experiment kinetics, the mean values of all time points were integrated by calculating the area under curves (AUC) defined by individual time points. Compared to cells incubated with CpG or CpG-scr, the CpG-siA20-treated BMDCs expressed A20 mRNA at significantly lower levels (Fig. 8A). This was specific for the siRNA directed at A20, since a construct containing a scrambled siRNA sequence (CpG-scr) did not have this effect. IκBa mRNA expression was shown to be increased in CpG-siA20 construct even more than in CpG treated DCs representing NF-κB activity (Fig. 8A). Similar results were obtained in JAWSII immature dendritic cell line (Fig. 8B).

Figure 8: A20 and IκBα in CpG/ CpG-construct treated DCs

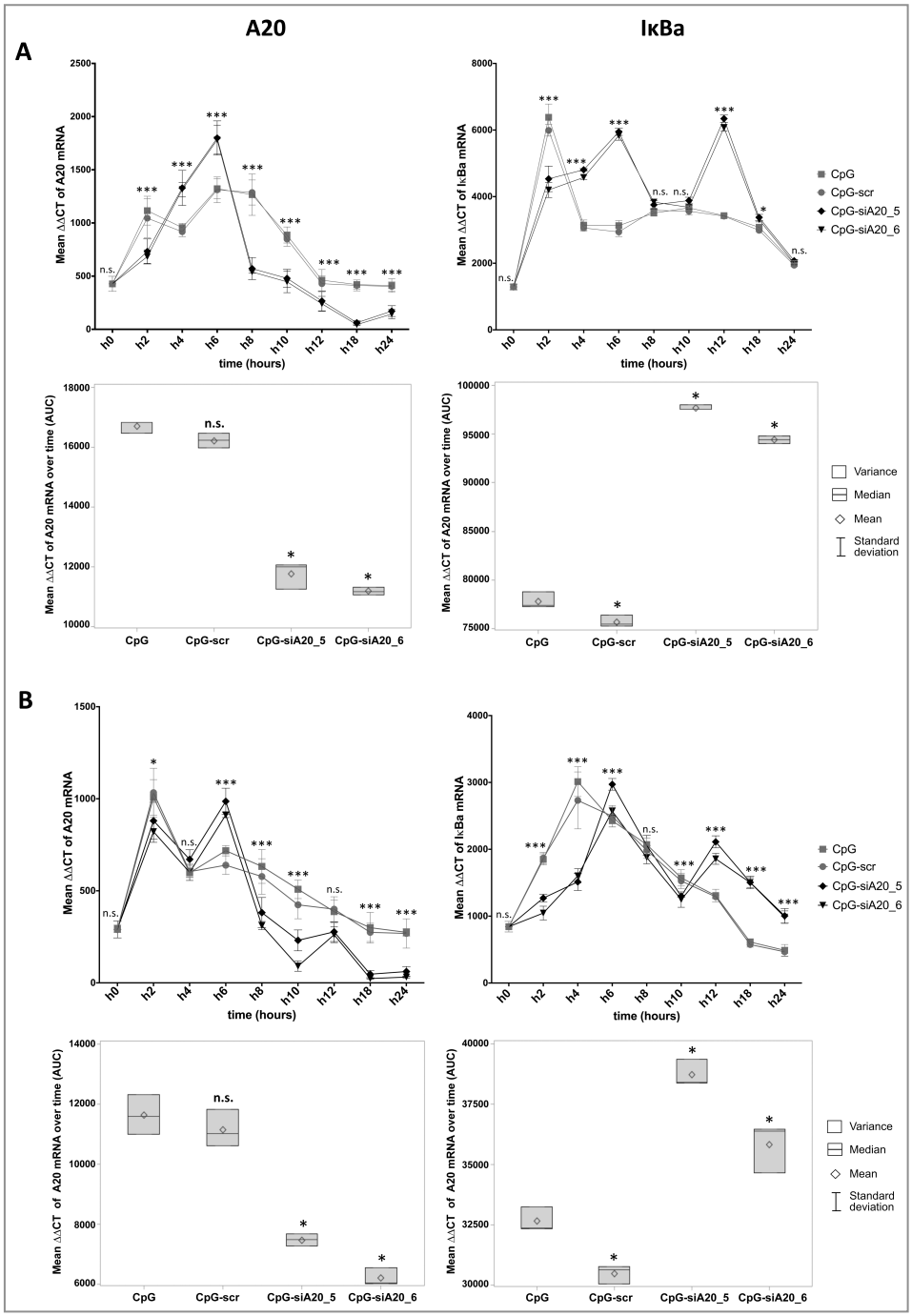

Figure 8: Expression of A20 and IκBα mRNA in CpG/ CpG-construct treated BMDCs and JAWSII cells. BMDCs and JAWSII cells have been stimulated with 1 nmol CpG/ CpG-scr/ CpG-siA20 constructs (CpG-siA20_5, CpG-siA20_6). Shown are kinetics from 0-24 hours and cumulated results of all time points (AUC) for mean values of A20 and IκBα mRNA (ΔΔCT) of one representative experiment, measured three times in duplicates, ß2MG normalized. **(A)** BMDCs at day 7 of culturing. **(B)** JAWSII suspension cells. Diagrams showing higher induction of cytokine expression in both *in vitro* systems after CpG-siA20 treatment in comparison to CpG/ CpG-scr. Performed statistical tests: Kruskal–Wallis one-way analysis of variance and Wilcoxon rank-sum test. n.s. indicates not significant, * indicates $p<0.05$, ** indicates $p<0.01$, and *** indicates $p<0.001$ compared to CpG treated cells.

The elevated expression of IκBα in A20-depleted cells demonstrated enhanced activation of the canonical NF-κB pathway and confirmed the functionality of the constructs.

The performed *in vitro* experiments in bone marrow-derived DCs and JAWSII cells confirmed the central role of A20 in controlling the NF-κB pathway activity. Linking siRNA against A20 to CpG was shown to be an effective tool for siRNA internalization and A20-silencing in dendritic cells.

7.3 CpG-siRNA A20 construct mediated DC stimulation *in vitro*

Previous experiments provided evidence of CpG-siA20 construct mediated NF-κB activation and A20 silencing. In order to assess the effects of CpG-siRNA-mediated A20 knockdown on DC function, mRNA levels of the pro-inflammatory cytokines IL-6 and TNF-α were analyzed in BMDCs and JAWSII cells that were left untreated or incubated with CpG only or CpG-conjugates. In both murine BMDCs and the immature murine DC line JAWSII a much stronger induction of IL-6 and TNF-α expression was observed in CpG-siA20 treated cells (Fig. 9A,B).

RT-qPCR analyses of CpG/ CpG-siA20 stimulated DCs underlined the stimulatory effect of simultaneous TLR9-pathway activation and A20 silencing. The increased expression of the pro-inflammatory cytokines IL-6 and TNF-α is an indication for immune-modulatory capacities *in vivo*.

Figure 9: IL-6 and TNF in CpG/ CpG-construct treated DCs

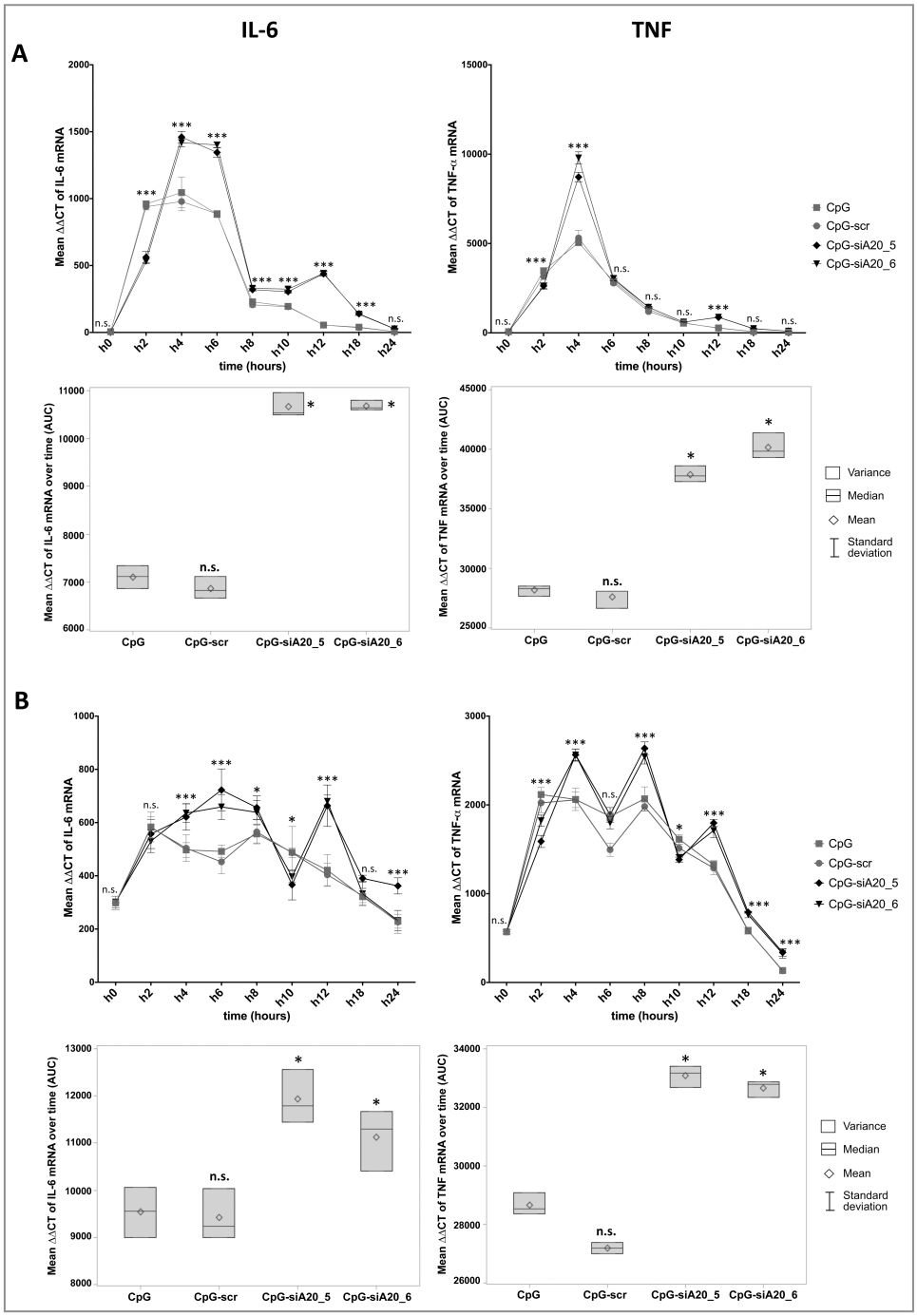

Figure 9: Expression of IL-6 and TNF-α mRNA in CpG/ CpG-construct treated BMDCs and JAWSII cells. BMDCs and JAWSII cells have been stimulated with 1 nmol CpG/ CpG-scr/ CpG-siA20 constructs (CpG-siA20_5, CpG-siA20_6). Shown are kinetics from 0-24 hours and cumulated results of all time points (AUC) for mean values of IL-6 and TNF-α mRNA (ΔΔCT) of one representative experiment, measured three times in duplicates, ß2MG normalized. **(A)** BMDCs at day 7 of culturing. **(B)** JAWSII suspension cells. Diagrams showing higher induction of cytokine expression in both *in vitro* systems after CpG-siA20 treatment in comparison to CpG/ CpG-scr. Performed statistical tests: Kruskal–Wallis one-way analysis of variance and Wilcoxon rank-sum test. n.s. indicates not significant, * indicates $p<0.05$, ** indicates $p<0.01$, and *** indicates $p<0.001$ compared to CpG treated cells.

7.4 CpG-siRNA A20 construct mediated immune stimulation *in vivo*

In vitro the CpG-siRNA A20 constructs proved to be capable of DC stimulation and A20 knockdown. The next step was the verification of CpG-siA20 construct activity *in vivo*. Therefor naïve healthy mice were treated with PBS or 1 nmol of CpG or CpG-siRNA constructs, respectively. CpG or FITC-labeled CpG-scr/CpG-siA20 constructs were injected intraperitoneal twice (0 and 24 hours). Peritoneal lavage was performed 36 hours after the first treatment for harvesting and analyzing construct uptake by immune cells at injection site. Fluorometric analyses revealed FITC-positive DCs, B cells, and NK cells. Deducting high background-/ self-fluorescence just parts of DCs and NK cells remained FITC-positive. Approximately 30% of DCs and 20-25% of NKs cells in the peritoneum inoculated FITC-labeled constructs at the analyzed time point (Fig. 10).

Figure 10: CpG-construct uptake *in vivo*

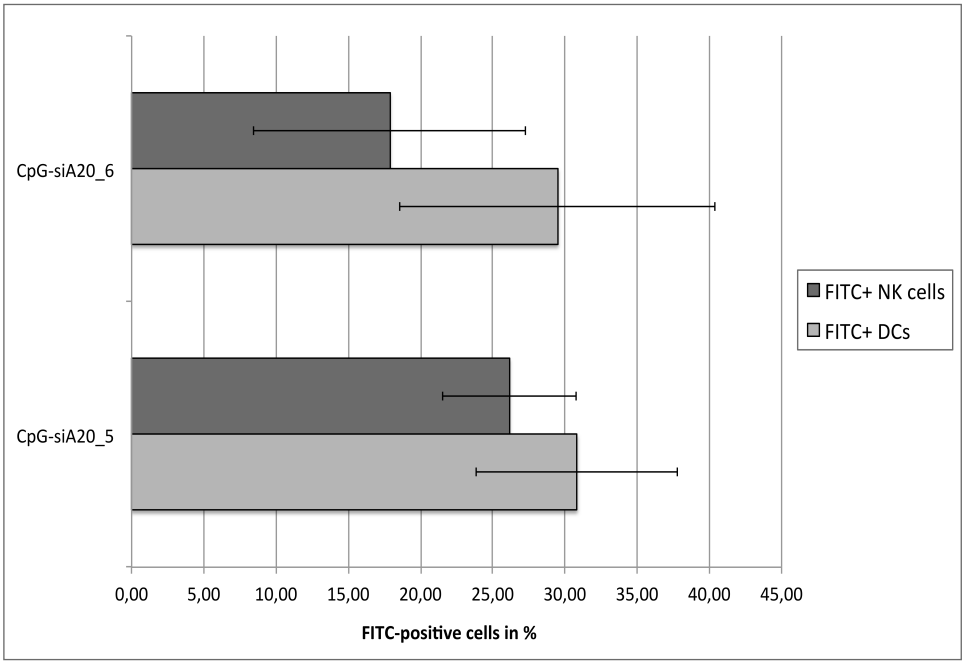

Figure 10: CpG-construct uptake by DCs and NK cells in peritoneum.
Healthy C57BL/6N mice (female, 8-10 weeks old, 5 mice/group) have been treated i.p. with 1 nmol CpG/ CpG-scr-FITC/ CpG-siA20-FITC (CpG-siA20_5, _6) constructs twice (0, 24 h). After 36 hours cells of the peritoneum were collected via peritoneal lavage. Shown are %ages of FITC-positive DCs (CD11c+ B220+) and NK cells (NK-1.1+ CD49b+) in the peritoneum. CpG-siRNA-FITC constructs were taken up to similar extent, irrespective of siRNA specifity (CpG-scr not shown).

This experiment confirmed the cellular uptake of CpG-siA20 constructs *in vivo* at injection site. In an additional experiment no FITC-positive cells were detectable at later time points (48 hours after first, 24 hours after second injection) in peritoneum. Furthermore, the overall amount of DCs was significantly lower compared to PBS and CpG-treated mice (Fig. 11). This could be an indication of successfully activated DCs leaving the peritoneal cavity for T cell priming. Interestingly, there was no major difference between CpG-siA20 and CpG-scr conjugates.

Figure 11: DCs in peritoneum after CpG-construct stimulation

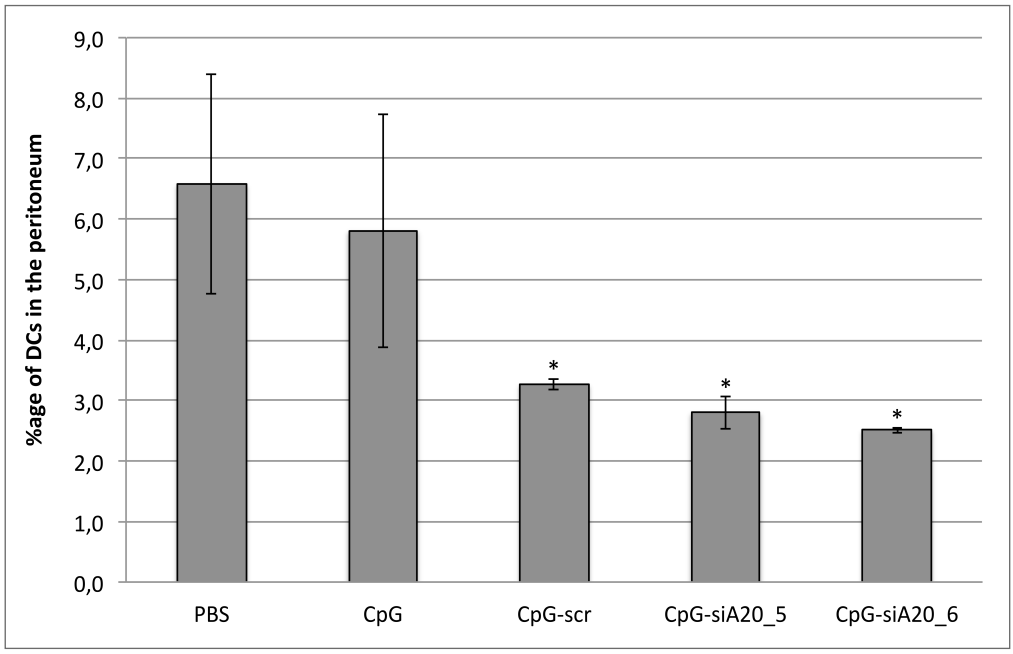

Figure 11: DCs leaving peritoneum after CpG-construct stimulation.
Healthy C57BL/6N mice (female, 8-10 weeks old, 5 mice/group) have been treated i.p. with 1 nmol CpG/ CpG-scr/ CpG-siA20 (CpG-siA20_5, _6) constructs twice (0, 24 hours). After 48 hours cells of the peritoneum were collected via peritoneal lavage. Shown are %ages of DCs (CD11c+ B220+) in the peritoneum depending on treatment. Diagram showing significantly lower expression of DCs after CpG-construct treatment as compared to CpG alone or PBS control. Performed statistical tests: Kruskal–Wallis one-way analysis of variance and Wilcoxon rank-sum test. n.s. indicates no significant differences, * indicates $p<0.05$ compared to CpG treated cells.

After intraperitoneal injection, the serum levels of several cytokines (IL-2, IL-6, IL-10, IL-12p70, TNF-α, IFN-γ) were measured over time by CBA to monitor secretion of immune-stimulatory factors.

Healthy mice were treated *in vivo* repeatedly (three times) every 48 hours with CpG or CpG-siA20 (CpG-siA20_5 plus CpG-siA20_6). The cytokines IL-2 and IL-12p70 showed no distinct changes during the examined period (12 days).

As expected from previous experiments, the assay revealed significantly higher concentrations of IL-6, TNF-α but also IFN-γ and IL-10 in serum isolated from animals treated with CpG or CpG-siRNA constructs compared to PBS-injected mice. Notably, in case of IL-6, TNF-α and IFN-γ the cytokine concentrations induced by the CpG-siA20 constructs were substantially higher than those triggered by treatment with CpG alone (Fig. 12).

Figure 12: Cytokines after i.p. CpG/ CpG-construct treatment

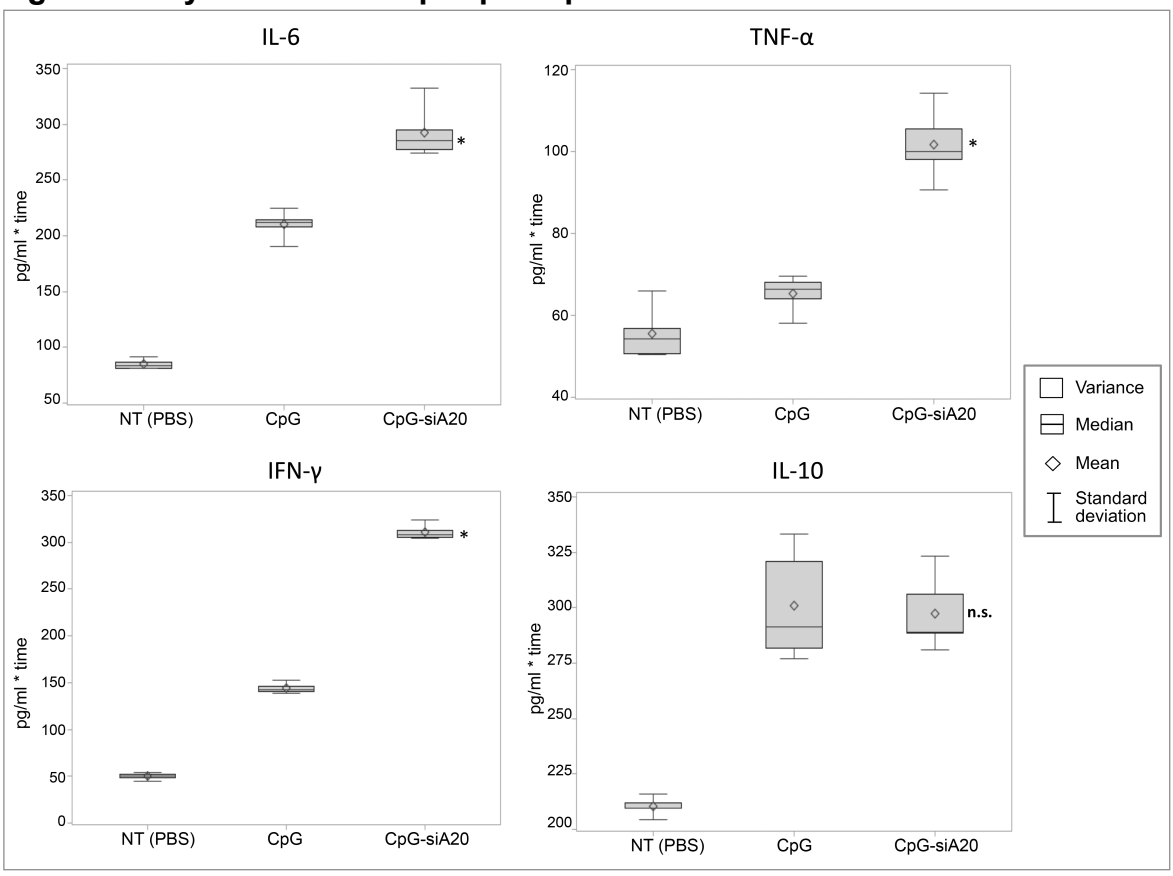

Figure 12: Cytokine expression after i.p. CpG/ CpG-construct treatment.
Healthy C57BL/6N mice (female, 8-10 weeks old, 5 mice/group) have been treated i.p. with 1 nmol CpG/ CpG-siA20 three times (day 0, 2, 4). Shown are cumulated results (AUC) of three time points within 12 days (day 1, 6, 12) for the cytokines IFN-γ, TNF-α, IL-6, and IL-10. Protein expressions in pg/ml has been analyzed by CBA and calculated via standard curves. Diagrams are showing significantly higher expression of IFN-γ, TNF-α, and IL-6 after CpG-siA20 treatment as compared to CpG alone and similar levels of IL-10. Performed statistical tests: Kruskal–Wallis one-way analysis of variance and Wilcoxon rank-sum test. n.s. indicates no significant differences, * indicates $p<0.05$ compared to CpG treated cells.

Whether the observed differences in cytokine induction between CpG and CpG-siA20 constructs were siRNA A20 specific or just due to unspecific siRNA linking was investigated further.

Healthy mice were treated with PBS or 1 nmol of CpG, CpG-scrambled siRNA or CpG-siRNA A20 constructs (CpG-siA20_5, CpG-siA20_6). Mice were treated repeatedly (two times) every 24 hours. After intraperitoneal injection, the serum levels of pro-inflammatory cytokines were measured at several time points using CBA. The assay confirmed the A20 siRNA specific higher induction of IL-6, TNF-α and IFN-γ. In serum isolated from animals treated with CpG-siA20 constructs the cytokine concentrations were significantly higher than those triggered by CpG or CpG-scrambled siRNA treatment (Fig. 13).

Figure 13: Cytokines after i.p. CpG/ CpG-construct treatment

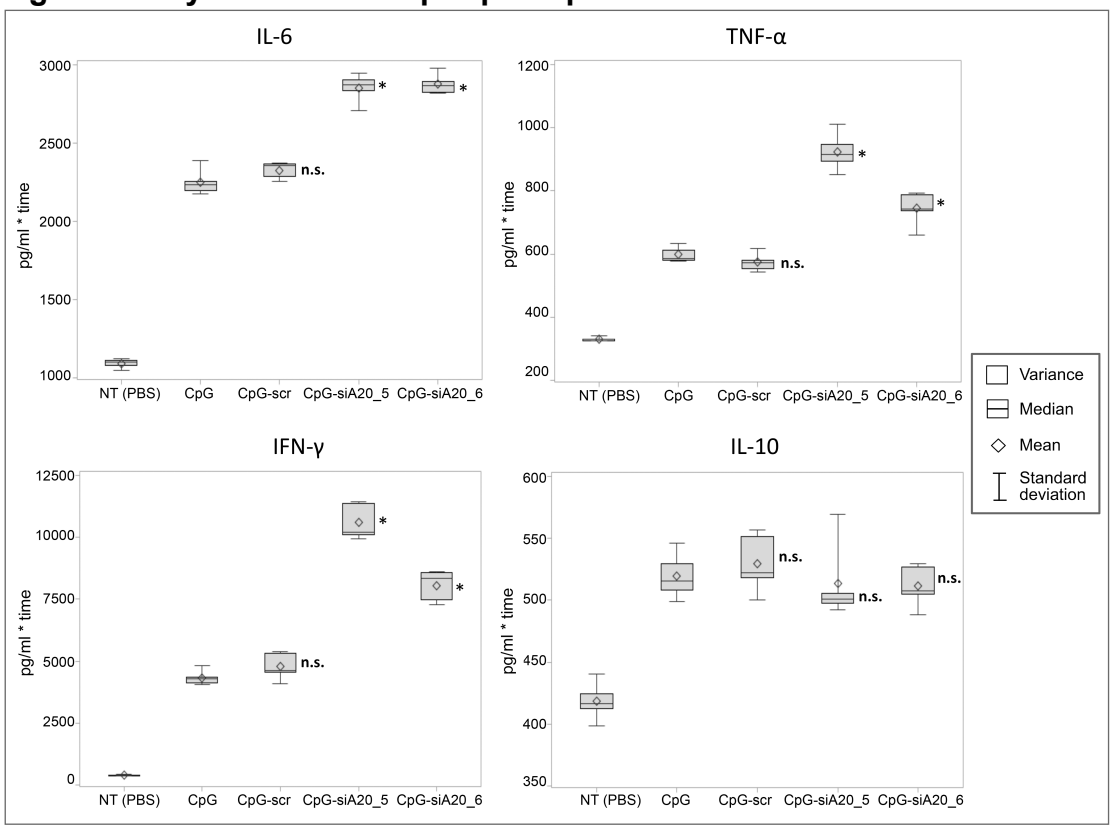

Figure 13: Cytokine expression after i.p. CpG/ CpG-construct treatment.
Healthy C57BL/6N mice (female, 8-10 weeks old, 5 mice/group) have been treated i.p. with 1 nmol CpG/ CpG-scr/ CpG-siA20 (CpG-siA20_5, _6) constructs twice (0, 24 hours). Shown are cumulated results (AUC) of five time points within 48 hours (3, 24, 30, 36, 48 hours) for the cytokines IFN-γ, TNF-α, IL-6, and IL-10. Protein expressions in pg/ml has been analyzed by CBA and calculated via standard curves. Diagrams are showing significantly higher expression of IFN-γ, TNF-α, and IL-6 after CpG-siA20 treatment as compared to CpG alone or controls and similar levels of IL-10. Performed statistical tests: Kruskal–Wallis one-way analysis of variance and Wilcoxon rank-sum test. n.s. indicates no significant differences, * indicates $p<0.05$ compared to CpG treated cells.

Looking at the kinetics for the period of 48 hours a prolonged or increased expression of the cytokines IL-6, TNF-α and IFN-γ is clearly visible (Fig. 14). The second CpG-siA20 application at 24 hours enhanced the expression, which was not detectable for CpG or CpG-scr control.

Figure 14: Cytokine kinetics after i.p. CpG/ CpG-construct treatment

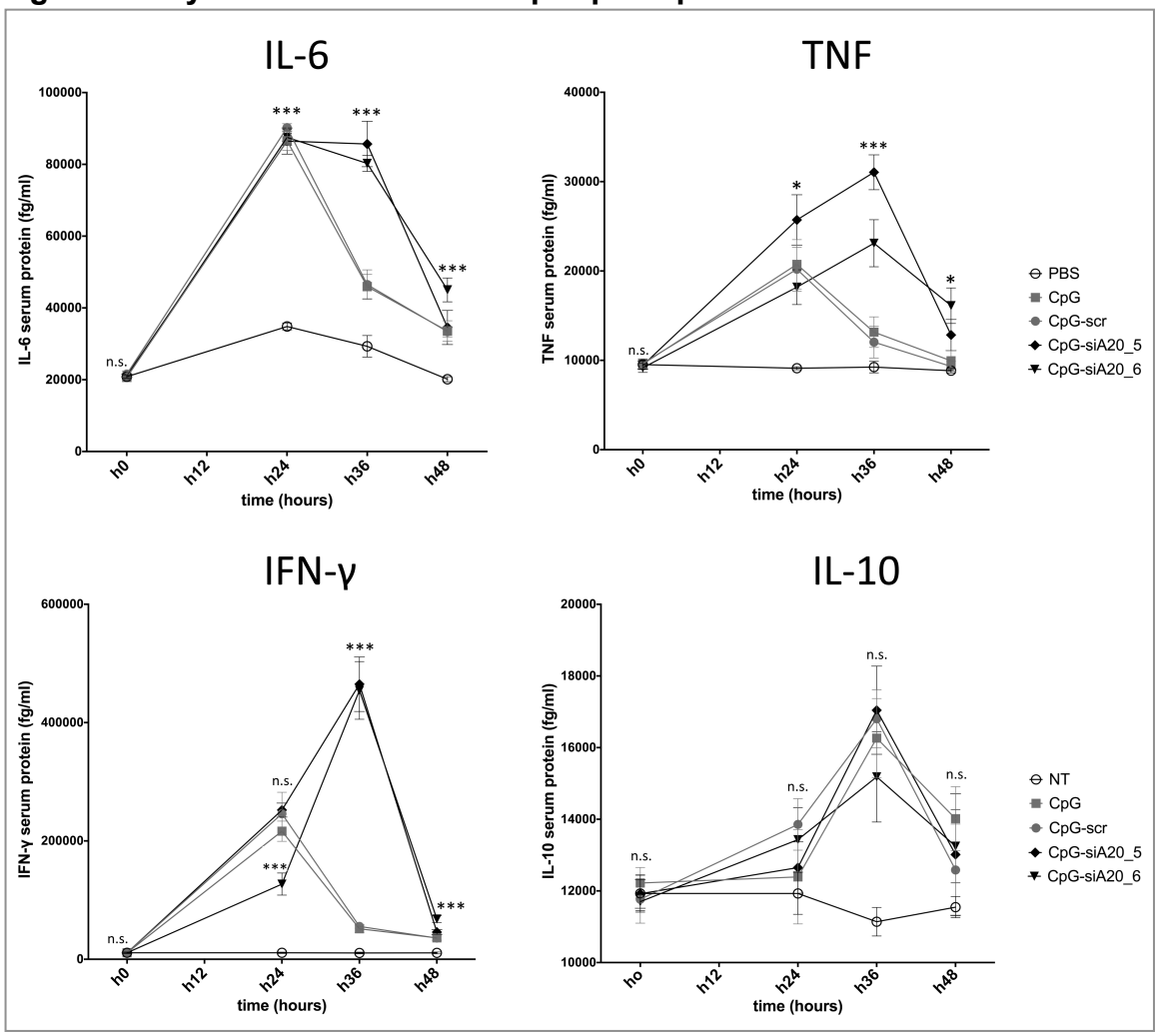

Figure 14: Cytokine expression kinetics after i.p. CpG/ CpG-construct treatment.
Healthy C57BL/6N mice (female, 8-10 weeks old, 5 mice/group) have been treated i.p. with 1 nmol CpG/ CpG-scr/ CpG-siA20 (CpG-siA20_5, _6) constructs twice (0, 24 hours). Shown are mean cytokine expressions (in fg/ ml) of five animals per group for the time points 0, 24, 36, and 48 hours; protein expression of the cytokines IFN-γ, TNF-α, IL-6, and IL-10 has been analyzed by CBA and calculated via standard curves. Diagrams are showing significantly higher expression of IFN-γ, TNF-α, and IL-6 after CpG-siA20 treatment as compared to CpG alone or controls and similar levels of IL-10. Performed statistical tests: Kruskal–Wallis one-way analysis of variance and Wilcoxon rank-sum test. n.s. indicates not significant, * indicates $p<0.05$, ** indicates $p<0.01$, and *** indicates $p<0.001$ compared to CpG treated cells.

The previous results clearly showed an A20 siRNA related increase of CpG mediated DC stimulation. To clarify whether the linking to CpG ODNs is necessary for siRNA delivery into the cells and A20 silencing function or if the presence of CpGs is sufficient for cellular uptake, an additional *in vivo* experiment was performed.

Healthy mice were treated with 1 nmol of CpG, CpG with unbound siRNA A20 (siA20_5, siA20_6), CpG-scrambled siRNA or CpG-siRNA A20 constructs (CpG-siA20_5, CpG-siA20_6) respectively. These mice were treated once (intraperitoneal injection) and the serum levels of pro-inflammatory cytokines were measured at several time points during the following 36 hours using CBA. The assay confirmed the previous results showing higher induction of IL-6, TNF-α and IFN-γ cytokine concentrations in CpG-siA20 constructs compared to CpG or CpG-scrambled siRNA (Fig. 15). A significant increase of IL-10 due to CpG-siA20 construct treatment compared to the control groups was also observed. Presumably this is a late effect, which was masked or delayed by repetitive treatments during the former studies.

For unbound siRNA in the presence of CpG could no differences be observed in cytokine induction compared to CpG alone (Fig. 15). Consequently, linking siRNA to CpG ODNs seems to be a requirement for internalization and siRNA-mediated gene silencing.

Figure 15: Cytokines after i.p. CpG/ CpG-construct treatment

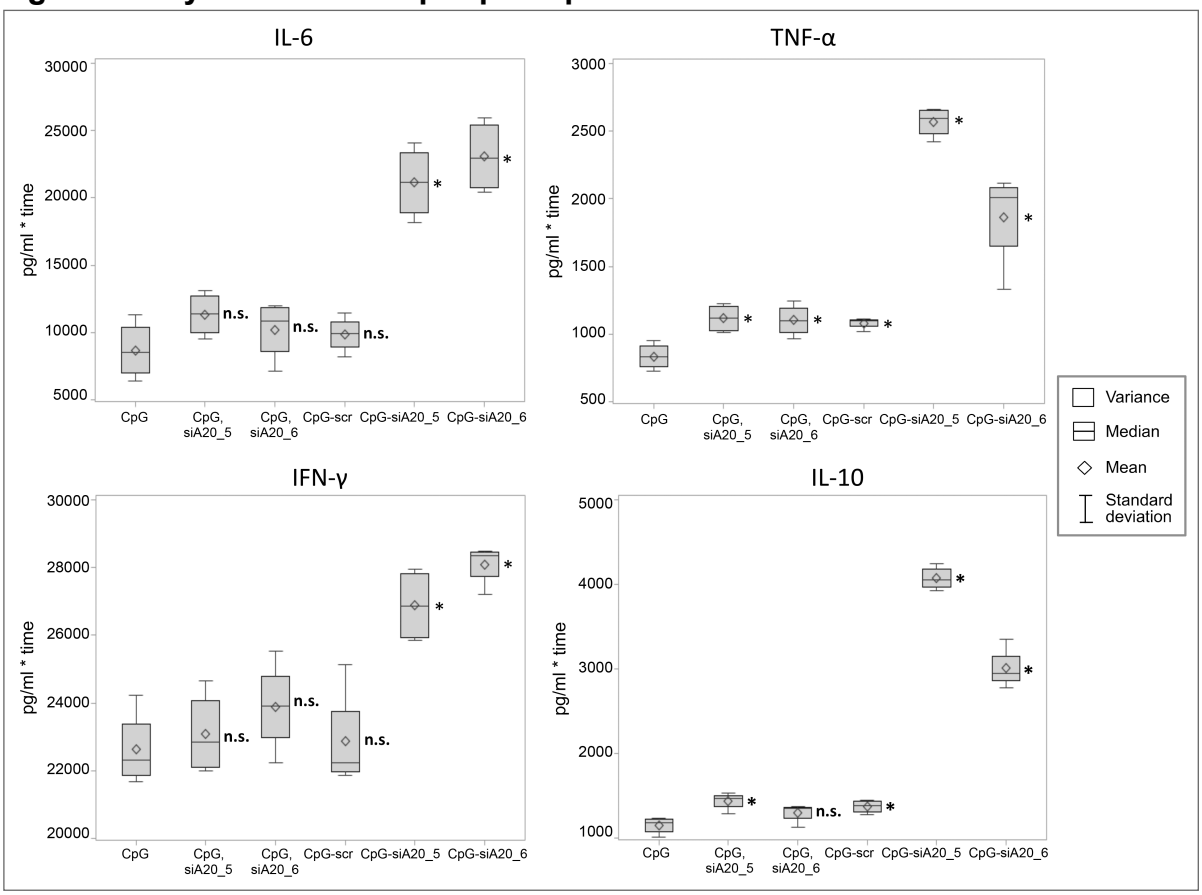

Figure 15: Cytokine expression after i.p. CpG/ CpG-construct treatment.
Healthy C57BL/6N mice (female, 8-10 weeks old, 4 mice/group) have been treated i.p. with 1 nmol CpG/ CpG with unlinked siA20 (siA20_5, _6)/ CpG-scr/ CpG-siA20 (CpG-siA20_5, _6) constructs once. Shown are cumulated results (AUC) of six time points within 36 hours (0, 3, 6, 12, 24, 36 hours) for the cytokines IFN-γ, TNF-α, IL-6, and IL-10. Protein expressions in pg/ml has been analyzed by CBA and calculated via standard curves. Diagrams are showing significantly higher expression of IFN-γ, TNF-α, IL-6, and IL-10 after CpG-siA20 treatment as compared to CpG alone or the controls. Performed statistical tests: Kruskal–Wallis one-way analysis of variance and Wilcoxon rank-sum test. n.s. indicates no significant differences, * indicates $p<0.05$ compared to CpG treated cells.

The performed *in vivo* experiments in healthy mice showed local CpG-construct uptake by dendritic cells as well as by NK cells and systemic immune-stimulation especially on cytokine level. In all treatment set-ups the stimulatory capacity of CpG-siA20 constructs exceeds the one of CpG or CpG-scr control significantly.

7.5 Effects of CpG-siRNA A20 construct treatment on B16 tumors *in vivo*

Strong immune-stimulatory capacities of the CpG-siA20 constructs were observed *in vivo* in healthy mice. Next, the immune-modulatory and anti-tumor properties of CpG-siA20 in a mouse tumor model were evaluated. Therefor the syngeneic melanoma tumor cell line B16-F1 was chosen.

The tumor cells were analyzed *in vitro* for direct effects due to CpG/ CpG-construct treatment before their *in vivo application*. By Analyzing A20, IL-6, and TNF-α via RT-qPCR no evident changes on mRNA expression could be observed, assuming no direct stimulatory effects on the tumor cells (data not shown). By the use of different camptothecin concentrations (2, 5, 10, 20 µM) it was tested whether the apoptosis sensitivity of CpG/ CpG-construct pre-treated cells differed to non-treated ones. Also in this question no distinct influence on B16 tumor cells was detectable (data not shown). After these pre-experiments B16-F1 cells approved for *in vivo* studies.

The melanoma cells were inoculated subcutaneously at the right flank of naïve healthy mice. Tumor size and health status of mice were controlled daily.

In all experiments the mice developed aggressively growing tumors under the skin (Fig. 16).

Figure 16: Murine melanoma tumor model

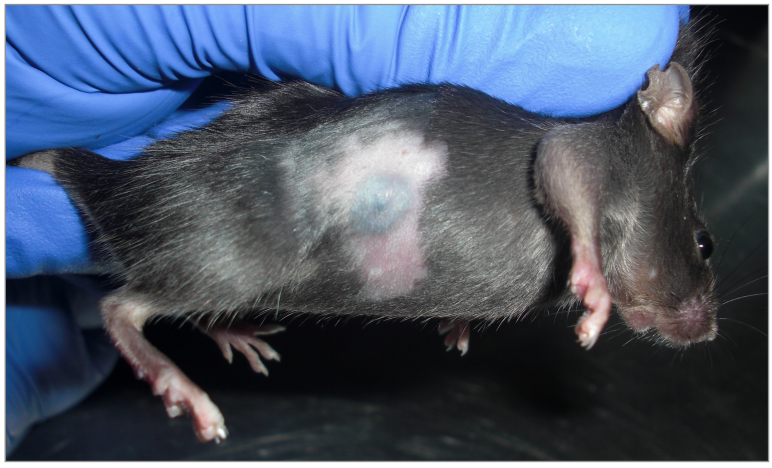

Figure 16: Murine tumor model of s.c. growing melanoma cells.
B16 melanoma cells (1x10^6) were injected s.c. after shaving in the right flank of C57BL/6 mice (female, 8 weeks old). The picture showing tumor development status of one representative mouse at day 10 after tumor cell injection and three days of daily peritumoral treatment with CpG-siA20 construct.

After the tumor reached a size of around 0.5 cm in diameter the treatment was started. CpG/ CpG-constructs or PBS as non-treated control were injected peritumorally at two sides of the tumor and the treatment was repeated at 24 h intervals for 7 days.
Three different experimental set-ups were tested for therapy optimization: Treatment start at day 7 applying 1 nmol CpG/ CpG-construct, start at day 4 also with 1 nmol and finally start at day 4 injecting 2 nmol. All of these experiments were performed at least two times.

During treatment period blood samples were collected every 24 hours, afterwards every 48 hours. Serum levels of several cytokines (IL-2, IL-4, IL-6, IL-10, IL-12p70, IL-17, TNF-α, IFN-γ) were measured by CBA.
The cytokines IL-2, IL-4, and IL-17 showed no distinct changes during the examined period (data not shown). Similar to naïve mice, tumor-bearing animals, which received the CpG or CpG-siRNA constructs showed higher serum levels of IL-6, TNF-α, IFN-γ and IL-12p70 compared to PBS-treated controls. Notably, the CpG-siA20 conjugates increased the concentration of TNF-α, IFN-γ and IL-12p70 significantly compared to CpG alone or the control CpG-scr construct (Fig. 17). In experiments with late treatment start at day 7, IL-6 was induced to a similar degree by all preparations containing CpG (Fig. 17A). This was unexpected, since CpG-siA20 administration had a very pronounced effect on this cytokine in cultured DCs and naïve mice. Initiation of the treatment 4 days after tumor cells inoculation confirmed the findings of the former trial. In this case, the CpG-siA20 conjugate increased the expression of all 4 cytokines, including IL-6 above the concentrations triggered by treatment of CpG alone or the control construct (Fig. 17B).
Increasing the amount of CpG/ CpG-constructs from 1 nmol to 2 nmol per treatment further improved the stimulatory capacity on cytokine level. All four cytokines were significantly higher expressed in CpG-siA20 treated mice compared to CpG of CpG-scr control groups (Fig. 17C).

Figure 17: Cytokines in tumor-bearing mice

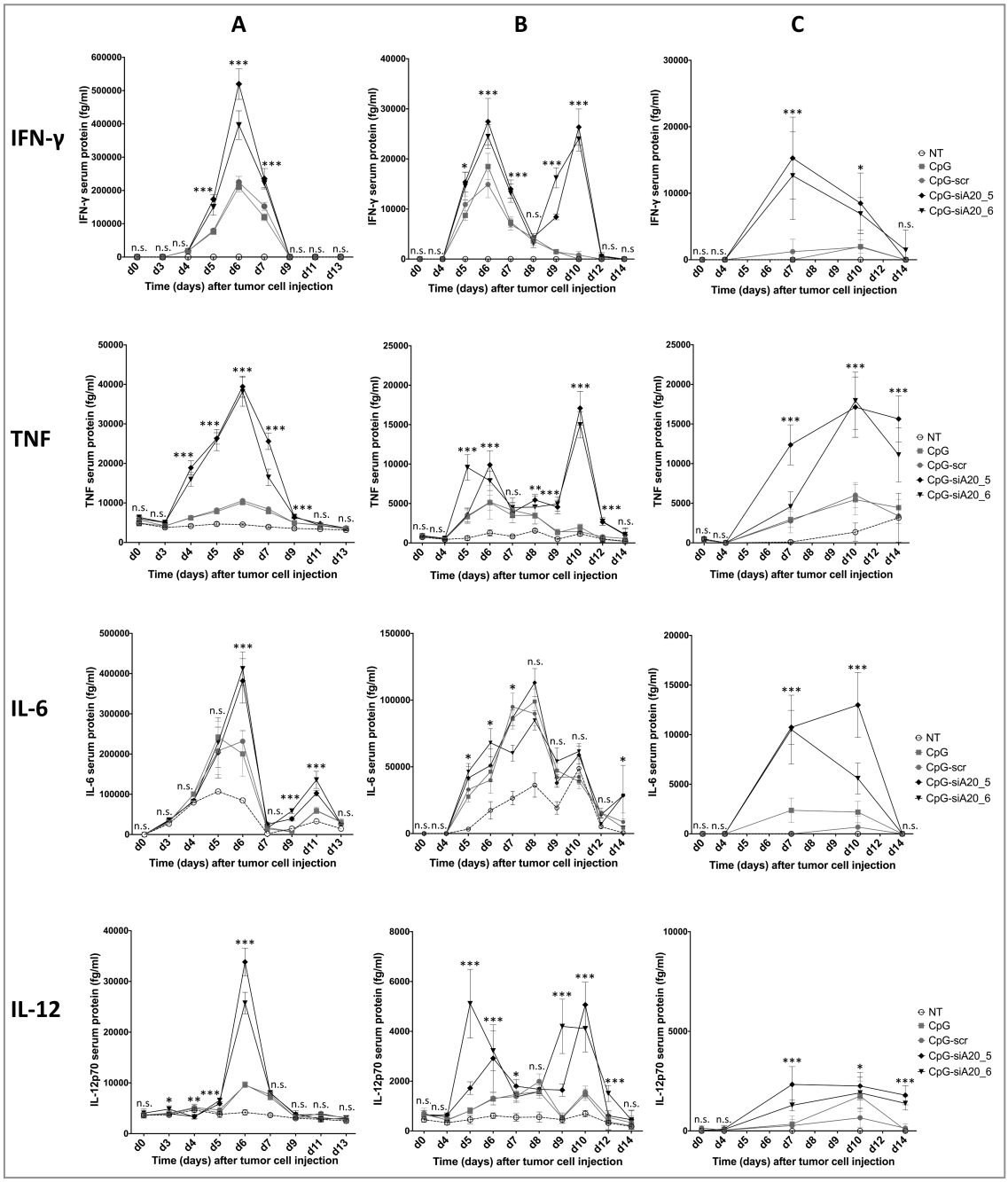

Figure 17: Cytokine expression in B16 melanoma-bearing mice after CpG/ CpG-construct treatment. C57BL/6N mice (female, 8 weeks old, 6 mice/group) with s.c. growing B16 tumors have been treated peritumorally with CpG/ CpG-scr/ CpG-siA20 (CpG-siA20_5, _6) constructs daily for seven days. Shown are mean values of 6 mice per group for 5-10 time points. Protein expression in pg/ml for the cytokines IFN-γ, TNF-α, IL-6, and IL-12p70 have been analyzed by CBA and calculated via standard curves. **(A)** Treatment start day 7 with 1 nmol; **(B)** Treatment start day 4 with 1 nmol; **(C)** Treatment start day 4 with 2 nmol. Diagrams are showing significantly higher expression of IFN-γ, TNF-α, and IL-12p70 after CpG-siA20 treatment as compared to CpG alone or the controls, IL-6 protein levels depending on treatment start. Performed statistical tests: Kruskal–Wallis one-way analysis of variance and Wilcoxon rank-sum test. n.s. indicates not significant, * indicates $p<0.05$, ** indicates $p<0.01$, and *** indicates $p<0.001$ compared to CpG.

In addition to the elevated cytokine serum levels, highly increased numbers of DCs were observed in the blood of CpG-siA20-treated animals. The percentage of circulating B cells was raised as well, surprisingly also in animals which were injected with CpG fused to scrambled siRNA (Fig. 18).

Figure 18: DCs and B cells in tumor-bearing mice

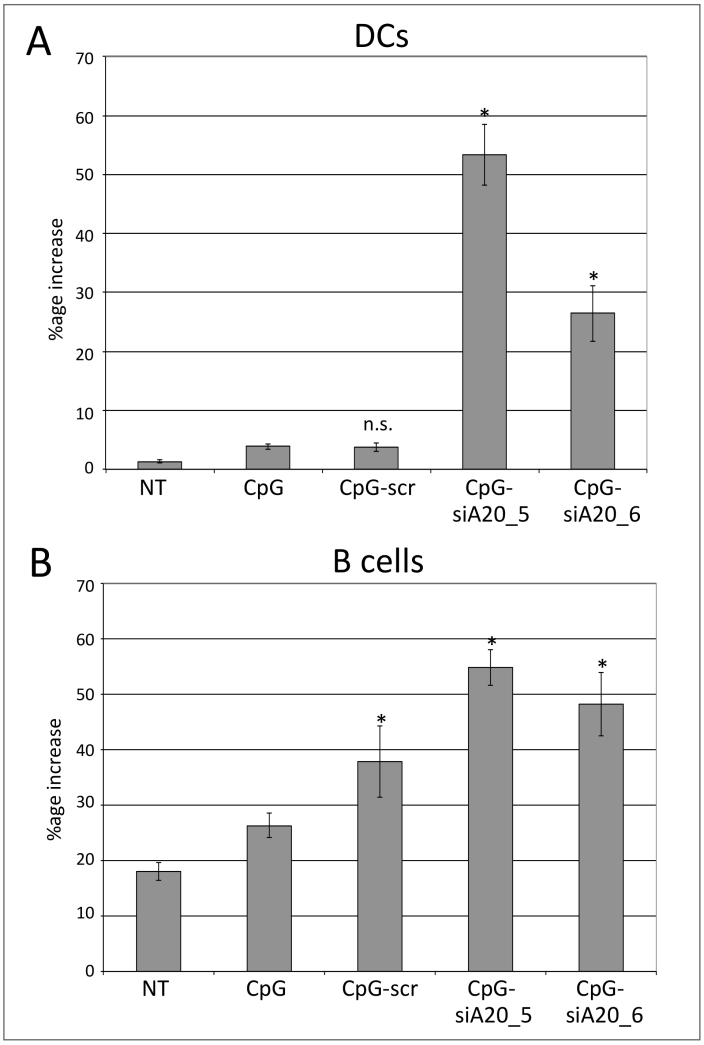

Figure 18:
Increase of DC and B cell numbers in blood of B16 melanoma-bearing mice.
C57BL/6N mice (female, 8 weeks old, 6 mice/group) with s.c. growing B16 tumors have been treated peritumorally with 1 nmol CpG/ CpG-scr/ CpG-siA20 (CpG-siA20_5, _6) constructs daily. Mice have been treated from day 4 after tumor cell challenge until day 10, blood collection for cellular analyses at day 10. Diagrams showing mean %age increase of DCs (CD11c+ B220+) and B cells (CD11c- B220+), comparing cell numbers before tumor cell injection (d0) with the one after 10 days depending on treatment; Performed statistical tests: Kruskal–Wallis one-way analysis of variance and Wilcoxon rank-sum test. n.s. indicates not significant, * indicates $p<0.05$ compared to CpG.

Another parameter indicating an enhanced immune response in CpG-siA20 treated animals was their greatly enlarged spleen. Splenomegaly was observed in all animals treated with CpG preparations but spleens isolated from CpG-siA20 animals were significantly bigger than those of controls (Fig. 19). Despite differences in size, the cellular composition of spleens was similar in all animal groups regardless of the organ size (data not shown).

Figure 19: Spleen in tumor-bearing mice

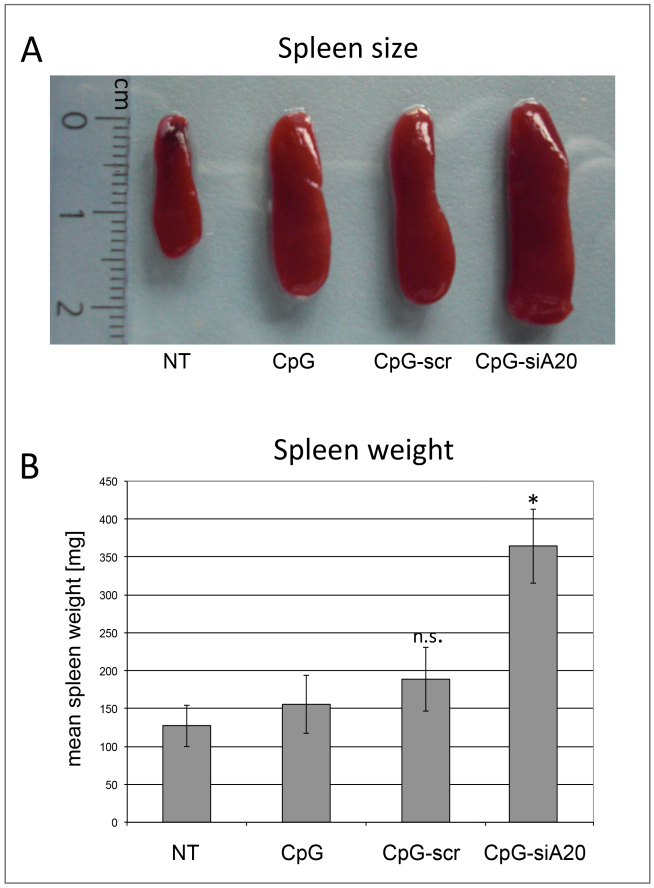

Figure 19: Spleen size of B16 melanoma-bearing mice depending on treatment.
C57BL/6N mice (female, 8 weeks old, 6 mice/group) with s.c. growing B16 tumors have been treated peritumorally with 1 nmol CpG/ CpG-scr/ CpG-siA20 (CpG-siA20_5, _6) constructs daily. Mice have been treated from day 4 after tumor cell challenge until day 10. **(A)** Picture showing one representative spleen per treatment group at the individual endpoint of experiment; mice showed increased spleen size depending on treatment. **(B)** Diagram showing mean spleen weight (in mg) of six mice per group. Performed statistical tests: Kruskal–Wallis one-way analysis of variance and Wilcoxon rank-sum test. n.s. indicates not significant, * indicates $p<0.05$ compared to CpG.

Splenocytes were analyzed for IDO (Indoleamine 2,3-dioxigenase) expression on mRNA level for determining potential immune suppressive effects starting from affected spleens. IDO expression seemed to increase depending on tumor growth respectively duration of tumor presence (Fig. 20). However, no significant changes correlating with treatment or spleen size could be observed (data not shown).

Figure 20: IDO expression in spleen

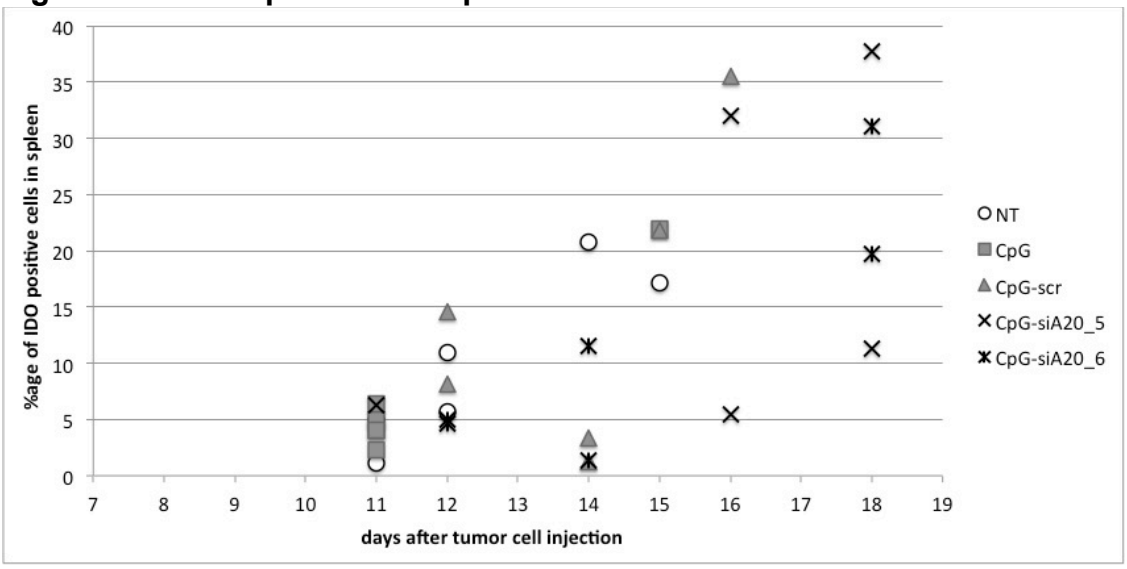

Figure 20: IDO expression in spleen of B16 melanoma-bearing mice.
C57BL/6N mice (female, 8 weeks old, 6 mice/group) with s.c. growing B16 tumors have been treated peritumorally with 1 nmol CpG/ CpG-scr/ CpG-siA20 (CpG-siA20_5, _6) constructs daily. Mice have been treated from day 4 after tumor cell challenge until day 10. FACS staining of isolated cells from spleen for IDO (Indoleamine 2,3-dioxigenase) expression at the individual end point of experiment for each mouse. Graphic shows %age of IDO positive cells for six mice per group from day 11 to day 18. IDO-positive cell numbers were increased over time but treatment independent.

Beside the described increase of circulating DC and B cell numbers, no significant cellular changes e.g. of T cell populations or NK cells could be observed in blood, as well as in draining lymph node and spleen at the analyzed time points (data not shown).

The stimulation and activation of the innate and adaptive immune response due to application of CpG/ CpG-constructs resulted in less aggressive growth of B16 melanoma tumors. In the first set of experiments, administration of 1 nmol ODN-constructs was started 7 days after B16 cells had been inoculated. With this treatment schedule a slight inhibition of tumor growth could be achieved in mice injected with CpG-siA20 constructs (CpG-siA20_5, CpG-siA20_6). Mice from these groups survived 3 to 4 days longer than the control animals until the tumor reached its limiting size (Fig. 21A).

Modification of the ODNs administration schedule in terms of earlier oligonucleotide injection (day 4) further improved the survival time of mice, which received siA20-specific conjugates. The tumor growth was noticeably inhibited and in one group, CpG-siA20_5, 50% of the animals survived until the end of the experiment on day 18 (Fig. 21B).

Figure 21: Survival curves

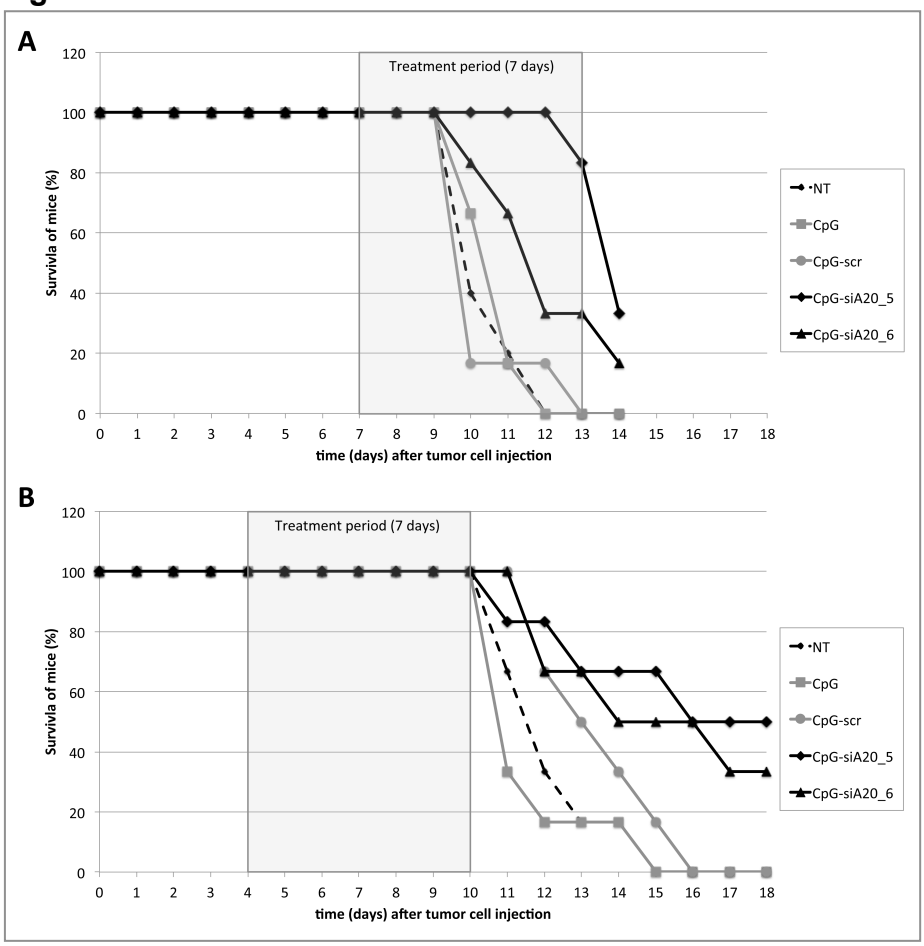

Figure 21: Survival curves of B16 melanoma-bearing mice depending on treatment. C57BL/6N mice (female, 8 weeks old, 6 mice/group) with s.c. growing B16 tumors have been treated peritumorally with 1 nmol CpG/ CpG-scr/ CpG-siA20 (CpG-siA20_5, _6) constructs daily. **(A)** Survival curve of mice with a treatment start at day 7 after tumor cell injection until end of experiment on day 14. **(B)** Survival curve of mice with a treatment start at day 4 after tumor cell injection until day 10. Diagrams showing survival of mice in % over time from time point of tumor cell injection until end of the experiment.

The prolongation of survival time is a result of tumor growth retardation. Mice getting CpG/ CpG-scr construct showed already a delayed tumor growth. CpG-siA20 constructs exceeding this effect even more. Like already described for survival time, the growth retardation is relative to treatment start and amount of applied CpG/ CpG-construct (Fig. 22A, 22B). Increasing the amount of CpG/ CpG-constructs from 1 nmol to 2 nmol per day slowed down the tumor growth significantly compared to non-treated mice. Since these experiments were stopped for all mice together at day 14 no clear statement can be made about survival time. However, tumor growing curves are providing an indication about the positive influence on further improved survival time (Fig. 22C).

Figure 22: Tumor growing curves

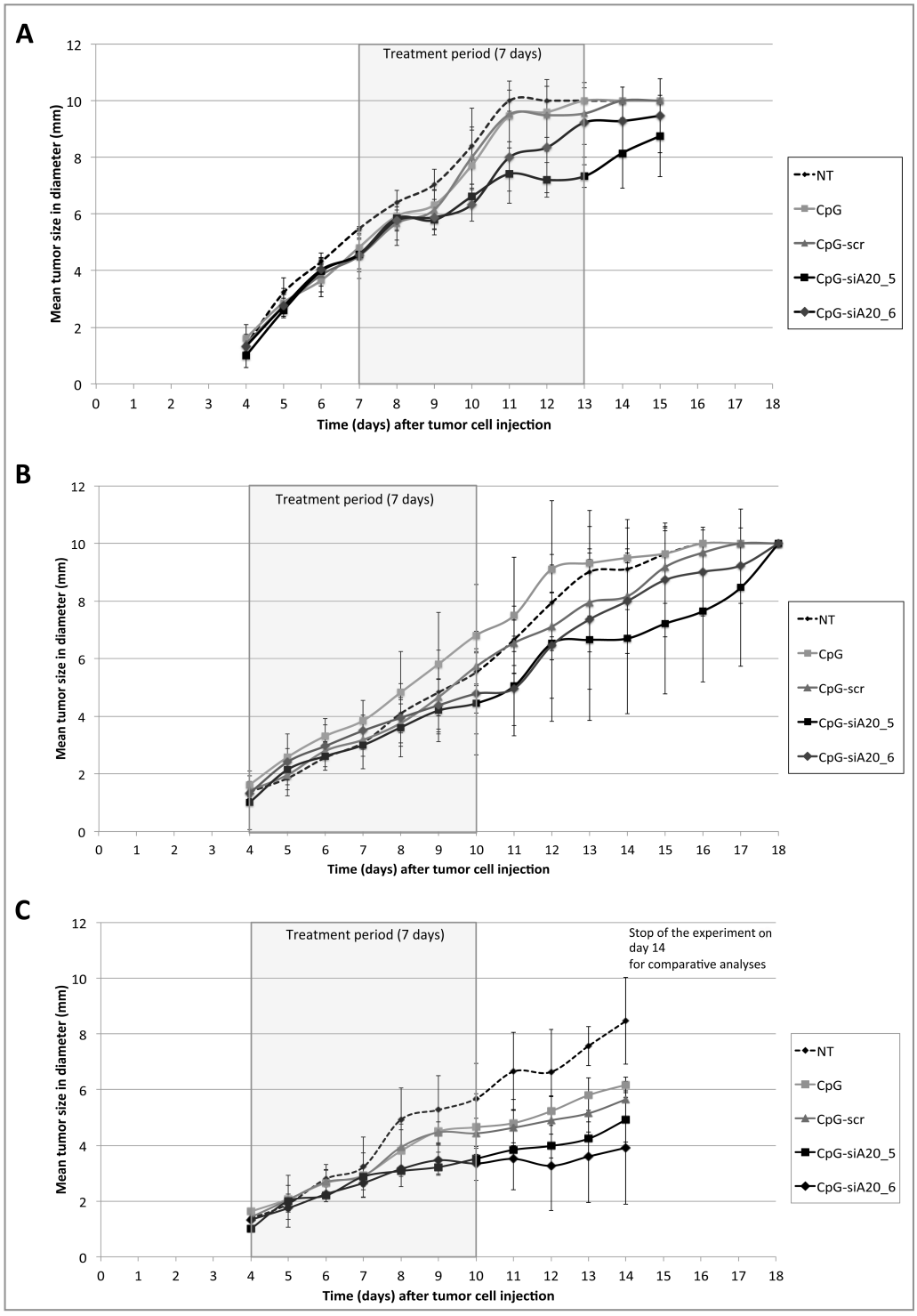

Fig. 22. Tumor growing curves of B16 melanoma after CpG/ CpG-construct treatment. Injection of 1x10^6 B16 melanoma cells s.c. at day 0, repetitive treatment (daily) with CpG/ CpG-scrambled RNA/ CpG-siRNA A20 for 7 days. **(A)** Treatment with 1 nmol CpG/ CpG-constructs starting at day 7. **(B)** Treatment with 1 nmol CpG/ CpG-constructs starting at day 4. **(C)** Treatment with 2 nmol CpG/ CpG-constructs starting at day 4. Graphics showing mean tumor size in mm diameter for six mice per group.

Despite the big variation between the individual mice in each group, the differences in tumor size are clearly visible (Fig. 23).

Figure 23: Mice with s.c B16 tumor

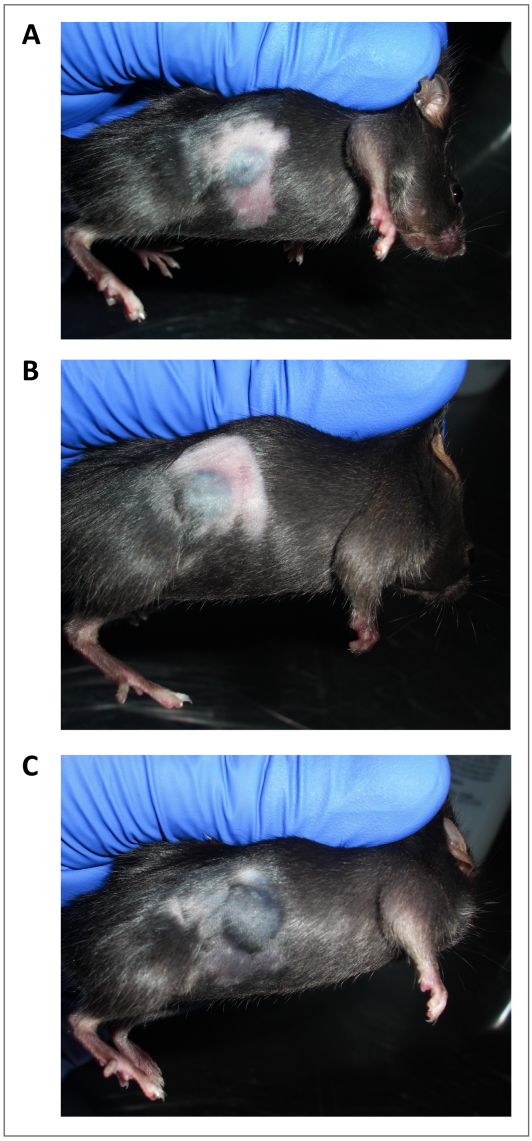

Figure 23: Mice with s.c. growing B16 melanoma tumors.
B16 melanoma cells (1x10^6) were injected s.c. in the right flank of C57BL/6 mice (female, 8 weeks old, 6 mice/group). The pictures are showing tumor development status at day 10 after injection and three days of daily peritumoral treatment. **(A)** One representative mouse after three repetitive treatments with CpG-siA20 construct. **(B)** One representative mouse after three repetitive treatments with CpG. **(C)** One representative mouse without treatment (PBS injections).

Summarizing the tumor size data from all experiments (1 nmol start day 7, 1 nmol start d 4, 2 nmol start d 4) revealed still clear differences. CpG-siA20 construct treated mice had significantly smaller tumors than CpG-treated mice (Fig. 24).

Figure 24: Tumor size comparison

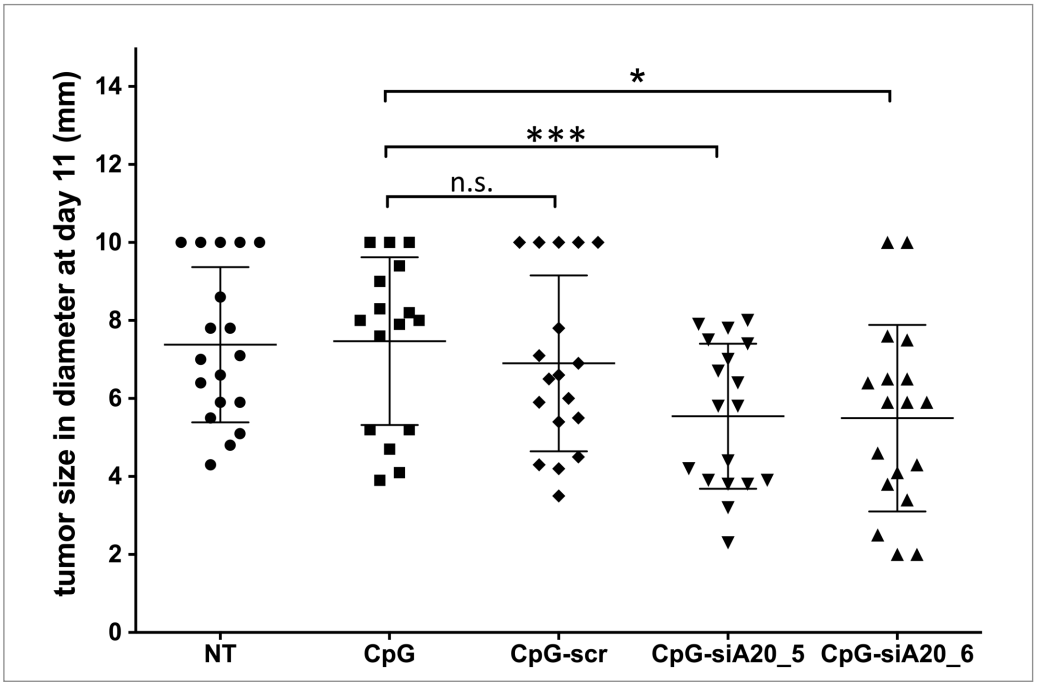

Fig. 24. Tumor size from all three treatment schedules at day 11. Injection of 1x10^6 B16 melanoma cells s.c. at day 0, repetitive treatment (daily) with CpG/ CpG-scrambled RNA/ CpG-siRNA A20 for 7 days. Shown is one exemplary experiment for each of the three treatment schedules (1 nmol start day 7, 1 nmol start d 4, 2 nmol start d 4). Graphic showing tumor size in mm diameter, mean values and variance for six mice per group per experiment (18 mice in total) at day 11. Dead mice appear with the final tumor size of 10 mm. Performed statistical tests: Kruskal–Wallis one-way analysis of variance and Wilcoxon rank-sum test. n.s. indicates not significant, * indicates $p<0.05$, ** indicates $p<0.01$, and *** indicates $p<0.001$ compared to CpG.

CpG-siA20 constructs showed to have strong stimulatory and immune-modulatory effects in healthy naïve mice as well as in tumor-bearing mice *in vivo*.

Next it was investigated whether CpG-siA20 oligonucleotides induced any tumor specific immune response.

B16 melanoma cells are known to express TRP-1 (tyrosinase-related protein-1) [77][79]. RT-qPCR analysis of B16 mRNA before tumor cell inoculation confirmed this (data not shown) outlining TRP-1 as a possible target for detecting tumor-specific immune responses. Circulating immune cells isolated from tumor-bearing mice (treatment start d4, 1 nmol CpG/ CpG-construct) were analyzed at day 11 after tumor cell injection. Cells were stained with FITC-labeled pentamers presenting peptide derived from tumor antigen Trp1, which is expressed by B16 cells, in regards to MHC class I haplotype $H2^b$. This complex specifically binds to Trp1-specific T cell receptors (TCRs).

As shown in Fig. 25, the percentage of CD8-positive cells that were co-stained with the Trp1-pentamer increased clearly when animals were treated with CpG-siA20 constructs.

Figure 25: Tumor-specific CTLs in blood

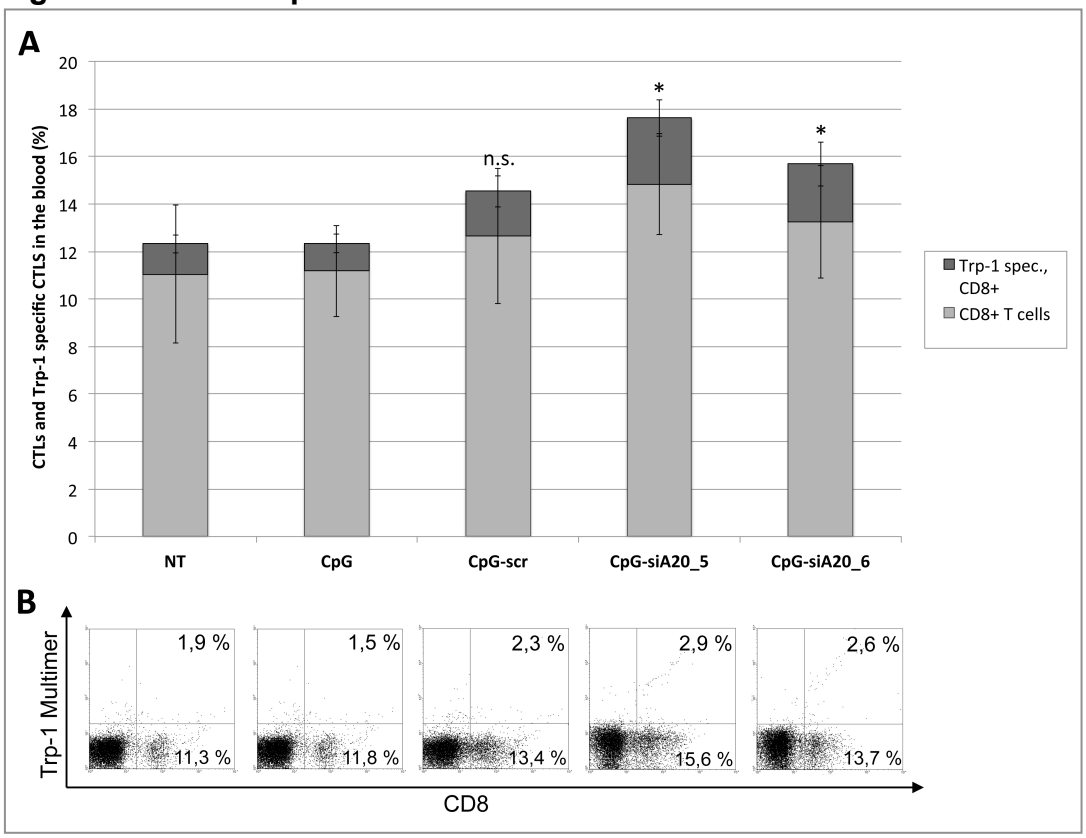

Figure 25: Tumor-specific CTLs in blood of B16 melanoma-bearing mice depending on treatment. C57BL/6N mice (female, 8 weeks old, 6 mice/group) with s.c. growing B16 tumors have been treated peritumorally with 1 nmol CpG/ CpG-scr/ CpG-siA20 (CpG-siA20_5, _6) constructs daily for 7 days, treatment start day 4. For cellular analyses blood has been collected at day 10, detection of Trp-1 tumor-specific CD8+ T cells has been performed by multimer staining. Shown are results from one representative experiment. **(A)** Diagram showing mean %age of CD8+ T cells and TRP-1 specific CTLs depending on treatment; Performed statistical tests: Kruskal–Wallis one-way analysis of variance and Wilcoxon rank-sum test. n.s. indicates not significant, *indicates $p<0.05$ compared to CpG. **(B)** Dot-Plot showing %age of Trp-1 specific CTLs for one representative animal per group. All CpG variants increased the number of tumor-specific CTLs most of all the CpG-siA20 constructs.

Increased levels of tumor-specific CTLs in blood of tumor-bearing mice treated with 1 nmol CpG/ CpG-constructs led to the question how this promising parameter looks like within the tumor. Therefore the next experiments (with 2 nmol CpG/ CpG-constructs) were stopped for all animals at the same time point. At day 14 the tumors from all animals were analyzed for Trp-1-specific and active (IFN-γ positive) CTLs.

The percentage of CD8-positive cells as well as the tumor-specific and active ones increased strongly inside the tumor when animals were treated with CpG-siA20 constructs compared to CpG or CpG-scr (Fig. 26).

Figure 26: Tumor-specific CTLs inside the tumor

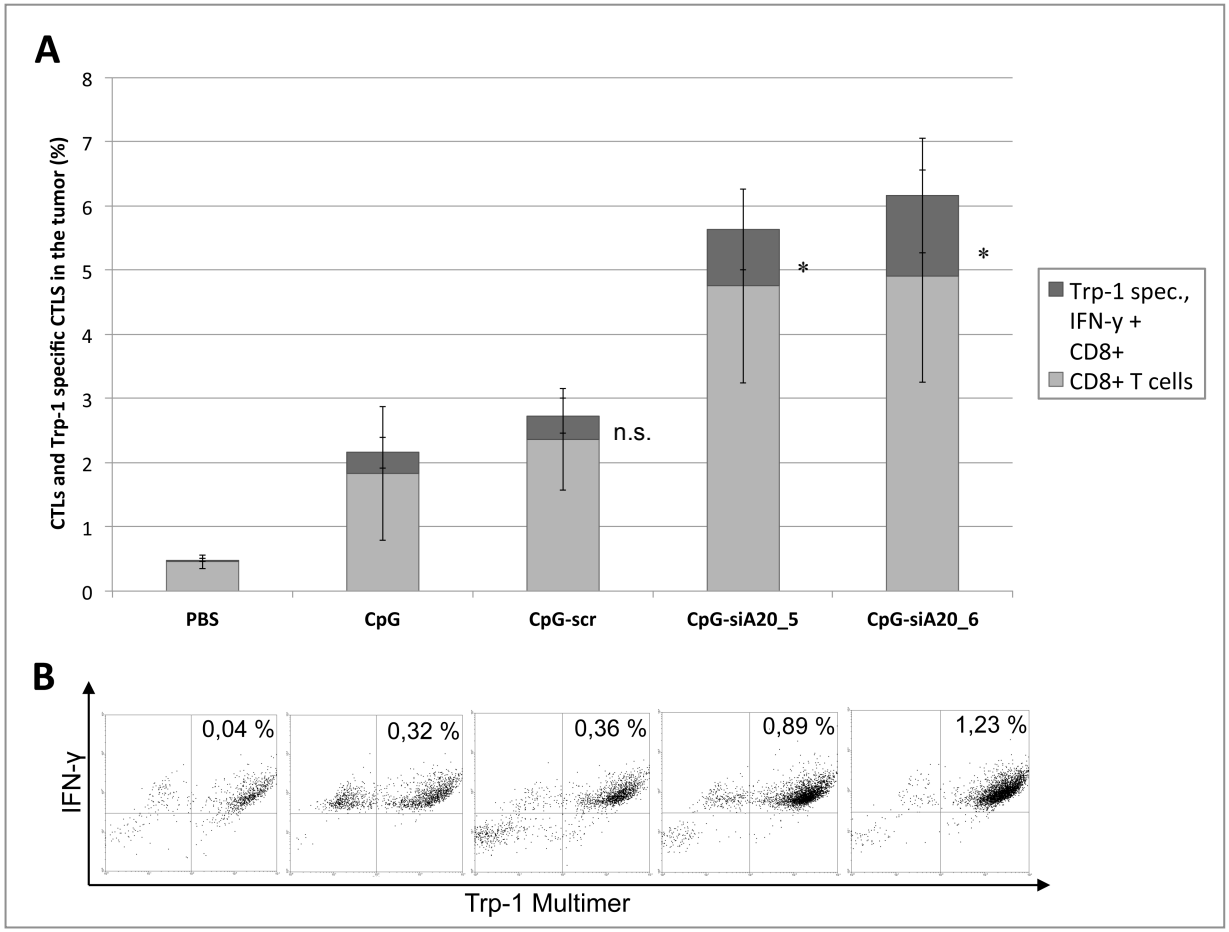

Figure 26: Tumor-specific CTLs in the tumor of B16 melanoma-bearing mice depending on treatment. C57BL/6N mice (female, 8 weeks old, 6 mice/group) with s.c. growing B16 tumors have been treated peritumorally with 2 nmol CpG/ CpG-scr/ CpG-siA20 (CpG-siA20_5, _6) constructs daily for 7 days, treatment start day 4. Tumor collection for cellular analyses at day 14 from all animals, detection of Trp-1 tumor-specific CD8+ T cells has been performed by multimer staining. **(A)** Diagram showing mean %age of CTLs and Trp-1 specific, active (IFN-γ positive) CTLs of 6 mice/ group depending on treatment; Performed statistical tests: Kruskal–Wallis one-way analysis of variance and Wilcoxon rank-sum test. n.s. indicates not significant, *indicates $p<0.05$ compared to CpG. **(B)** Dot-Plot showing %age of Trp-1 specific, active (IFN-γ positive) CTLs related to all lymphocytes inside the tumor for one representative animal per group. All CpG variants increased the number of tumor-specific CTLs most of all the CpG-siA20 constructs.

The level of tumor-specific CD8+ cells correlated with the retardation of tumor growth indicating the efficient induction of a tumor-specific CTL response upon the combined TLR stimulation and A20 attenuation.

Since activation of the cytotoxic arm of the immune system should result in killing of transformed cells, the tumors were checked for the presence of dead or dying cells. At the individual end point of experiment (treatment start d4, 1 nmol CpG/ CpG-construct) the tumors were analyzed using Annexin V/7-AAD staining assay. While CpG alone and CpG-scr construct did not cause significant apoptosis within the tumor, the percentage of dead cells in CpG-siA20 treated groups was substantially elevated, reaching up to 25% of all B16 cells (Fig. 27).

Figure 27: Tumor cell apoptosis

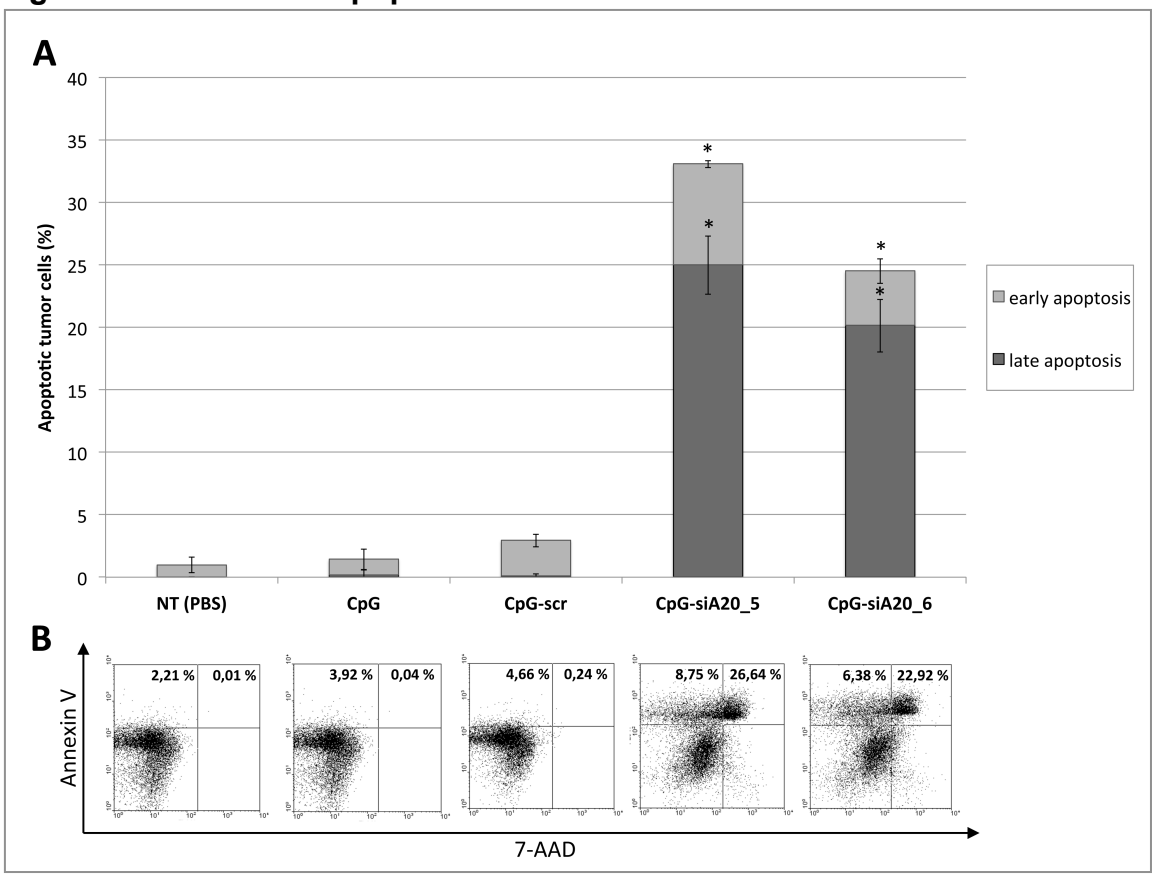

Figure 27: B16 tumor cell apoptosis depending on treatment.
C57BL/6N mice (female, 8 weeks old, 6 mice/group) with s.c. growing B16 tumors have been treated peritumorally with 1 nmol CpG/ CpG-scr/ CpG-siA20 (CpG-siA20_5, _6) constructs daily from day 4 until day 10. Detection of early and late apoptosis of the tumor cells has been performed at the individual end of experiment for each mice using Annexin V/7-AAD. **(A)** Diagram showing mean %age of early (Annexin V positive) and late (7-AAD, Annexin V positive) apoptotic cells for 6 mice/ group; Performed statistical tests: Kruskal–Wallis one-way analysis of variance and Wilcoxon rank-sum test. n.s. indicates not significant, *indicates $p<0.05$ compared to CpG. **(B)** Dot-Plot showing %age of early (Annexin V positive) and late (7-AAD, Annexin V positive) apoptotic cells for one representative animal per group. Especially the CpG-siA20 constructs increased the number of apoptotic tumor cells.

Again, the level of dead tumor cells correlated with the levels of tumor-specific CTLs and slower growth of the tumors. In addition to apoptosis analysis the tumor cells were tested for cell cycle distribution using Propidium iodide method. Strikingly lots of cells were observed in G0-/ G1-phase (75%) but this seemed characteristic for all analyzed samples irrespectively of treatment (data not shown).

The analyses of CpG-siA20 constructs in comparison to CpG/ CpG-scr control in a B16 tumor model showed elevated immune-stimulatory effects manifesting in pro-inflammatory cytokine expression, increased numbers of infiltrating tumor-specific CTLs, and more apoptotic tumor cells. Taken together these factors slowed down tumor growth and by this prolonged the survival of mice.

7.6 CpG-siRNA A20 construct mediated human DC stimulation *in vitro*

In mice, CpG-siA20 constructs have been shown to be a promising tool for selective immune cell stimulation. In humans, the immune cells expressing the target molecule TLR9 differ to those in mice. While in mice immune cells of the myeloid lineage (including monocytes, macrophages and myeloid DCs) express TLR9 and respond to CpG stimulation, in humans, mainly B cells and plasmacytoid DCs express TLR9.
Peripheral DCs isolated from healthy donors` blood and newly designed constructs for the human system were the basis for the first human *in vitro* testing.
Eight healthy donor DCs were treated with 0.5 nmol CpG, CpG-scr or CpG-siA20 (CpG-siA20_59, CpG-siA20_60) constructs and analyzed.

One parameter for CpG-construct function was activation of the NF-κB pathway monitored by IκBa mRNA expression (RT-qPCR). All donor DCs showed responses to CpG/ CpG-construct stimulation whereby time point and intensity differed individually. Most of the donor DCs showed higher stimulatory responses due to CpG-siA20 compared to CpG or CpG-scr treatment (Fig. 28).

Figure 28: NF-κB stimulation in human DCs

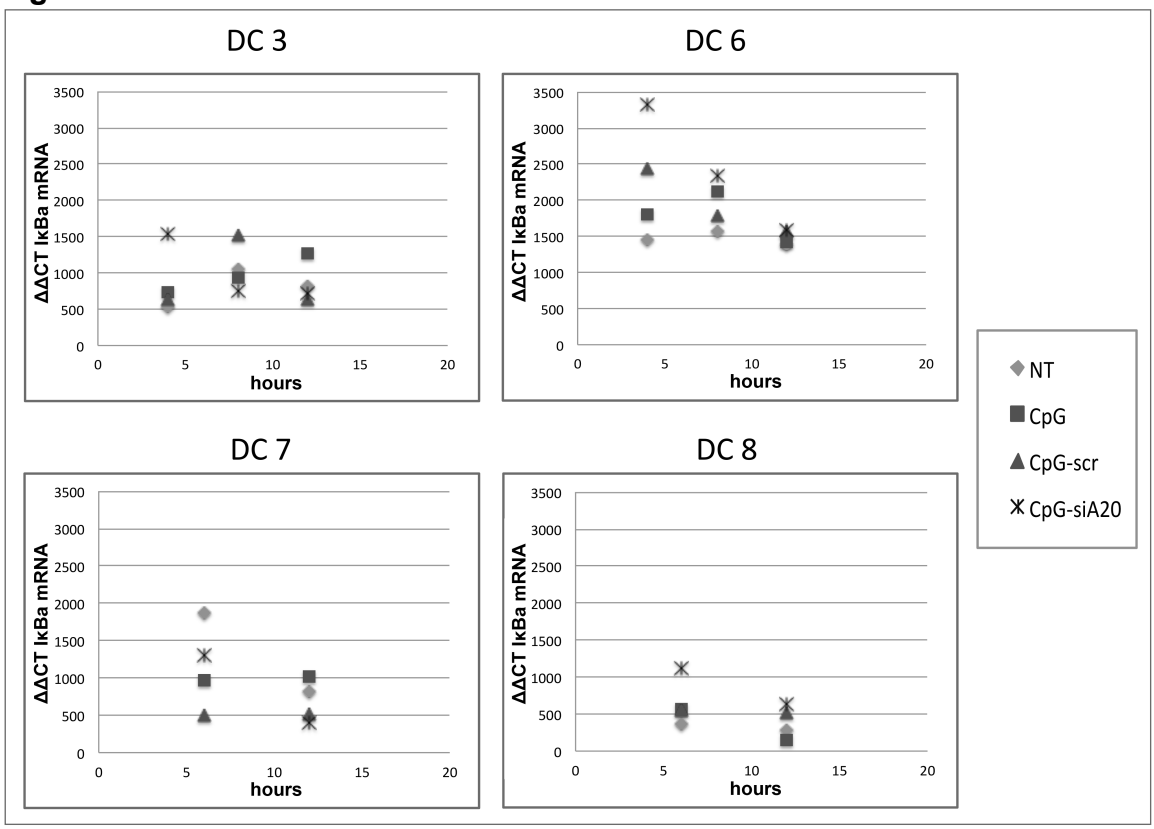

Figure 28: NF-κB stimulation in human DCs after CpG/ CpG-construct treatment *in vitro*. Human DCs isolated from healthy donor blood via positive and negative bead selection have been stimulated with 0.5 nmol CpG, CpG-scrambled siRNA (CpG-scr) or CpG-siRNAs against A20 (CpG-siA20_59, CpG-siA20_60). Shown are 4 out of 8 representative donors. For mRNA analyses cells were collected after 4, 8, 12 hours or after 6 and 12 hours; IκBa mRNA expression levels (ΔΔCT) were measured using RT-qPCR and normalized with ß2MG. All healthy donor DCs are showing responses to CpG/ CpG-construct stimulation whereby time point and intensity differs individually. Most of the donor DCs showed higher stimulatory responses due to CpG-siA20 compared CpG or CpG-scr treatment.

Beside NF-κB activation cytokine expression is a good indicator of DC activation. Performing CBA expression of the cytokines IL-2, IL-6, IL-12p70, TNF-α, and IFN-γ were analyzed at several time points (4, 8, 12 hours or 1, 2, 3, 4, 5, 6, 8, 10, 12 hours) after CpG/ CpG-construct administration.

The cytokines IL-2, IL-12p70, IFN-γ were not detectable using this i*n vitro* system. All healthy donor DCs showed IL-6 induction for all tested CpG/ CpG-construct stimulations whereby time point and intensity differed individually. Five donors showed low IL-6 induction (DC 1, 2, 4, 5, 6) and the others high induction (DC 3, 7, 8) in response to CpG/ CpG-construct stimulation. Nearly all donor DCs showed higher stimulatory responses to CpG-siA20 than for CpG or CpG-scr (Fig. 29).

Figure 29: IL-6 expression in human DCs

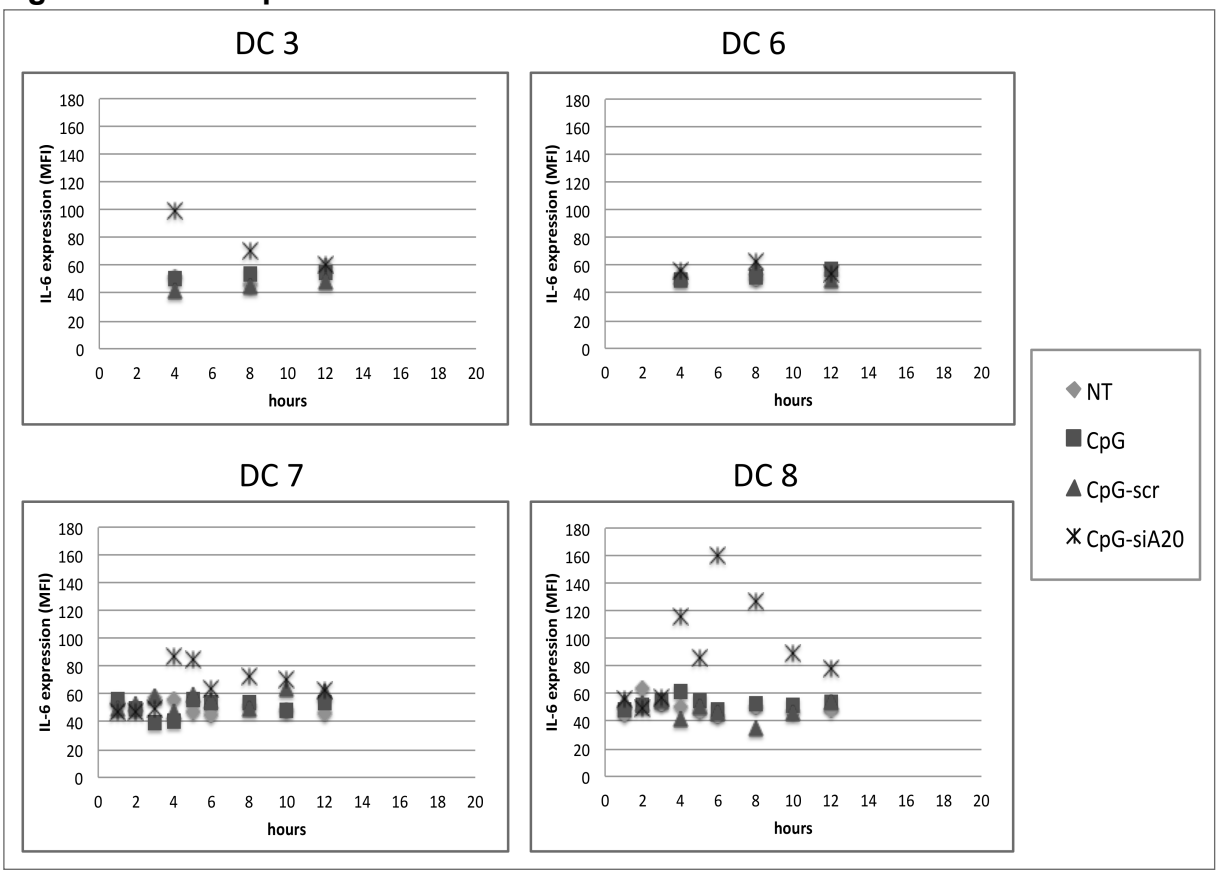

Figure 29: Effects of CpG/ CpG-constructs on human DCs *in vitro*. Human DCs isolated from healthy donor blood via positive and negative bead selection have been stimulated with 0.5 nmol CpG, CpG-scrambled siRNA (CpG-scr) or CpG-siRNA against A20 (CpG-siA20_59, CpG-siA20_60). Shown are 4 out of 8 representative donors. For cytokine analyses cell culture supernatants were collected after 4, 8 and 12 hours or after 1, 2, 3, 4, 5, 6, 8, 10, 12 hours; IL-6 protein levels were measured using CBA and calculated by a standard curve. All healthy donor DCs are showing responses to CpG/ CpG-construct stimulation whereby time point and intensity differs individually. Nearly all donor DCs showed higher stimulatory responses due to CpG-siA20 compared CpG or CpG-scr treatment.

Another cytokine, which was induced due to CpG/ CpG-construct stimulation, though only at a low level, was TNF-α. All healthy donor DCs were showing responses to CpG containing formulations whereby time point and intensity differed individually. Half of the donors showed low TNF induction (DC 1, 3, 4, 5) and half high induction (DC 2, 6, 7, 8) in response to CpG/ CpG-construct stimulation. All donor DCs showed higher stimulatory TNF responses due to CpG-siA20 than compared CpG or CpG-scr (Fig. 30).

Figure 30: TNF-α expression in human DCs

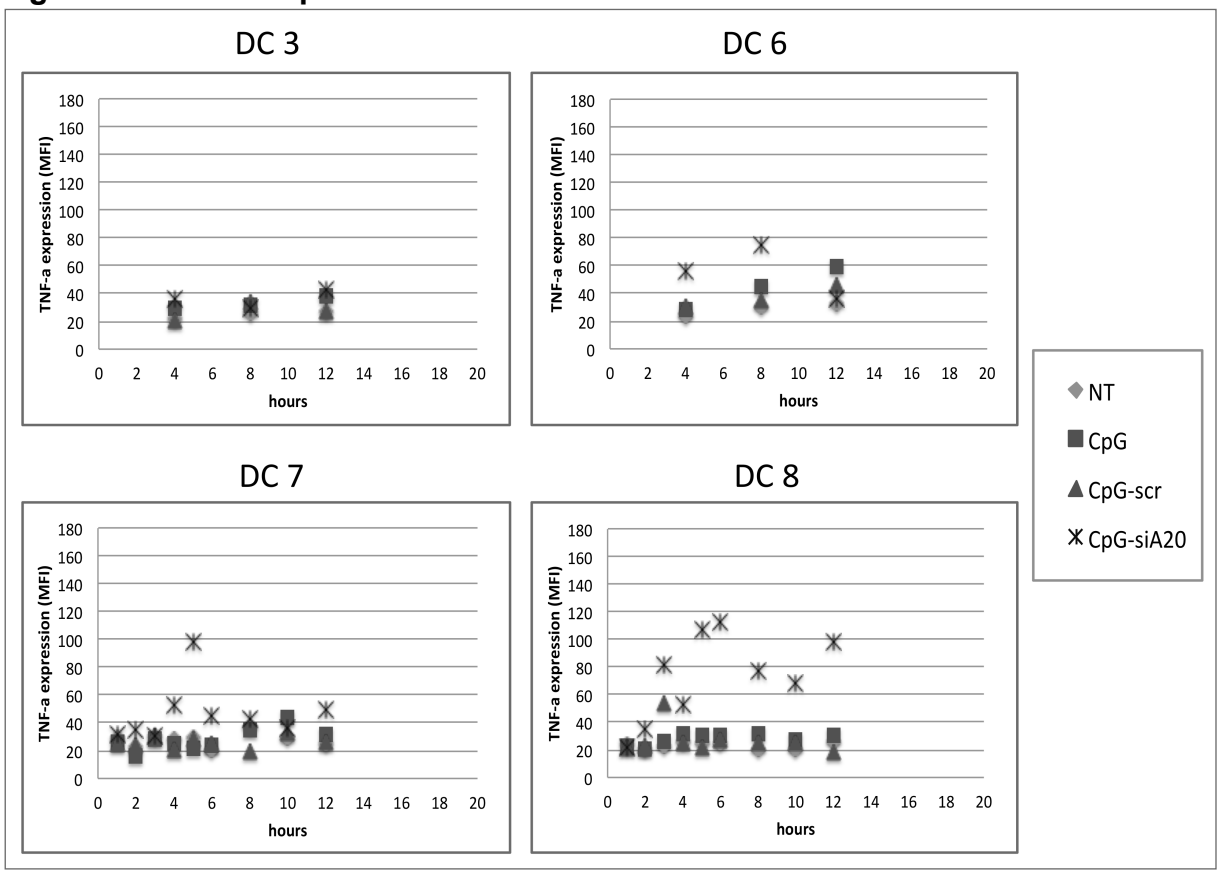

Figure 30: Effects of CpG/ CpG-constructs on human DCs *in vitro*. Human DCs isolated from healthy donor blood via positive and negative bead selection have been stimulated with 0.5 nmol CpG, CpG-scrambled siRNA (CpG-scr) or CpG-siRNA against A20 (CpG-siA20_59, CpG-siA20_60). Shown are 4 out of 8 representative donors. For cytokine analyses cell culture supernatants were collected after 4, 8 and 12 hours or after 1, 2, 3, 4, 5, 6, 8, 10, 12 hours; TNF-α protein levels were measured using CBA and calculated by a standard curve. All healthy donor DCs are showing responses to CpG/ CpG-construct stimulation whereby time point and intensity differs individually. Nearly all donor DCs showed higher stimulatory responses due to CpG-siA20 compared CpG or CpG-scr.

The promising results from murine *in vitro* and *in vivo* experiments could partially be confirmed in the tested human *in vitro* system. Initial results indicate elevated NF-κB activation alongside increased IL-6 and TNF-α cytokine secretion in response to CpG-siA20 compared to CpG or CpG-scr control. Although further experiments are needed to investigate the full impact of CpG-siA20 constructs on human DCs and the other TLR9 expressing target cells of the CpG-headed immune cell stimulation, the CpG-siA20 constructs showed already to be an innovative tool for effective and targeted cell stimulation in humans too.

8 DISCUSSION

A competent patient immune system is an important basis for cancer immunotherapies. Frequent tumor-induced immune suppression is thereby one of the main obstacles in this field, which needs to be overcome. Silencing of the natural NF-κB inhibitor A20 in DCs leads to an enhanced stimulatory capacity of DCs. This switch from immune suppressive factors to immune effector functions can probably disrupt a tumor induced immune tolerance. The dual role of CpG ODNs in targeting and stimulating TLR9-expressing DCs is an ideal tool for targeted siRNA delivery in parallel to cell stimulation. In this study, one synthetic molecule combining these activities was synthesized adopting a strategy established by Kortylewski and coworkers [39]. This molecule consists of a CpG ODN linked to a siRNA against A20. This molecule is easy to apply and presents the basis for a local, targeted and transient A20 knockdown in tumor associated cell types, especially in DCs, directly *in vivo.*

8.1 Generation of a long-term growth factor dependent mouse DC line

DCs hold a central role in the immune system, by regulating the switch between tolerant and activated states [5]. Depending on their maturation state and the cytokines they express, DCs may either create an immune suppressive microenvironment or support the expansion of tumor-associated antigen specific T cells. For *in vitro* analyses of CpG/ CpG-construct function on mouse DCs a long-term growth factor dependent bone marrow-derived DC (BMDC) culture was established. Bone marrow progenitor cells treated *in vitro* with GM-CSF differentiate into BMDCs, which phenotype resembles the naturally occurring DCs [43][44]. GM-CSF addition is leading to DC, monocyte/ macrophage and granulocyte cell differentiation [45]. Separation of the unwanted cell populations from the generated cell mixture via their different adherence properties resulted in enriched DC cultures. These DCs were suitable *in vitro* model systems for studying stimulatory capacities and cytokine secretion after stimulation. However, the separated DCs showed limited survival even under steady GM-CSF supplementation. Co-culturing with the unwanted cell populations was found to facilitate a long-term culturing of the wanted BMDCs.

The underlying mechanisms are not fully understood presuming a beneficial environment for DC maintenance.

Depending on generation protocol, the maturation condition of each BMDC culture differs and has to be elevated by fluorometric analyses of activation markers. BMDCs are known to be easily activated during handling, such as processing, culturing, and purification [46]. In our hands only 20% of BMDCs showed CD80 and CD86 activation marker expression, which is an indication for mainly immature DC phenotypes. After three weeks of culturing the phenotype changed to more mature DCs showing 70-90% CD80, CD86 positive cells which remained for the rest of culturing time (more than one year).

The DC line JAWSII displayed a secondary model system for construct *in vitro* testing. JAWSII is an immortalized immature DC line, which has been established from the bone marrow cultures of $p53^{-/-}$ C57BL/6 mice. This cell line is used for studies of anti-tumor [47][48] and pathogen-specific [49] immunity. JAWSII, consisting of two cell types, adherent monocytes and suspension DCs, were separated prior use in *in vitro* analyses.

Both murine DC models were suitable testing systems for CpG-construct internalization and stimulation. However, BMDCs resemble the natural occurring DCs better than the immortalized cell line JAWSII.

8.2 A20 knockdown in mouse DCs *in vitro*

The TNFAIP3 gene encoding the A20 protein has been recently identified as an essential factor, which regulates the maturation of DCs, negatively according to their production of inflammatory cytokines and general stimulatory properties [28]. A20 silenced DCs show enhanced expression of co-stimulatory molecules and pro-inflammatory cytokines [28].

Cellular uptake and intracellular trafficking to the endoplasmic reticulum represent major technical obstacles for effective siRNA mediated A20 silencing in DCs. During the last years several new delivery systems were developed. Some of them were inadequate for *in vivo* applications because of inherent risks (viral vectors) [50][51][52], high toxicity or low efficiency (liposomes, cationic polymers) [53]. However, others seem to be promising (peptides, nanoparticles) [54]. In combination with antibodies or cell-specific ligands, some of these complexes, e.g. nanoparticles, are even capable of targeted cellular deliveries [55]. The dual role of CpG ODNs in targeting and stimulating TLR9-expressing DCs displays an ideal tool for specific A20 siRNA delivery in parallel to cell stimulation.

Treatment of bone marrow derived DCs or JAWSII cells with CpG-siA20 conjugates led to rapid construct internalization and A20 knockdown.

The A20 downregulation was followed by elevated NF-κB signaling and cytokine secretion, which were superior compared to CpG alone or to CpG fused with irrelevant siRNA. Proving A20 silencing on protein level was complicated by the fast feedback mechanisms between A20 and NF-κB. A20 was upregulated initially in all samples treated with CpG or CpG-siRNA constructs. At a later time, 20 hours after treatment, the amount of A20 protein decreased selectively in cells treated with CpG-siA20 constructs. However, already 4 hours later the A20 protein signal had returned to higher levels than those in control cells. In our opinion the reason for this phenomenon is the fact that A20 is a NF-κB target itself. Hence, the augmented activity of NF-κB due to initial A20 depletion ultimately leads to a rebound with increased A20 levels along with other NF-κB targets like IκBα, IL-6 or TNF-α.

8.3 CpG-siRNA A20 construct mediated DC stimulation *in vitro*

The maturation of DCs, required for effective immune response, can be accelerated by providing stimuli such as inflammatory cytokines or cross-linking of co-stimulatory receptors. It has been demonstrated that activated through their TLRs DCs are capable of inducing tumor-specific cytotoxic T cell [56]. Triggering TLRs activates multiple transcription factors, which ultimately induce the expression of characteristic cytokines and surface molecules, which indicate a phenotype of mature and fully functional DCs [57].

The CpG-siA20 construct can be applied without the need of any additional transfer or vector systems, a major advantage compared to other approaches aiming A20-depletion. A20 silencing in addition to CpG-mediated DC stimulation leads to enhanced/ prolonged immune-stimulatory responses.

Activated DCs produce many cytokines, for example IFN-α, IL-6, IL-12 and TNF-α [8][58]. CpG-siA20 induced DC activation was analyzed by performing RT-qPCR to detect the mRNA levels of IκBα, IL-6, and TNF-α. Upregulation of IκBα gene expression is a consequence of NF-κB activation and a general sign of cellular activation due to TLR9 stimulation and of A20 silencing [59].

The cytokine IL-6 plays an important role in the regulation of immune responses and is produced among others by activated DCs [60][61]. TNF-α is a pro-inflammatory cytokine involved in cell stimulation and activation in response to inflammatory stimuli [62]. Expression of these three NF-κB targets demonstrates successful DC activation and cytokine production.

8.4 CpG-siRNA A20 construct mediated immune stimulation *in vivo*

CpG-siRNA A20 construct uptake and mediated cell stimulation has been verified *in vitro* in murine DCs. *In vivo* this has been tested first in healthy C57BL/6N wild type mice before transferring to the tumor model. The intraperitoneal application strategy was chosen for monitoring local effects on directly exposed immune cells as well as systemic effects on cytokine levels. Just in one application set, 12 hours after the second of two daily injections, cells with internalized FITC-labeled constructs were detectable in the peritoneum. Especially DCs and NK cells, to lower extent also B cells, were FITC-positive after construct injection. Kortylewski et al. showed internalization by MΦ, DCs, and myeloid cells at injection site in tumor-free mice [39]. For more precise analysis of immune cell populations taking up CpG-siRNA constructs *in vivo,* another fluorescent marker would be more suitable because of high self-fluorescence of the cells of interest. Also more dense time points would be needed for not missing construct positive cells before leaving peritoneal cavity. In consequence to these critical points no definite assertion concerning *in vivo* construct uptake could be done so far.

Besides cellular siRNA uptake, there are additional hurdles *in vivo*, such as serum stability, aggregation with serum proteins, and uptake by phagocytes [63][64]. As demonstrated by multiple studies, much higher silencing activities could be obtained by increasing the length of siRNA oligonucleotides [65]. Even better efficiency may be obtained when the gene targeting sequence is presented in the context of the naturally occurring miRNA backbones [66]. Moreover, increasing the serum stability and reducing the negative charge of the conjugates by chemical modifications might result in more efficient and sustained A20 knockdown [67].

The choice of CpG ODN type is another important factor for effective immune-stimulation and induction of antigen-specific immune responses. In this study a CpG B-class ODN, called CpG 1668, was used for murine *in vitro* and *in vivo* experiments. B-class ODNs can enhance antigen cross-presentation and induce the development of an adaptive T cell response, whereas CpG A-class ODNs mainly impact NK cells and innate immunity [68][69]. B-class ODNs were shown to be more effective for the treatment of EL4 lymphoma than A-class ODNs [68]. Treatment of B16 melanoma was more effective with A-class than with B-class CpG ODN suggesting NK cell mediated tumor reduction [68]. For future studies on CpG-siRNA A20 function, CpG class could be more adapted to tumor model type and induced immunologic effects to exploit their full potential. A promising solution could be CpG C-type ODNs, which combine stimulatory capacities of CpG A- and B-class [69]. The repertoire of synthetic CpG oligonucleotides differing in their immune-stimulatory properties and cell specificity is constantly expanding and some types are already submitted to the pre-/clinical trials [70][71][72]. Despite or even because of plenty of structural optimization possibilities, the utilization of CpG ODNs for targeted delivery of siRNA displays a promising tool for selective *in vivo* gene silencing.

A20 silencing in TLR9 expressing immune cells, especially DCs, was supposed to induce strong immune stimulation. The levels of pro-inflammatory cytokines in serum increased in all animals, which received CpG or CpG fused to siRNA. However, A20 specific siRNA constructs increased the concentration of IL-6, TNF-α and IFN-γ significantly more than CpG alone or its fusion with irrelevant siRNA.

A20 silencing in addition to CpG-mediated cell stimulation led to enhanced/ prolonged immune-stimulatory responses. A risk of this immune stimulatory agent is the possibility of enhanced immunogenicity to self-proteins. By this they may trigger the development of autoimmune disease or increase the susceptibility to pathogenic agents that cause toxic shock. A20 deficiency in DCs leads to activated DCs, B cells, T cells, and autoantibodies which can cause a pathology with features of systemic autoimmune diseases [27]. On the other hand, CpG-treated animals (mice, non-human primates) showed no macroscopic or microscopic evidence of tissue damage or inflammation [68][73]. In several Phase I and II studies the use of CpG ODNs was tested to optimize the immunotherapy of patients. None of the CpG exposed patients developed signs or symptoms of autoimmune disease [73].

In this study using CpG/ CpG-siRNA constructs, there were no signs of immune suppression by increased IDO expression in spleens detectable, which was described after systemic application of high doses of CpG [74]. In our experiments performing transient A20 knockdown there were no signs of toxicity detectable. However a screening for autoimmune related symptoms and diagnostic parameters (e.g. fever, complete blood count, C-reactive protein elevation), could be a reasonable addition for future experimental set ups.

8.5 Effects of CpG-siRNA A20 construct treatment on B16 tumors *in vivo*

The immune-stimulatory effects of CpG-siRNA A20 constructs were tested for capability of inducing anti-tumor effects in C57BL/6N wild type mice *in vivo*. The tumor model of choice was the murine melanoma cell line B16. These tumor cells established after subcutaneous injection local tumors under the skin. The B16 cells were chosen as they originating from the same mouse strain used for *in vivo* studies. They express known tumor antigens and the tumor cells were well visible due to their high melanin content. The fast and aggressive growing character of these tumor cells was an underestimated disadvantage of this model, since the untreated melanoma tumors reached their final size of 1 cm in diameter already after 10-12 days. A more slowly growing tumor would have been beneficial to increase the therapeutic window.

The described approach using CpG-siRNA constructs for A20 silencing displays a targeted stimulation of TLR9 expressing cells. Therefore, B16 tumor cells were analyzed for TLR9 expression before use. TLR expression has been observed in some tumor entities showing diverse effects due to their stimulation reaching from apoptosis induction to cell proliferation [75][76][77]. The B16-F1 cell line used in this study showed no TLR9 expression on mRNA level. Additionally performed co-culturing of tumor cells with CpG/ CpG-siRNA constructs revealed no direct effects on NF-κB target gene expressions.

To evaluate the potential of detecting tumor-specific immune responses, B16 melanoma cells were analyzed for known tumor antigen expression [77][79] on mRNA level. The B16-F1 cell line used in this study showed veritable Trp-1 antigen expression outlining a good basis for tumor model experiments.

One million tumor cells were inoculated under the skin at the right flank of the mice to generate a model of established solid tumors. Since the aim was to target immune cells in the immunosuppressive tumor environment, repeated peritumoral treatments with 1 or 2 nmol CpG/ CpG-constructs were performed. The intensity of induced immune-stimulation was majorly monitored by systemic cytokine expression in blood. It was possible to monitor changes in serum cytokine levels during the whole experimental period, since only a few drops of blood are needed for the analyses. The cytokines showed prompt treatment responses with the highest fold change from all analyzed parameters and comparable results in all experiments irrespectively of treatment schedule. Regardless of the stage of tumor growth, the injection of conjugates increased serum concentrations of IL-6, TNF-α, IFN-γ and IL-12p70 cytokines. The elevation of IL-12 may be particularly important. It has been shown recently in human monocyte-derived DCs that the immune-stimulatory effect of A20 depletion, measured as the capacity to induce a Th1 response, is critically dependent on the secretion of this cytokine by DCs. This is in agreement with the well-known fact that IL-12 promotes activation of NK, NKT, Th1 and Tc1 cells [30][57][80][81].

IFN-γ plays an important role in context of CTL and NK cell killing of tumor cells. CpG-activated NKT cells produce IFN-γ, which enhances DC maturation and promotes further IFN-γ production and tumor-specific responses by CD8+ T cells [82].

Interestingly, IL-10, an immunosuppressive cytokine known to be expressed by DCs was elevated in all treated groups regardless of the A20 targeting. Nevertheless, this resulted not in changes on Treg side at the analyzed time points.

Recently it was shown that Th-1 cells can lead to cancer cell senescence, a state of stable or permanent growth arrest, by producing IFN-γ and TNF [83][84]. Since these cytokines were highly induced due to CpG-siA20 stimulation cell cycle analyses of the isolated tumor cells were performed. Increased cell cycle G1/S ratio should by an indicator for cancer cells being in a permanently non-proliferating state [83]. At the analyzed time point (day 14 after tumor cell injection) the comparison of cell cycle distribution revealed no treatment-related differences. Cytokine-induced tumor cell senescence could not be approved as the driving force behind the anti-tumor effects of CpG-siA20 constructs. Analyses of tumor cell status at more time points ought to clarify this issue.

However, only in mice treated with CpG-siA20 conjugates the rise of soluble inflammatory factors in the serum was accompanied by a dramatic increase of the percentage of tumor-antigen-specific CD8+ T cells. The activation of cytotoxic CD8+ T cells upon CpG treatment had been described in various tumor and vaccination model systems [85][86][87][88]. Experiments using CD8-ko mice [87] or antibody-mediated CD8 depletion [88] showed the direct involvement of CTLs in tumor regression/eradication. Although the tumor progression could not be stopped in this study, simultaneous stimulation of TLR9 and A20 knockdown resulted in its substantial delay. A strong induction of cell death within these tumors clearly correlated with slower growth. Why such a strong activation of the immune system did not led to tumor eradication remains to be addressed. B16 is among the most aggressive tumor types, refractory to most treatment approaches [88][90]. Secondly, the performed experiments demonstrate that the outcome differed depending on the size of tumor at treatment initiation. The differences between A20-inhibited and control animals could possibly have been magnified by further reducing the interval between tumor inoculation and injection of the conjugates. However, purpose of this study was to validate construct function in a system where the tumors were well established for treatment rather than tumor prevention schedule.

8.6 CpG-siRNA A20 construct mediated human DC stimulation *in vitro*

The CpG-siRNA A20 constructs showed strong immune-stimulatory capacities and promising anti-tumor effects *in vivo* in mice. For transferring this approach to the human system new constructs were designed consisting of a CpG targeting human TLR9 and siRNA silencing human A20 or scrambled siRNA without function as a control.

In mice, immune cells of the myeloid lineage (including monocytes, macrophages and myeloid DCs) express TLR9 and respond to CpG stimulation, whereas in humans, these cell types generally do not express TLR9 and cannot be directly activated by CpG ODNs [35]. In humans pDCs and B cells are the only immune cells that can be directly stimulated by CpG ODNs. NK cell activation and IFN-γ induction seem to be indirect effects mediated through pDCs [91][92].

CpG ODNs are also capable of promoting peptide-specific CTL response in the human system. *In vitro* peptide-specific cytotoxic activity was present after treatment of PBMCs plus T cells with CpG A-, B-, and C-class ODNs, whereas A-type CpGs were more effective than the others [93]. However, so far only B-type CpG is in use for clinical treatments [94]. For our first *in vitro* testing of human CpG-siRNA A20 constructs A-type CpG ODN and human DCs isolated from healthy donor`s blood has been used.

All CpG containing agents induced NF-κB stimulation and IL-6, TNF-α cytokine secretion whereby CpG-siA20 constructs had stronger effects in most donor DCs. Time point and intensity of stimulatory response varied between individual donors showing no correlation with age, gender or blood group. Donor background and details about blood handling before handed over for cell preparation, were unknown and could have influenced experimental outcomes. For the analysis all DC populations (pan-DCs) were isolated from the donor blood. Since TLR9 in humans is mainly expressed by plasmacytoid DCs, further experiments with this subpopulation would be of interest. Beside the observed stimulatory effects on NF-κB activation and cytokine production further results according the peptide-specific cytotoxic activity and anti-tumor potential would also be interesting supplements.

9 CONCLUSIONS AND OUTLOOK

An important requirement for effective cancer immunotherapy is a potent patients` immune system. Therefore supplementation with immune stimulating reagents is usually necessary. The novel CpG-siRNA A20 construct used in this project combines CpG-mediated stimulation of TLR9 expressing cells with targeted A20 silencing for prolonged NF-κB activation. The construct enables a local, targeted and transient A20 knockdown in tumor associated cell types, especially in DCs, directly *in vivo.* Construct-mediated NF-κB activation in DCs is leading to a multitude of activating and stimulating factors culminating in activation of antigen presenting cells, antigen-specific cytotoxic T cells, and a strong Th1 response.

The major objectives of this study were to examine whether TLR9 mediated A20 silencing via CpG-siRNA constructs is possible and if this knockdown acts synergistically to the CpG ODN induced cell stimulation. Employing bone marrow-derived DCs and the immature DC line JAWSII construct uptake and dendritic cell stimulation *in vitro* were shown successfully. Furthermore, it was proven that silencing of A20 enhances the CpG-induced activation of NF-κB followed by increased expression of IL-6 and TNF-α. A further purpose was to utilize these constructs to stimulate immune cells directly *in vivo*. CpG-siRNA A20 constructs were incorporated by TLR9 expressing immune cells and induced strong immune-stimulatory responses after intraperitoneal application in healthy mice.

Final goal was to improve the anti-tumor immune response and break tumor-induced immunosuppression for prolongation of survival. In mouse tumor model experiments subcutaneous growing B16 melanoma tumors were treated. Peritumoral CpG-siRNA A20 injections induced potentiated anti-tumor immune responses, manifested by elevated cytokine expression, increased numbers of activated tumor-specific cytotoxic T cells, and high levels of tumor cell apoptosis. Despite very fast and aggressive growing tumor cells, delayed tumor growth and prolongation of survival could be accomplished. The performed experiments revealed concentration and treatment schedule dependent treatment outcomes. The sooner the treatments starts, the better. The optimal construct concentration as well as the duration of treatment remaining to be clarified.

In summary, the experimental results show that the simultaneous activation of TLR9 and attenuation of A20 expression in DCs using the *in vivo* deliverable CpG-siRNA conjugate is capable of inducing a strong and specific immune response against an established tumor. This approach represents an attractive alternative to current therapeutic trials employing TLR agonists alone and/or manipulating DCs *ex vivo*. CpG ODNs as well as siRNA part of the constructs facilitate several modification opportunities for improved and tumor-specific therapeutical effects. Therefore, the novel CpG-siA20 construct represents an adjustable and targeted immune stimulatory approach with a great potential. First experiments in human system confirm the potentiated function of TLR9 stimulation in parallel to A20 silencing for improving DC activation. Further experiments are needed to show future perspective of this promising new adjuvant in improving cancer immunotherapy.

10 LIST OF FIGURES

11 REFERENCES

[1] Stewart TJ, Greeneltch KM, Lutsiak ME, Abrams SI. (2007) Immunological responses can have both pro- and antitumor effects: implications for immunotherapy. Expert Rev Mol Med. 9(4):1-20. Review.

[2] Dunn GP, Old LJ, Schreiber RD. (2004) The immunobiology of cancer immunosurveillance and immunoediting. Immunity. 21(2):137-48. Review.

[3] Dunn GP, Old LJ, Schreiber RD. (2004) The three Es of cancer immunoediting. Annu Rev Immunol. 22:329-60. Review.

[4] Rabinovich GA, Gabrilovich D, Sotomayor EM. (2007) Immunosuppressive strategies that are mediated by tumor cells. Annu Rev Immunol. 25:267-96. Review.

[5] Whiteside TL, Odoux C. (2004) Dendritic cell biology and cancer therapy. Cancer Immunol Immunother. 53(3):240-8. Epub 2003 Dec 18. Review.

[6] Steinman RM, Hawiger D, Liu K, Bonifaz L, Bonnyay D, Mahnke K, et al. (2003) Dendritic cell function in vivo during the steady state: a role in peripheral tolerance. Ann N Y Acad Sci. 2003 Apr;987:15-25. Review.

[7] Macatonia SE, Hosken NA, Litton M, Vieira P, Hsieh CS, Culpepper JA, et al. (1995) Dendritic cells produce IL-12 and direct the development of Th1 cells from naive CD4+ T cells. J Immunol. 154(10):5071-9.

[8] Cella M, Scheidegger D, Palmer-Lehmann K, Lane P, Lanzavecchia A, Alber G. (1996) Ligation of CD40 on dendritic cells triggers production of high levels of interleukin-12 and enhances T cell stimulatory capacity: T-T help via APC activation. J Exp Med. 1996 Aug 1;184(2):747-52.

[9] Satthaporn S, Eremin O. (2001) Dendritic cells (I): Biological functions. J R Coll Surg Edinb. 2001 Feb;46(1):9-19. Review.

[10] Nefedova Y, Nagaraj S, Rosenbauer A, Muro-Cacho C, Sebti SM, Gabrilovich DI. (2005) Regulation of dendritic cell differentiation and anti-tumor immune response in cancer by pharmacologic-selective inhibition of the janus-activated kinase 2/signal transducers and activators of transcription 3 pathway. Cancer Res. 65(20):9525-35.

[11] Yang AS, Lattime EC. (2003) Tumor-induced interleukin 10 suppresses the ability of splenic dendritic cells to stimulate CD4 and CD8 T-cell responses. Cancer Res. 63(9):2150-7.

[12] Bharadwaj U, Li M, Zhang R, Chen C, Yao Q. (2007) Elevated interleukin-6 and G-CSF in human pancreatic cancer cell conditioned medium suppress dendritic cell differentiation and activation. Cancer Res. 67(11):5479-88.

[13] Janeway CA Jr, Medzhitov R. (2002) Innate immune recognition. Annu Rev Immunol. 2002;20:197-216. Review.

[14] Akira S, Uematsu S, Takeuchi O. (2006) Pathogen recognition and innate immunity. Cell. 124(4):783-801. Review.

[15] Kadowaki N, Ho S, Antonenko S, Malefyt RW, Kastelein RA, Bazan F, Liu YJ. (2001) Subsets of human dendritic cell precursors express different toll-like receptors and respond to different microbial antigens. J Exp Med. 194(6):863-9.

[16] Song XT, Evel-Kabler K, Shen L, Rollins L, Huang XF, Chen SY. (2008) A20 is an antigen presentation attenuator, and its inhibition overcomes regulatory T cell-mediated suppression. Nat Med. 14(3):258-65. doi: 10.1038/nm1721.

[17] Malynn BA, Ma A. (2009) A20 takes on tumors: tumor suppression by an ubiquitin-editing enzyme. J Exp Med. 206(5):977-80. doi: 10.1084/jem.20090765. Review.

[18] Skaug B, Jiang X, Chen ZJ. (2009) The role of ubiquitin in NF-kappaB regulatory pathways. Annu Rev Biochem. 78:769-96. doi: 10.1146/annurev.biochem.78.070907.102750.

[19] Wertz IE, O'Rourke KM, Zhou H, Eby M, Aravind L, Seshagiri S, Wu P, Wiesmann C, Baker R, Boone DL, Ma A, Koonin EV, Dixit VM. (2004) De-ubiquitination and ubiquitin ligase domains of A20 downregulate NF-kappaB signalling. Nature. 430(7000):694-9.

[20] Chanudet E, Ye H, Ferry J, Bacon CM, Adam P, Müller-Hermelink HK, Radford J, Pileri SA, Ichimura K, Collins VP, Hamoudi RA, Nicholson AG, Wotherspoon AC, Isaacson PG, Du MQ. (2009) A20 deletion is associated with copy number gain at the TNFA/B/C locus and occurs preferentially in translocation-negative MALT lymphoma of the ocular adnexa and salivary glands. J Pathol. 217(3):420-30. doi: 10.1002/path.2466.

[21] Zhang SQ, Kovalenko A, Cantarella G, Wallach D. (2000) Recruitment of the IKK signalosome to the p55 TNF receptor: RIP and A20 bind to NEMO (IKKgamma) upon receptor stimulation. Immunity. 12(3):301-11.

[22] De Valck D, Jin DY, Heyninck K, Van de Craen M, Contreras R, Fiers W, Jeang KT, Beyaert R. (1999) The zinc finger protein A20 interacts with a novel anti-apoptotic protein which is cleaved by specific caspases. Oncogene. 18(29):4182-90.

[23] Heyninck K, Beyaert R. (2005) A20 inhibits NF-kappaB activation by dual ubiquitin-editing functions. Trends in Biochemical Sciences. 30:1-4.

[24] Krikos A, Laherty CD, Dixit VM. (1992) Transcriptional activation of the tumor necrosis factor alpha-inducible zinc finger protein, A20, is mediated by kappa B elements. Journal of Biological Chemistry. 267:17971-17976.

[25] Lee EG, Boone DL, Chai S, Libby SL, Chien M, Lodolce JP, Ma A. (2000) Failure to regulate TNF-induced NF-kappaB and cell death responses in A20-deficient mice. Science. 289(5488):2350-4.

[26] Turer EE, Tavares RM, Mortier E, Hitotsumatsu O, Advincula R, Lee B, Shifrin N, Malynn BA, Ma A. (2008) Homeostatic MyD88-dependent signals cause lethal inflammation in the absence of A20. J Exp Med. 205(2):451-64. doi: 10.1084/jem.20071108.

[27] Kool M, van Loo G, Waelput W, De Prijck S, Muskens F, Sze M, van Praet J, Branco-Madeira F, Janssens S, Reizis B, Elewaut D, Beyaert R, Hammad H, Lambrecht BN. (2011) The ubiquitin-editing protein A20 prevents dendritic cell activation, recognition of apoptotic cells, and systemic autoimmunity. Immunity. 35(1):82-96.

[28] Song X-T, Kabler K E, Shen L, Rollins L, Huang X F, Chen S-Y. (2008) A20 is an antigen presentation attenuator, and its inhibition overcomes regulatory T cell–mediated suppression. *Nature Medicine.* 258 - 265.

[29] Tacken PJ, Zeelenberg IS, Cruz LJ, van Hout-Kuijer MA, van de Glind G, Fokkink RG, et al. (2011) Targeted delivery of TLR ligands to human and mouse dendritic cells strongly enhances adjuvanticity. Blood. 118(26):6836-44.

[30] Breckpot K, Aerts-Toegaert C, Heirman C, Peeters U, Beyaert R, Aerts JL, et al. (2009) Attenuated expression of A20 markedly increases the efficacy of double-stranded RNA-activated dendritic cells as an anti-cancer vaccine. J Immunol. 182(2):860-70.

[31] Kadowaki N, Ho S, Antonenko S, Malefyt RW, Kastelein RA, Bazan F, Liu YJ. (2001) Subsets of human dendritic cell precursors express different toll-like receptors and respond to different microbial antigens. J Exp Med. 194(6):863-9.

[32] Richardson MA, Ramirez T, Russell NC, Moye LA. (1999) Coley toxins immunotherapy: a retrospective review. Altern Ther Health Med. 5:42-47.

[33] Hoption Cann SA, Van Netten JP, Van Netten C. (2003) Dr William Coley and tumour regression: A place in history or in the future? Postgrad Med J. 79:672-680.

[34] Krieg AM, Yi AK, Matson S, Waldschmidt TJ, Bishop GA, Teasdale R, Koretzky GA, Klinman DM. (1995) CpG motifs in bacterial DNA trigger direct B-cell activation. Nature. 374(6522):546-9.

[35] Bauer S, Wagner H. (2002) Bacterial CpG-DNA licenses TLR9. Curr Top Microbiol Immunol. 270:145-54. Review.

[36] Hemmi H, Takeuchi O, Kawai T, Kaisho T, Sato S, Sanjo H, Matsumoto M, Hoshino K, Wagner H, Takeda K, Akira S. (2001) A Toll-like receptor recognizes bacterial DNA. Nature. 2000 Dec 7;408(6813):740-5. Erratum in: Nature. 409(6820):646.

[37] Wagner H. (2002) Interactions between bacterial CpG-DNA and TLR9 bridge innate and adaptive immunity. Curr Opin Microbiol. 5(1):62-9. Review.

[38] Häcker H, Vabulas RM, Takeuchi O, Hoshino K, Akira S, Wagner H. (2000) Immune cell activation by bacterial CpG-DNA through myeloid differentiation marker 88 and tumor necrosis factor receptor-associated factor (TRAF)6. J Exp Med. 192(4):595-600.

[39] Kortylewski M, Swiderski P, Herrmann A, Wang L, Kowolik C, Kujawski M, et al. (2009) In vivo delivery of siRNA to immune cells by conjugation to a TLR9 agonist enhances anti-tumor immune responses. Nat Biotechnol. 27(10):925-32.

[40] Nechaev S, Gao C, Moreira D, Swiderski P, Jozwiak A, Kowolik CM, et al. (2013) Intracellular processing of immunostimulatory CpG-siRNA: Toll-like receptor 9 facilitates siRNA dicing and endosomal escape. J Control Release. 170(3):307-15. doi: 10.1016/j.jconrel.2013.06.007.

[41] Van Voorhis WC, Hair LS, Steinman RM, Kaplan G. (1982) Human dendritic cells. Enrichment and characterization from peripheral blood. J Exp Med. 155(4):1172-87.

[42] Reid SD, Penna G, Adorini L. (2000) The control of T cell responses by dendritic cell subsets. Curr Opin Immunol. 12(1):114-21. Review.

[43] Inaba K, Inaba M, Romani N, Aya H, Deguchi M, Ikehara S, et al. (1992) Generation of large numbers of dendritic cells from mouse bone marrow cultures supplemented with granulocyte/macrophage colony-stimulating factor. J Exp Med. 176(6):1693-702.

[44] Inaba K, Swiggard WJ, Steinman RM, Romani N, Schuler G, Brinster C. (2009) Isolation of dendritic cells. Curr Protoc Immunol. Chapter 3:Unit 3.7. doi: 10.1002/0471142735.im0307s86.

[45] Scheicher C, Mehlig M, Zecher R, Reske K, Seiler F, Hintz-Obertreis P. (1993) Recombinant GM-CSF Induces in Vitro Differentiation of Dendritic Cells from Mouse Bone Marrow. Advances in Experimental Medicine and Biology Volume 329, pp 269-273.

[46] Jiang X, Shen C, Rey-Ladino J, Yu H, Brunham RC. (2008) Characterization of Murine Dendritic Cell Line JAWS II and Primary Bone Marrow-Derived Dendritic Cells in Chlamydia muridarum Antigen Presentation and Induction of Protective Immunity. Infect Immun. 76(6): 2392–2401. Published online 2008 March 24. doi: 10.1128/IAI.01584-07.

[47] Pajtasz-Piasecka E, Rossowska J, Szyda A, Krawczenko A, Dus D. (2007) Generation of anti-tumor response by JAWS II mouse dendritic cells transduced with murine interleukin 12 genes. Oncol Rep. 17(5):1249-57.

[48] Xu Y, Darcy PK, Kershaw MH. (2007) Tumor-specific dendritic cells generated by genetic redirection of Toll-like receptor signaling against the tumor-associated antigen, erbB2. Cancer Gene Ther. 14(9):773-80.

[49] Otsu S, Gotoh K, Yamashiro T, Yamagata J, Shin K, Fujioka T, Nishizono A. (2006) Transfer of antigen-pulsed dendritic cells induces specific T-Cell proliferation and a therapeutic effect against long-term Helicobacter pylori infection in mice. Infect Immun. 74(2):984-93.

[50] Check E. (2005) Gene therapy put on hold as third child develops cancer. Nature 433:561.

[51] Hacein-Bey-Abina S, Von Kalle C, Schmidt M, McCormack MP, Wulffraat N, Leboulch P, et al. (2003). LMO2-associated clonal T cell proliferation in two patients after gene therapy for SCID-X1. Science. 302:415-419.

[52] Raper SE, Chirmule N, Lee FS, Wivel NA, Bagg A, Gao GP, et al. (2003) Fatal systemic inflammatory response syndrome in a ornithine transcarbamylase deficient patient following adenoviral gene transfer. Mol Genet Metab. 80:148-158.

[53] Laufer SD, Detzer A, Sczakiel G, Restle T. (2010) Selected Strategies for the delivery of siRNA in vitro and in vivo. RNA Technologies and their applications. Springer-Verlag. 29-58. DOI 10.1007/ 978-3-642-12168-5_2.

[54] Shim MS, Kwon YJ. (2010) Efficient and targeted delivery of siRNA in vivo. FEBS J. 277(23):4814-27. doi: 10.1111/j.1742-4658.2010.07904.x.

[55] Jeong JH, Mok H, Oh YK, Park TG. (2009) siRNA conjugate delivery systems. Bioconjug Chem. 20:5-14.

[56] Warger T, Osterloh P, Rechtsteiner G, Fassbender M, Heib V, Schmid B, Schmitt E, Schild H, et al. (2006) Synergistic activation of dendritic cells by combined Toll-like receptor ligation induces superior CTL responses in vivo. Blood. 108(2):544-50.

[57] Smyth MJ, Hayakawa Y, Takeda K, Yagita H. (2002) New aspects of natural-killer-cell surveillance and therapy of cancer. Nat Rev Cancer. 2(11):850-61. Review.

[58] Mellman I, Steinman RM. (2001) Dendritic cells: specialized and regulated antigen processing machines. Cell. 106(3):255-8. Review.

[59] Bottero V, Imbert V, Frelin C, Formento JL, Peyron JF. (2003) Monitoring NF-kappa B transactivation potential via real-time PCR quantification of I kappa B-alpha gene expression. Mol Diagn. 7(3-4):187-94.

[60] Horn F, Henze C, Heidrich K. (2000) Interleukin-6 signal transduction and lymphocyte function. Immunobiology. 202(2):151-67.

[61] Kishimoto T. (2010) IL-6: from its discovery to clinical applications. Int Immunol. 22(5):347-52. doi: 10.1093/intimm/dxq030. Epub 2010 Apr 21. Review.

[62] Idriss HT, Naismith JH. (2000) TNF alpha and the TNF receptor superfamily: structure-function relationship(s). Microsc Res Tech. 50(3):184-95. Review.

[63] Alexis F, Pridgen E, Molnar LK, Farokhzad OC. (2008) Factors affecting the clearance and biodistribution of polymeric nanoparticles. Mol Pharm. 5:505-515.

[64] Xie FY, Woodle MC, Lu PY. (2006) Harnessing in vivo siRNA delivery for drug discovery and therapeutic development. Drug Discov Today. 11:67-73.

[65] Snead NM, Wu X, Li A, Cui Q, Sakurai K, Burnett JC, Rossi JJ. (2013) Molecular basis for improved gene silencing by Dicer substrate interfering RNA compared with other siRNA variants. Nucleic Acids Res. 41(12):6209-21. doi: 10.1093/nar/gkt200.

[66] Fellmann C, Hoffmann T, Sridhar V, Hopfgartner B, Muhar M, Roth M, et al. (2013) An optimized microRNA backbone for effective single-copy RNAi. Cell Rep. 5(6):1704-13. doi: 10.1016/j.celrep.2013.11.020.

[67] Abdur Rahman SM, Sato H, Tsuda N, Haitani S, Narukawa K, Imanishi T, et al. (2010) RNA interference with 2',4'-bridged nucleic acid analogues. Bioorg Med Chem. 18(10):3474-80. doi: 10.1016/j.bmc.2010.03.076.

[68] Ballas ZK, Krieg AM, Warren T, Rasmussen W, Davis HL, Waldschmidt M, Weiner GJ. (2001) Divergent therapeutic and immunologic effects of oligodeoxynucleotides with distinct CpG motifs. J Immunol. 167(9):4878-86.

[69] Marshall JD, Fearon K, Abbate C, Subramanian S, Yee P, Gregorio J, et al. (2003) Identification of a novel CpG DNA class and motif that optimally stimulate B cell and plasmacytoid dendritic cell functions. J Leukoc Biol. 73(6):781-92.

[70] Gray RC, Kuchtey J, Harding CV. (2007) CpG-B ODNs potently induce low levels of IFN-alphabeta and induce IFN-alphabeta-dependent MHC-I cross-presentation in DCs as effectively as CpG-A and CpG-C ODNs. J Leukoc Biol. 81(4):1075-85.

[71] Katsuda M, Iwahashi M, Matsuda K, Miyazawa M, Nakamori M, Nakamura M, et al. (2011) Comparison of different classes of CpG-ODN in augmenting the generation of human epitope peptide-specific CTLs. Int J Oncol. 39(5):1295-302. doi: 10.3892/ijo.2011.1146.

[72] Wooldridge JE, Weiner GJ. (2003) CpG DNA and cancer immunotherapy: orchestrating the anti-tumor immune response. Curr Opin Oncol. 15(6):440-5.

[73] Klinman D. (2004) Immunotherapeutic uses of CpG oligodeoxynucleotides. Nature Rev Immunol 4, 1-10.

[74] Wingender G, Garbi N, Schumak B, Jüngerkes F, Endl E, von Bubnoff D, et al. (2006) Systemic application of CpG-rich DNA suppresses adaptive T cell immunity via induction of IDO. Eur J Immunol. 36(1):12-20.

[75] Jan Zeromski, Iwona Mozer-Lisewska, Mariusz Kaczmarek. (2008) Significance of Toll-like Receptors Expression in Tumor Growth and Spreading: A Short Review. Cancer Microenviron. 1(1): 37–42. doi: 10.1007/s12307-008-0005-4

[76] Huang B, Zhao J, Li H, He KL, Chen Y, Chen SH, et al. (2005) Toll-like receptors on tumor cells facilitate evasion of immune surveillance. Cancer Res. 65(12):5009-14.

[77] Sommariva M, De Cecco L, De Cesare M, Sfondrini L, Ménard S, Melani C, et al. (2011) TLR9 agonists oppositely modulate DNA repair genes in tumor versus immune cells and enhance chemotherapy effects. Cancer Res. 71(20):6382-90. doi: 10.1158/0008-5472.CAN-11-1285.

[78] Negroiu G, Dwek RA, Petrescu SM. (2005) Tyrosinase-related protein-2 and -1 are trafficked on distinct routes in B16 melanoma cells. Biochem Biophys Res Commun. 328(4):914-21.

[79] Ghanem G, Fabrice J. (2011) Tyrosinase related protein 1 (TYRP1/gp75) in human cutaneous melanoma. Mol Oncol. 5(2):150-5. doi: 10.1016/j.molonc.2011.01.006. Review.

[80] Ferlazzo G, Morandi B, D'Agostino A, Meazza R, Melioli G, Moretta A, et al. (2003) The interaction between NK cells and dendritic cells in bacterial infections results in rapid induction of NK cell activation and in the lysis of uninfected dendritic cells. Eur J Immunol. 33(2):306-13.

[81] Trinchieri G. (2003) Interleukin-12 and the regulation of innate resistance and adaptive immunity. Nat Rev Immunol. 3(2):133-46. Review

[82] Zhao J, Bagchi S, Wang C-R. (2014) Type II natural killer T cells foster the antitumor activity of CpG-oligonucleotides. OncoImmunology. Vol 3:e1-1.

[83] Braumüller H, Wieder T, Brenner E, Aßmann S, Hahn M, Alkhaled M, et al. (2013) T-helper-1-cell cytokines drive cancer into senescence. Nature. doi:10.1038/nature11824.

[84] Wieder T, Braumüller H, Brenner E, Zender L, Röcken M. (2015) Changing T-cell enigma: Cancer killing or cancer control?. Cell Cycle. 12:19, 3335-3342, DOI: 10.4161/cc.26060.

[85] Miconnet I, Koenig S, Speiser D, Krieg A, Guillaume P, Cerottini JC, et al. (2002) CpG are efficient adjuvants for specific CTL induction against tumor antigen-derived peptide. J Immunol. 168(3):1212-8.

[86] Davila E, Celis E. (2000) Repeated administration of cytosine-phosphorothiolated guanine-containing oligonucleotides together with peptide/protein immunization results in enhanced CTL responses with anti-tumor activity. J Immunol. 165(1):539-47.

[87] Baines J, Celis E. (2003) Immune-mediated tumor regression induced by CpG-containing oligodeoxynucleotides. Clin Cancer Res. 9(7):2693-700.

[88] Wu A, Oh S, Gharagozlou S, Vedi RN, Ericson K, Low WC, et al. (2007) In vivo vaccination with tumor cell lysate plus CpG oligodeoxynucleotides eradicates murine glioblastoma. J Immunother. 30(8):789-97.

[89] William M. Siders, Kristin L. Vergilis, Carrie Johnson, Jacqueline Shields and Johanne M. Kaplan. (2003) Induction of Specific Anti-tumor Immunity in the Mouse with the Electrofusion Product of Tumor Cells and Dendritic Cells. Molecular Therapy. 7, 498–505.

[90] Fleshman JW. (2000) Athogenesis: Tumor cell lines and application in experimental animal studies. In: Reymond MA, Bonjer HJ, Köckerling F. Port-site and Wound Recurrences in Cancer Surgery. Springer Science & Business Media.

[91] Hornung V, Rothenfusser S, Britsch S, Krug A, Jahrsdörfer B, Giese T, et al. (2002) Quantitative expression of toll-like receptor 1-10 mRNA in cellular subsets of human peripheral blood mononuclear cells and sensitivity to CpG oligodeoxynucleotides. J Immunol. 168(9):4531-7.

[92] Rothenfusser S, Hornung V, Krug A, Towarowski A, Krieg AM, Endres S, et al. (2001) Distinct CpG oligonucleotide sequences activate human gamma delta T cells via interferon-alpha/-beta. Eur J Immunol. 31(12):3525-34.

[93] Rothenfusser S, Hornung V, Ayyoub M, Britsch S, Towarowski A, Krug A, et al. (2004) CpG-A and CpG-B oligonucleotides differentially enhance human peptide-specific primary and memory CD8+ T-cell responses in vitro. Blood. 103(6):2162-9.

[94] Katsuda M, Iwahashi M, Matsuda K, Miyazawa M, Nakamori M, Nakamura M, et al. (2011) Comparison of different classes of CpG-ODN in augmenting the generation of human epitope peptide-specific CTLs. Int J Oncol. 39(5):1295-302.

12 DECLARATION

Hiermit erkläre ich, dass diese Arbeit bisher von mir weder an der Mathematisch-Naturwissenschaftlichen Fakultät der Ernst-Moritz-Arndt-Universität Greifswald noch einer anderen wissenschaftlichen Einrichtung zum Zwecke der Promotion eingereicht wurde. Ferner erkläre ich, dass ich diese Arbeit selbständig verfasst und keine anderen als die darin angegebenen Hilfsmittel und Hilfen benutzt und keine Textabschnitte eines Dritten ohne Kennzeichnung übernommen habe.

Greifswald, _____ _____

Floriane Braun

13 PUBLICATIONS

In vivo silencing of A20 *via* TLR9-mediated targeted siRNA delivery potentiates anti-tumor immune response

Braun FCM, van den Brandt J, Thomas S, Lange S, Schrank J, Gand C, Przybylski GK, Schmoeckel K, Bröker BM, Schmidt CA, Grabarczyk P
PLoS One. 2015 Sep.

Identification of multiple complex rearrangements associated with deletions in the 6q23-27 region in Sézary syndrome

Iżykowska K, Zawada M, Nowicka K, Grabarczyk P, Braun FC, Delin M, Möbs M, Beyer M, Sterry W, Schmidt CA, Przybylski GK
J Invest Dermatol. 2013 Nov;133(11):2617-25. doi: 10.1038/jid.2013.188. Epub 2013 Apr 18.

Tumor suppressor TNFAIP3 (A20) is frequently deleted in Sézary syndrome

Braun FC*, Grabarczyk P*, Möbs M, Braun FK, Eberle J, Beyer M, Sterry W, Busse F, Schröder J, Delin M, Przybylski GK, Schmidt CA
* Both authors contributed equally to this study
Leukemia. 2011 Sep;25(9):1494-501. doi: 10.1038/leu.2011.101. Epub 2011 May 31.

Immunomodulatory effects of sorafenib on peripheral immune effector cells in metastatic renal cell carcinoma

Busse A, Asemissen AM, Nonnenmacher A, Braun F, Ochsenreither S, Stather D, Fusi A, Schmittel A, Miller K, Thiel E, Keilholz U
Eur J Cancer. 2011 Mar;47(5):690-6. doi: 10.1016/j.ejca.2010.11.021.

Systemic immune tuning in renal cell carcinoma: favorable prognostic impact of TGF-beta 1 mRNA expression in peripheral blood mononuclear cells

Busse A, Asemissen A, Nonnenmacher A, Ochsenreither S, Fusi A, Braun F, Stather D, Schmittel A, Miller K, Thiel E, Keilholz U
J Immunother. 2011 Jan;34(1):113-9. doi: 10.1097/CJI.0b013e3181fb6580.

14 DANKSAGUNG

An dieser Stelle möchte ich all jenen danken, die durch ihre fachliche und persönliche Unterstützung zum Gelingen dieser Arbeit beigetragen haben.

Frau Prof. Dr. Barbara Bröker (Institut für Immunologie und Transfusionsmedizin, Universität Greifswald) möchte ich für die Betreuung meiner Dissertation und die inspirierenden Diskussionen danken.

Mein besonderer Dank gilt Prof. Dr. Christian Andreas Schmidt (KIMC, Universitätsmedizin Greifswald). Sie haben mich stets ermutigt eigene Ideen zu entwickeln und meinen Weg zu gehen. Danke für Ihre Förderung und Unterstützung.

Ein großer Dank gebührt Dr. Piotr Grabarczyk (KIMC, Universitätsmedizin Greifswald), dessen gute Ideen Grundlage dieser Arbeit und stets eine Inspiration waren. Dein wissenschaftliches Können ist mir ein großes Vorbild.

Bei Dr. Jens van den Brandt (ZSFV, Universität Greifswald) möchte ich mich besonders bedanken für die Unterstützung und Zusammenarbeit bei den Tierversuchen und darüber hinaus. Ohne Ihre Hilfe wäre diese Arbeit so nicht möglich gewesen.

Für die schönen Mikroskopischen Aufnahmen möchte ich mich bei Dr. Raghavendra Palankar (ZIK-HIKE, Universität Greifswald) bedanken.

Ein großer Dank geht auch an Dr. Bernd Jäger (Institut für Biometrie und Informatik, Universität Greifswald) für die Ruhe und Geduld bei der statistischen Auswertung meiner Daten.

Ebenfalls danken möchte ich Olfert Landt (TIB Molbiol, Berlin) für Anleitung und Diskussionen in CpG-Fragen zu Beginn des Projektes.

Bedanken möchte ich mich auch bei Katrin Schmoeckel (Institut für Immunologie und Transfusionsmedizin, Universität Greifswald) für die Starthilfe bei dem Schritt in die *in vivo* Versuche und viele gute Tipps.

Meinen lieben Kollegen Martin Delin, Juliane Schrank, Claudia Gand, Passorn Winkler, Sören Thomas, Sandra Lange und Kathrin Aßmus möchte ich für die schöne gemeinsame Zeit im Labor danken. Ihr wart stets zur Stelle mit Rat und Tat und habt mir den Arbeitsalltag verschönert. Es war toll Seite an Seite mit euch zu arbeiten.
Auch den anderen Mitarbeitern der KIMC, vor allem Antje Mertin und Jana Schicka, möchte ich für die Unterstützung und gute Zusammenarbeit danken.

Bedanken möchte ich mich insbesondere bei Sören Thomas. Es war schön dich mit im A20-Team zu haben und ich freue mich, dass du das Projekt mit so viel Begeisterung und Engagement weitergeführt hast.

Juliane Schrank möchte ich besonders herzlich danken für viele Jahre Unterstützung, Zusammenarbeit und Freundschaft. Ich werde immer gerne an unsere gemeinsame Studien- und Arbeitszeit zurückdenken.

Ein ganz besonderer Dank gilt meiner ganzen Familie, die mich stets unterstützt und an mich geglaubt hat. Ich bin sehr glücklich euch alle zu haben.
Von ganzem Herzen möchte ich meinem Mann danken. Deine Liebe, Geduld und Glaube an mich hat mir viel Kraft gegeben. Obwohl uns all zu oft viele Kilometer trennten, warst und bist du immer in meinem Herzen.